Cape Peninsula University of Technology

SUPERCRITICAL FLUID FRACTIONATION PROCESS DEVELOPMENT: A TECHNO-ECONOMIC EVALUATION OF RETROFITTING AN AROMA PRODUCTION FACILITY

by

SIOBHAN CHLOÉ HENDRICKS

Thesis submitted in fulfilment of the requirements for the degree

Master of Engineering in Chemical Engineering

in the Faculty of Engineering and the Built Environment
at the Cape Peninsula University of Technology

Supervisor: Mr T.F.N. Madzimbamuto
Co-supervisor: Prof. T.V. Ojumu

Bellville
May 2022

DECLARATION

I, **Siobhan Chloé Hendricks**, declare that the contents of this thesis represent my own unaided work, and that the thesis has not previously been submitted for academic examination towards any qualification. Furthermore, it represents my own opinions and not necessarily those of the Cape Peninsula University of Technology.

Signed	May 2022 **Date**

ABSTRACT

An aroma–rich, aqueous condensate is produced as a by-product from the triple-effect evaporation of apple juice during the production of sugar from the fruit juice. At about 1% content of organic compounds, an opportunity exists to add value to this product by concentrating the aroma compounds and reducing the bulk of the water content. In doing so, the non-aroma imparting organic compounds contained may also be selectively removed, and thus increasing the value of the product. Besides its application as food and beverage, a concentrated aroma can find use is perfumery and other scented products.

This work investigated the feasibility of further concentrating an aroma-rich, but highly dilute aqueous condensate by-product using supercritical CO_2 (sCO_2) as the selective solvent. The compounds of interest were hexenal and trans-2-hexenal (representing the desired, aroma compounds), and hexanol (an organic compound that does not contribute to the desired aroma). Initially, a theoretical approach to the problem was taken to investigate the possibility of enrichment of the organic compounds from their aqueous mixture, as well as separation of the organic compounds. This was achieved using a series of equilibrium flash calculations representing a counter-current column. Experimental vapour-liquid equilibria data of binary solute-CO_2 for each of the compounds, obtained from the literature, was used to develop a model to represent the phase behaviour of the system. The SRKKD thermodynamic model in Aspen Plus® was shown to adequately represent the system behaviour.

An outcome representing the possibility of concentration, but the unlikelihood of separation of the hexanol from the aroma compounds was obtained at this stage. This outcome led to further investigation at pilot plant, experimental level, using a synthetic mixture of the main components of a typical condensate from a fruit-sugar factory. The sample and the dense gas were fed counter-currently through the column, and the concentrated extract separated from the solvent in a series of separators. Pilot plant experiments were conducted at 40 & 50^oC and 70 & 100 bar at a solvent to feed ratio of 5.

Flow and composition data was obtained from the series of experiments. The data was used to develop a process model, using the commercial simulator Aspen Plus®. The model parameters were adjusted to fit the flow and composition experimental data. Good prediction of the process performance was obtained from model. The model was thus used to predict the performance of the process at conditions other than those investigated experimentally. Different process lay-out scenarios were investigated. In this way, it was possible to predict the conditions required for optimum operation of the process.

The results showed that, in agreement with the theoretical study, the concentration of organic components in the feed was relatively easily achievable. Somewhat unexpectedly, the results

showed that hexanol was removed to a greater extent than had been predicted by the model. Optimum conditions were selected at 40^{o}C, 70 bar and S/F ratio of 5. Energy requirements for the complete process, according to the model was 348 MJ/kg product. Both the product quality and yield indicate that the process holds potential for further development, possibly towards achieving a commercial process.

ACKNOWLEDGEMENTS

Firstly, I would like to thank God almighty for giving me the perseverance to complete this research project.

I wish to thank:

- My supervisor, Mr Tafirenyika Madzimbamuto, for his amazing supervision and continuous support even when I was slacking. I will forever be grateful for his patience, encouragement, persistent guidance, and expertise in the research field. His invaluable and excellent advice will always remain with me.
- My co-supervisor, Prof Tunde Ojumu for his motivation, dedication to excellence, needed knowledge and the role he played in making my research project a success.
- Ms Hannelene Small for her willingness to always assist and her advice.
- The girls (Vianka, Geraldine and Zezethu) for their assistance with my experiments and all the 'non-fun' times in the laboratory. You have helped me a lot and thank you for sharing your knowledge and time with me.
- My mom and dad for the endless love, support, and encouragement.

The financial assistance of the National Research Foundation and Nedbank towards this research is acknowledged. Opinions expressed in this thesis and the conclusions arrived at, are those of the author, and are not necessarily to be attributed to the National Research Foundation and Nedbank.

CONTENT

LIST OF FIGURES

LIST OF TABLES

GLOSSARY

Terms and Acronyms

CC	Counter-current
CF	Correction factor
EoS	Equation of state
PR	Peng Robinson
scCO₂	Supercritical CO_2
SFE	Supercritical fluid extraction
SFF	Supercritical fluid fractionation
SRKKD	Soave-Redlich-Kwong EoS with Kabadi Danner mixing rules

S/F	Solvent-to-feed ratio
VLE	Vapour-liquid equilibrium
Raffinate	Enriched liquid phase
Extract	Enriched vapour phase
Total aromas/ valuables	Hexanal and *trans*-2-hexenal
Total organics	Hexanal, *trans*-2-hexenal, and hexanol

List of Symbols

Symbol	***Description***	***Unit***
A	Area	m^2
c_i	Concentration	mg/L
C_p	Specific Heat Capacity	$kJ/(kg.K)$
D_{ij}	Mass diffusivity	m^2/s
F	Feed flow rate	$kmol/hr$
g_l	Group contribution parameter	
G_i	Sum of group contributions	
H	Enthalpy	J
$\hat{H}$	Specific Enthalpy	J/kg
J	Mass flux	kg/m^2 s
K_{ij} *or* α_{ij}	Distribution coefficient between component i and j	
k_{ij}	Binary interaction parameter for SRK correlations	
k_T	Isothermal compressibility	m^2/N
m	Mass	kg
$\dot{m}$	Mass flow rate	kg/hr
M_W	Molar mass	$kg/kmol$
n	Number of moles	mol
$\dot{n}$	Molar flow rate	mol/hr
P	Pressure	bar
P_c	Critical pressure	bar
P^*	Vapour pressure	Pa
Q	Heat added or removed	kJ
R	Universal gas constant, 8.314 $kJ/kmolK$	
t	Time	hr
T	Temperature	℃
T_c	Critical temperature	℃
u	Velocity	m/hr
$\hat{U}$	Internal energy	kJ
$\hat{U}$	Specific internal energy	kJ
V	Volume	m^3
V_m	Malar volume	$m^3/kmol$
x	Liquid fractions	
y	Vapour fractions	
z	Height	m

Greek and other symbols

Δ	Delta	
μ	Dynamic Viscosity	$Pa.s$
ρ	Density	kg/m^3
σ	Standard deviation	
$\bar{X}$	Average	

Subscripts

c	Critical
i	Component i

j	Component j
L	Liquid
V	Vapour

CHAPTER ONE

Introduction

1. INTRODUCTION

This work investigated the added value of a sub-concentration process for the enrichment of an apple aroma byproduct obtained from a fruit-sugar production facility. In this chapter, the background and problem statement established the purpose of the study. In addition, the objectives and thesis delineation are presented to fulfil the aim.

1.1. Background and Motivation

Typically, a fruit, spice or vegetable aroma is a combination of a few hundred individual aroma compounds, that together make up a few parts per million of the entire product. Equally so, their use in processed foods, beverages and fragrances are limited to these orders of magnitude (Rowe, 2005; Gonçalves *et al.*, 2018; Saffarionpour and Ottens, 2018).

Processes exist in which sugar is produced from fruit juice, such as apple juice, by concentrating the sugar through triple effect evaporation, followed by crystallisation. The triple effect evaporation is usually fitted with equipment to capture the fruit aroma-rich vapour, which is used as the essence in beverage manufacture. This condensed vapour, however, contains only up to 1% aroma compounds and is therefore highly dilute (Root, 1996).

As a result, the product requires further purification to isolate or concentrate the desirable apple aroma compounds. Conventional methods such as distillation or evaporation require high operating temperatures that pose challenges to thermal labile compounds (Dixon & Hewett, 2000). Low boiling points of valuable aromas close to that of the alcohols might present difficulty in separation. In addition, organics form azeotropes (constant boiling point with constant vapour and liquid composition) with water and alcohols, which will not be separable by distillation (Rao, 1989; Turton *et al.*, 1998; Crocker, 2009; Frey, 2009; Seader *et al.*, 2011).

The over-arching aim of this investigation was to evaluate the added value of the apple aroma byproduct obtained through further concentration using supercritical CO_2 as the selective solvent. The feed material was the aroma-rich condensed vapour obtained from the triple effect evaporation of apple juice. The process to be developed was to be retrofitted to the flowsheet model of a generic fruit sugar manufacturing process.

1.1.1. Overview: Fruit Aroma

Aroma, commonly known as flavour or odour, finds many applications in the processing industry. They are added to final products to enhance the aroma profile of products such as perfumes, beverages, and insecticides. Or used as-is in aromatherapy, cosmetic products, and air fresheners. The use of aroma dates to the 5th century. It was used as and added to perfumes, oils and spices in ancient Greece and Rome, and many were sourced locally. Others were imported from the Middle East (Classen*, et al*., 1994). In modern industry, aromas, depending on their application, product specification and aroma profile requirement, can be found, and indeed added to, food, beverages, spices, wine, fragrances, perfumes and essential oils (Anthony, 2007).

The aroma profile consists of volatile compounds. It constitutes the bulk of most aromas identified that contribute to the smell or odour. In addition, it affects the overall taste of the aroma/flavour perceived. However, only a fraction of these compounds identified contribute to the characteristic aroma of the specific fruit (López & Echeverría, 2010). Factors such as genetic, environmental, and harvesting practices play a key role in the aroma profile and biosynthesis thereof (Gonçalves *et al.*, 2018). Over the past seven decades, significant improvements in cultivation, cultural practices and advancements in technology have contributed to the preservation of fruit. However, improvement is still lacking in fruit aromas' overall production and preservation (Elhadi M. Yahia, 1994).

1.1.2. Apple Aroma

Apples are one of the most important fruit crops in terms of their market share in South Africa (HortGro, 2017). According to Sheth (2018), worldwide apple production was over 50 million tonnes in 2018. With China being the largest producer. South Africa also produces different apples mainly consumed in the local markets (HortGro, 2017). The demand for apples on local and international markets has increased. Therefore, an increase in the contribution of the apple economy to South Africa's GDP is expected (HortGro, 2017; Plaza, 2019).

Apples comprise water, carbohydrates, aromas, organic acids and are rich in simple sugars. The flavour of the fruit is contributed by taste (perception of chemicals by taste buds) and aroma/odour (perception of chemicals by receptors in the nose). Taste is mainly determined by simple sugars and acids, whereas odour depends on the volatility of the aroma and perception of the receptors located in the nose (Elhadi M. Yahia, 1994; Espino-Díaz *et al.*, 2016).

Apple aroma consists of a complex mixture of volatile compounds, with over 300 volatile compounds identified, predominantly made up of alcohols, ketones, aldehydes, esters, and ethers. The compounds that significantly contribute to apples' characteristic scent or odour are

the carbon 6 alcohols and aldehydes, constituting a small fraction of all the compounds identified in apple aroma. 1-hexanal, *trans*-2-hexenal, 1-hexanol, 1-butanol and ethyl-2-methyl butyrate are a few of many compounds identified in apple aroma. Compounds described having the characteristic apple scent/aroma present in most apple varieties are 1-hexanal and *trans*-2-hexenal (Elhadi M. Yahia, 1994; Corbo *et al*., 2002; Lane *et al*., 2002; Root & Barrett, 2004; Symoneaux *et al*., 2006; Espino-Díaz *et al.*, 2016).

In contrast, volatile compounds, generally alcohols such as 1-hexanol and 1-butanol, which constitute the bulk of the aroma, have no contribution to apple aroma and are described as compounds unsought for in the final product. Thus, separating or concentrating the valuable and undesirable compounds in apple aroma would result in a higher quality product that fetches a higher value on the market. (Mckenzie, 1988; Dixon and Hewett, 2000; Gardini *et al.*, 2002; Root and Barrett, 2004; Symoneaux *et al.*, 2006; Xu *et al*., 2007; López and Echeverría, 2010)

Biosynthesising apple aroma presents challenges due to the complexity of the volatile profile. Volatile compounds present in apple aroma produced through metabolic pathways to make up the volatile profile. Conditions such as climate changes, fruit ripening, post-handling factors, etc., have a significant impact on the products produced through these metabolic pathways. Thus, making it difficult to fabricate the process (Espinosa *et al.,* 2002; López & Echeverría, 2010).

Commercially apple aroma is recovered from the production of concentrated juice through evaporation, distillation or partial condensation (Börjesson *et al.*, 1996; Arthey & Ashurst, 1996; Jiang *et al*., 2010). A process concentrating fruit sugars extracted from apples recovers apple aroma as a byproduct during the evaporation stage. The sugar product comprises fructose, sucrose, and glucose to substitute for artificial sugars used in other industries. The product is flavour free and has a sugar concentration of 70/71^{o}Brix, with apple aroma condensate as a byproduct (Root, 1996).

A traditional apple juice concentrate process requires the following steps: fruit pulping, filtration, evaporation, pasteurisation and crystallisation/cooling (Schultz, 1969). During the evaporation stage, the aroma and most of the water is recovered in its vapour form, leaving a concentrate without a scent, mainly containing fructose or sucrose. Extracting aroma compounds through means of high temperatures, such as that required during evaporation @ 90^{o}C, compromises the quality of thermally labile compounds, consequently adulterating the final product produced (Börjesson *et al.*, 1996; Saffarionpour and Ottens, 2018).

1.1.3. Current conventional methods

Distillation, evaporation and solvent extraction are examples of conventional methods to concentrate natural organic flavours and aroma. (López & Echeverría, 2010). These methods are considered cheaper, readily available, and easy to operate and construct compared to newer technologies. Distillation is a separation technique used for splitting liquid mixtures into their respective individual components by applying heat. Differences in boiling point and volatility of the components in the mixture establish the principle or mechanism of separation (McCabe *et al.*, 1993). However, the application of aroma distillation finds its use in producing fruit spirits (Spaho, 2017).

Evaporation comprises the boiling of a weak, aqueous solution to produce a more concentrated product during evaporation. However, the aroma compounds are co-evaporated, and they turn up in the vapour phase (McCabe *et al*., 1993; Geankoplis, 2003). Solvent Extraction is one of the standard methods used to extract volatile and non-volatile compounds that make up an organic or non-organic solvent to extract compounds from a solid or liquid matrix (Attokaran, 2011). General advantages and disadvantages for the methods described above are listed in Table 1-1.

Table 1-1: Common advantages and disadvantages of conventional methods (McCabe *et al.*, 1993; Reverchon & De Marco, 2006; Crocker, 2009; López & Echeverría, 2010)

ADVANTAGES	DISADVANTAGES
– Simple to operate and easy to construct. – Low production and maintenance costs. – Suitable for large-scale production processes. – High yields. – Organic solvents are cheap and widely available.	– Harsh conditions cause the degradation of thermally labile compounds. – Energy-intensive process. – Organic solvents used are toxic, flammable and solvent-free product not guaranteed. – Several processing steps are involved.

Other less common methods, such as pervaporation and supercritical fluid fractionation (SFF), have shown effectiveness, efficiency and pose a lesser threat to the environment when compared to these traditional methods. In addition, it has not been well-established in the South African industry.

1.1.4. Alternative process route – Supercritical Fluid Fractionation (SFF)

Selective extraction with CO_2, however, may overcome all the drawbacks previously described. In its supercritical state, CO_2 performs best at temperatures just above its critical parameters, i.e. 31°C and 7.4 bar, where its density is highest (Brunner, 2009). These conditions are equally benign concerning thermally labile compounds, and the process's effect on the environment is virtually negligible, as the process does not produce additional CO_2. No boiling of water is involved, and the solvent is continuously recycled. Thus the costs of processing are low (Reverchon & De Marco, 2006).

Literature reveals that the use of SFE using CO_2 can be feasible for the concentration of aroma compounds in essential oils, for the fractionation of fish and vegetable oils to concentrate the tocopherols, esters and other non-saponifiable compounds found in animal and vegetable oils (Reverchon, 1997; Laitinen & Kaunisto, 1999; Mukhopadhyay, 2000; Gracia *et al*., 2007; Del Valle *et al.*, 2014). The counter-current fractionation of the key apple aroma compounds present in apple juice using supercritical CO_2 was reported by Bejarano & del Valle, (2017). The process showed feasibility in fractionating water and organics with a product obtained rich in key volatile compounds. Although the water concentration decreased significantly, the final product comprised a low concentration of organic compounds. Improving product quality such that the aroma fetches a higher value on the market will result in an economically viable product. Therefore, the research aimed to demonstrate the feasibility of retrofitting the suggested process to a current aroma production facility.

1.1.5. Purpose of the study

The purpose of this study was to develop a value addition process for the enrichment of an apple aroma byproduct obtained from a fruit sugar manufacturing process. In addition, the feasibility of enriching the product with the aroma compounds at the expense of the non-aroma organic compounds was also investigated.

1.2. Problem statement

The projected increase in flavourings and fragrances market results in increased demand, and apple aroma is no exception (Lucintel, 2020; TheInsightPartners, 2021). South Africa produces a large variety of fruit, especially in the Ceres and Groenland regions of the Western Cape (HortGro, 2017). Apples constitute the bulk of the fruit produced there, both for domestic and international markets. With the fruit processed into apple juice, dried apples and cider (Plaza, 2019), less known is that a large portion of the annual crop finds use in processing sugars, such as fructose and sucrose. The process route is well established.

Thermal processes used commercially tend to be expensive, particularly where the boiling of water is involved. In addition, thermally labile compounds that comprise many flavours tend to

degrade. Further, the flavour fraction obtained during evaporation tends to be much diluted in water. The risk of retaining residual solvent in the product rules out the use of solvent extraction in modern processes due to adverse consumer preference for this production method and the growing unacceptability of the environmental impact of such processes.

Thus, the demand for an alternative process route for the concentration on apple aroma has arisen. As previously discussed, SFF is a method that finds application in the concentration of apple aroma, and it has shown feasibility in separation by Bejarano & del Valle, (2017). In the current study process layout scenarios for the method of extraction proposed was produced to be retrofitted to an existing processing facility and compared based on their technical feasibility and product quality to determine which process are best suited for the counter-current (CC) fractionation of key apple aroma constituents using $scCO_2$. Further, an order of magnitude study was performed to establish the economic viability of the process.

1.3. Research aim and objectives

The over-arching aim of this study was to investigate the retrofitting of a sub-concentration to an existing fruit-sugar producing facility for enriching an apple aroma byproduct.
The following objectives were formulated

1. To develop a process model in Aspen Plus®, and to validate the model using experimental and literature data based on the SFF of the apple aroma byproduct.
2. To predict the multicomponent phase behaviour and separability of the compounds in the system based on literature binary phase behaviour data.
3. To optimise the current process layout and recommend the best-suited process by comparing process route layout scenarios based on product quality, energy consumption, technical feasibility, and economic viability for the fractionation of apple aroma concentrate.

1.4. Thesis delineation

The limitations of the research were:

- The model solution was key apple aroma compounds in South African produced apple aroma concentrate.

1.4.1. Delineation

The current research focuses on producing a best-suited process layout scenario based on product quality and energy consumption and investigating the economic evaluation thereof; however, the following was not included in this research project:

- The process layout scenarios presented were based on process route layouts for the fractionation column only. It does not include other major processing units; therefore, each layout's energy requirement was not evaluated.
- Piping and instrumentation were not included in the economic evaluation.
- Optimisation of other major units was not considered.

1.5. Significant contributions

The current investigation was structured to provide the following significant novel contributions:

1. New data on the CC fractionation of apple aromas using $scCO_2$ for an apple aroma model solution based on an apple aroma concentrate obtained from the South African industry.
2. An Aspen Plus® process model validated with literature and experimental data that predicted the separation of apple aroma compounds from fruit juice
3. An Aspen Plus® process model for retrofitting the fractionation of apple aroma compounds to a current process layout in industry.
4. Comparison of process layout scenarios for the fractionation of apple aroma based on product quality, product yield and organics recovery for South African produced apple aroma.

1.6. Thesis Outline

Chapter	Content
1 Introduction	The current chapter, chapter 1, provided a summary of the background of the research, the current method and alternative process routes used to produce apple aroma, the purpose of the study, the problem statement, the research aim and objectives, hypothesis and questions, significance of the study, limitations, and thesis delineation
2 Literature Review	Literature review on SFF using CO_2 and application thereof, the traditional method, phase behaviour of compounds in the system, thermodynamic modelling and process modelling of the system. Information is provided on previous studies conducted for similar applications and a traditional process currently used in the industry. This chapter also includes a discussion of the expected phase behaviour of the compounds in the relevant system. In addition, thermodynamic modelling of phase behaviour and economic studies using the upscale method is included in this chapter. This fulfilled the first objective of the research.
3	The material and methods employed to investigate the hypothesis of the study. The approach to each objective, materials used, the experimental

Materials and Methods	approach, and the data analysis are provided. A brief introduction to process modelling is also provided in this chapter using the Aspen Plus® process simulator. This fulfilled the second and third objectives.
4 Results	Steady-state was established in terms of thermal, mechanical, and hydrodynamic measurements during pilot plant experiments. Mass balance data obtained from pilot plant experiments were used to evaluate energy consumption and product quality validated the process model developed in the Aspen Plus® process simulator. In addition, the model was validated with literature data to attain objective 1 and shown accuracy in phase behaviour predictions above S/F ratios of 5 and at higher feed concentrations. Objective 2 was achieved through the investigation of the validated model at 40 – 60°C, 80 – 140 bar and S/F ratios of 5 – 15 the separability of the mixture was determined. Process layout considerations are compared based on product quality, organics recovery and yield to fulfil the requirements of objective 3. Based on separability data, separation occurs as a single-stage thus a single flash unit was suitable for the investigation of the phase behaviour of optimum process parameters, which was attained through a sensitivity analysis in the Aspen Plus® process simulator.
5 Discussion	This chapter fulfilled the aim of this investigation and answered the research questions. Results indicated that separation occurs as a single-stage, however, this was as a result of the polarity of the compounds in the system as confirmed by Bejarano & del Valle (2017). Therefore, $scCO_2$ is more than capable of extracting apple aroma constituents from a dilute aqueous solution with a near perfect separation. An order of magnitude economic evaluation in terms of energy consumption was 348 MJ/kg product because of high processing capacity. However, the significant organics concentration indicated an increased product value. In addition, energy requirements can be reduced.

CHAPTER TWO

Literature Review

2. LITERATURE REVIEW

This section provides the literature review to achieve objectives set in Chapter 1. Literature references are provided to support the description of the current knowledge on the sources and properties of apple aroma, the traditional methods of extraction, the suggested methods of concentration, and the physiochemical background of the suggested technology.

2.1. Introduction

Recently, consumer preferences have swung away from the consumption of synthetic flavours and aromas, to the more naturally produced flavour. The increased demand for natural flavour enhancers in food and beverages forecasts a growth in the aroma chemical market (TheInsightPartners, 2021). Apple aroma comprises complex and diverse chemical compounds. Volatile compounds make up a fraction of it. These compounds comprise the characteristic of the scent or odour of the aroma profile (Flath *et al*., 1967). On the other hand, other compounds that are not characteristic (aroma-like) to the aroma profile constitute the bulk thereof. Distillation and evaporation are typical examples of conventional methods to concentrate and extract natural apple aroma compounds from fruit or fruit juice (Root, 1996). The potential of newer extraction methods, such as supercritical fluid extraction (SFE), has yet to be recognised in the South African industry. SFE has shown feasibility in the fractionation of apple aroma constituents; however, application on an industrial scale shows the economic viability in the South African industry.

2.2. Apple aroma

Apple aroma finds use in industries such as the cosmetic, food and beverages and spice industry. It is either sold as a final product or added to other end products such as perfumes, beverages, soaps, detergents. Sources of apple aroma are present in raw fruit or follow the synthetic route. Due to the low concentration of valuable volatiles present in unprocessed fruit, the need for synthetically produced products derived. However, a swing in consumer preference has resulted in increased value in natural produced flavours. In addition, natural flavours tend to fetch a value on the market, at 10 or higher parallel to synthetic products (Mckenzie, 1988; Arthey & Ashurst, 1996; Root & Barrett, 2004).

2.2.1. Economic market share

According to BCCPublishing (2014), in 2006, the flavour and fragrances market was worth approximately 6.3 billion US dollars, increasing to approximately 23.9 billion US dollars in 2013 (BCCPublishing, 2014). Sabanoglu (2020) reports that the global market was approximately worth 28.5 billion US dollars in 2017, increasing to approximately 35 billion US dollars in 2019 (Sabanoglu, 2020).

The global flavours and fragrances market increased by 1,16 billion US dollars on average per year between 2006 and 2013 (7 years), increasing to an average of 3.25 billion US dollars per year between 2017 and 2019. As a result of changing consumer preferences and growing customers buying more natural products or products containing natural ingredients, the market expects continuous growth. Additionally, the market benefits from increasing income amongst the middle class (Lucintel, 2020).

A decline in the global flavours and fragrance market following 2020 due to the COVID-19 pandemic projected an increased market value for 2021 (Lucintel, 2020). The South African food and flavour enhancer market projects a compound annual growth rate of 5,1% for 2020 – 2025. The market witnessed significant growth due to growing consumer awareness. Thus, extracting aromas from natural sources would hold economic value. However, counter fit products containing inferior alternative ingredients might impede the market growth. (MordorIntelligence, 2019). But the growing demand for aroma chemicals for enhancing taste in food and beverages is likely to drive the aroma chemicals market (TheInsightPartners, 2021).

The increased market value shows that the flavour and fragrances market does not expect a decline. The growing consumer preference is a large contributor to the growing market. Thus, aromas extracted from natural sources such as fruit will fetch a higher value on the market. In addition, the growing market indicates that the value of flavour and fragrances are increasing. Therefore, indicating economic viability for the fractionation of apple aroma compounds.

2.2.2. Physical characteristic

Apple aroma is described as a clear liquid that has the characteristic scent of apples. Below is a list of the physical characteristics of apple aroma as obtained from Associated Fruit Processors (n.d.) (Associated Fruit Processors, n.d.):

Appearance	:	Colourless liquid
Scent/odour	:	Green, earthy, sweet
Concentration	:	180 – 210-fold
Specific Gravity d 20/20	:	0.9900 – 0.9980
Refractive Index (20 ^{o}C)	:	1.3390 – 1.3490

2.2.3. Chemical (volatiles) Composition

The volatile compounds present in apple aroma are either characterised to have an apple-like odour or undesired to the aroma profile. The compounds that contribute significantly to the overall flavour and aroma perceived in raw apple juice are present in minute concentrations due to high concentrations of carbohydrates and proteins (López & Echeverría, 2010). Within this low concentration, over 300 volatile compounds are identified in apple aroma.

Predominantly, comprised of alcohols, ketones, aldehydes, esters, lactones and terpenes (Jiang et al., 2010; Espino-Díaz *et al*., 2016).

Flath *et al*. (1967) identified and classified volatile apple aroma compounds into desired compounds that have an apple-like odour and undesired compounds which has no any direct resemblance to apple aroma. Root (1996) further divided six general apple aroma components that contribute to the quality of the apple aroma or essence as represented in Table 2-1:

Table 2-1 Desired and undesired compounds identified in apple aroma by Root, (1996:20):

Desired compounds	
Ethyl 2-methyl butyrate	Ripe apple aroma
1-Hexanal	Green apple aroma
trans-2-hexenal	Green apple aroma
Undesired compounds	
Ethyl acetate	Aeroplane glue aroma
1-butanol	Solvent or petroleum aroma
c-3-Hexanol	Green grass aroma

The compounds listed in Table 2-1 summarise the 56 volatile compounds identified by Flath *et al*. (1967) in delicious apple essence extract including 21 components unreported by previous researchers. The author further refined the compounds based on their olfactory thresholds in ppm (V/V). Alcohols, aldehydes, and esters comprised the 18 compounds evaluated. The alcohols had the highest olfactory thresholds (lowest concentration perceived by human sense of smell) in comparison to the esters and aldehydes. Furthermore, the three compounds listed as desired compounds in Table 2-1 have an apple-like character and essential contributors to apple aroma. These compounds contribute significantly to the overall aroma profile and comprise aldehydes and esters. Alcohols and, surprisingly, esters present in high concentrations have an odour/scent completely off from apples and thus lands themselves as undesired compounds (Flath *et al*., 1967). Koch (1976) acknowledged the sensory value of *trans*-2-hexenal in apple aroma essence in terms of its odour intensity. A reduction of the total aldehydes concentration in conjunction with increasing synthetic *trans*-2-hexenal nearly established the original odour of the original apple juice perceived (Koch, 1976).

Dimick & Hoskin (1983) further identified 266 volatile compounds present in apple aroma. With esters constituting the bulk of the apple aroma numerically. Nevertheless, the esters do not contribute significantly to the characteristic scent of apple aroma. The esters with a molecular weight between 100 to 300 g/mol contribute to the fruity odour present in apple aroma (Dimick & Hoskin, 1983). The carbon 6 alcohols and aldehydes formed during lipid oxidation significantly contribute to apple aroma's characteristic scent or odour. The alcohols contribute quantitatively mainly to the apple aroma. However, other compounds such as ketones, ethers,

acids, lactones, terpenes, and other hydrocarbons are also present in apple aroma but in significantly low to moderate concentrations. Overall, the quantity and type of volatile compounds, production patterns, fruit skin colour or C6 aldehydes primarily determines the overall aroma profile (Dimick & Hoskin, 1983).

The complexity of the aroma profile is presented in biosynthesising apple aroma. It involves metabolic pathways affected by factors such as fruit ripening, postharvest handling, climate change, etc. (López & Echeverría, 2010; Espino-Díaz *et al.*, 2016). The main products produced from metabolic pathways of fatty and amino acids are volatile compounds. Such as aldehydes, esters, and alcohols. The presence of enzymes such as lipoxygenase (LOX) and alcohol dehydrogenase (ADH) affects the volatile profile as it plays a crucial role in the production of volatile compounds apples (Espinosa *et al.,* 2002). The volatile profile changes with fruit maturation. Before maturation, most aldehydes are present and in the highest concentration. During harvesting, the alcohol content increases. After harvesting, the concentration of the esters rapidly increases (Espino-Díaz *et al*., 2016). Thus, the type and amount of volatile compounds present in apple aroma vary significantly amongst apple varieties. The factors influencing the production of these volatiles is impossible to accurately establish a set concentration for each volatile compound present in apple aroma. In addition, apple genetics is crucial in the volatile profile. Therefore, a comparison of the volatile profiles enables the identification of volatile compounds specific to apple aroma. Compounds described as having the characteristic scent/odour of apple adds value to the apple aroma. Synthesising volatile compounds to make up apple aroma as a more accessible process route has established itself; however, it will not replicate the aroma naturally extracted from the fruit. Table 2-2 shows a summary of the primary apple aroma volatile compounds found in apples as identified in a review by Espino-Díaz *et al.* (2016).

Table 2-2 Summary of volatile compounds identified in a study by Espino-Díaz *et al.* (2016)

Volatile compound	Total identified	Compounds found in highest concentration
Aldehydes	10	*trans*-2-hexenal and hexanal
Alcohols	9	Ethanol, 1-hexanol and 1-butanol
Esters	16	Hexyl acetate, butyl acetate, 2-methyl butyl acetate and hexyl hexanoate

The aldehydes in Table 2-2 were identified in the fruit before maturation, after ultra-low oxygen (ULO) and apple juice at harvesting. Hexanal and *trans*-2-hexenal were present in all the different apple varieties. They presented the highest concentration in the Golden Reinders apple variety after ULO compared to the other aldehydes present in apples. In the apple varieties Bisbee Spur Delicious and Golden Delicious, respectively, before maturation of the apples, an abundance of nonanal was identified by Mattheis *et al.* (1991) and Vallat *et al*.,

(2005) (Espino-Díaz et *al*., 2016). However, this compound was not present in any of the other apple varieties.

In terms of mass fraction, 1-hexanol and 1-butanol are abundant alcohols in the Granny Smith, Golden Delicious apples, and ethanol in the Mondial Gala. The esters, hexyl acetate, 2-methyl butyl acetate, and hexyl hexanoate, are abundant in the Pink Lady apple variety. In contrast, butyl acetate presents the highest concentration in the Mondial Gala apple variety. The alcohols generally comprise the highest fraction of volatile compounds in apple aroma. However, esters are numerically the most significant contributor to the apple aroma profile varying from 80% in the Golden Delicious variety to 98% in Starking Delicious. Esters described as sweet and fruity usually contribute to the overall apple aroma. However, a mixture of total esters perspicuously will not acquire desired apple-like characteristics as they present complex interactions (Espino-Díaz *et al*., 2016; Niu *et a*l., 2019). Dixon and Hewett (2000) identified the following aldehydes and alcohols based on their relative acidity of alcohol dehydrogenation of acetaldehyde and ethanol in an apple variety in Table 2-3:

Table 2-3 List of aldehydes and alcohols identified in Cox's Orange Pippin Apples (Dixon & Hewett, 2000)

Aldehyde identified	Alcohol identified
propanal	propan-1-ol
butanal	propan-2-ol
2-methylpropanal	butan-1-ol
pentanal	2-methylpropan-1-ol
hexanal	pentan-1-ol
trans-2-hexenal	hexan-1-ol
	trans-2-hexan-1-ol

In Table 2-3, propanal presented the highest % activity of ADH, 30.1, as opposed to a relatively lower 10 % activity ADH for hexanal and *trans*-2-hexenal for this apple variety. The alcohol, *trans*-2-hexen-1-ol, comprised a notably high % activity ADH of 121.3, which is higher when relative to other alcohols identified (>50%). Hexan-1-ol constitutes 18.3 % activity ADH, which falls under the lower percentage of alcohols. C6 aldehydes, characteristic of apple aroma, presented the most insufficient % activity ADH of all compounds identified in the apple variety. Thus, compounds with low % activity can be assumed to be valuable volatile compounds in apple aroma (Dixon & Hewett, 2000).

Börjesson *et al.* (1996) prepared a model apple juice aroma solution to establish whether pervaporation presents feasibility in recovering key apple aroma compounds. The model solution comprised out of the following compounds (Börjesson *et al.*, 1996) shown in Table 2-4.

Table 2-4 Volatile compounds identified by Börjesson *et al.* (1996) for a model apple juice solution

Organic Group	Volatile compound
Esters:	ethyl acetate, ethyl butanoate, ethyl-2-methyl butanoate, isopentyl acetate and hexyl acetate
Aldehydes:	*trans*-2-hexenal
Alcohols:	isobutanol, butanol, isopentanol and hexanol

Gas Chromatography (GC) and Gas Chromatography-Mass Spectroscopy (GC-MS)) analysis of apple juice permeate acquired the concentrations of the compounds in Table 2-4. The author experimented on the model solution instead of apple juice itself, because of the low concentration of the aroma compounds in apple juice and for analysis purposes. Upon analysis of the apple juice permeate, the author found difficulty in separating the ethanol peak from the ethyl acetate peak. Thus, the author decided to exclude ethanol from the model solution, in conjunction with the fact that ethyl acetate has a greater significance in apple aroma when compared to ethanol, even though both ethanol and ethyl acetate has the most significant aroma threshold values (Börjesson *et al.*, 1996).

Bejarano & del Valle (2017) performed the counter-current fractionation of the key apple aroma components from a model apple aroma solution using supercritical CO_2. The author selected (E)-2-hexenal, hexanal and hexanol in combination with distilled water to comprise the feed investigated to fabricate apple aroma. (E)-2-hexenal and hexanal were identified as the key components for the model apple aroma solution, and hexanol as undesired. (E)-2-hexenal is also referred to as *trans*-2-hexenal (Bejarano & Del Valle, 2017).

Although alcohols comprise the most significant concentration quantitatively in apple aroma, the carbon 6 aldehydes and esters, present in small amounts, adds a higher value in terms of their intensity. The carbon 6 unsaturated aldehydes, hexanal and *trans*-2-hexenal, have a descriptive green apple-like odour (Dimick & Hoskin, 1983; Mehinagic *et al*., 2004) of all volatile compounds previously reported. Dimick & Hoskin (1983) describes hexanal as desirable in terms of its contribution to the aroma profile and *trans*-2-hexenal important to the aroma intensity. The carbon 6 alcohol hexanol has a descriptive earthy (Mehinagic *et al*., 2004) like odour and is most abundant in all apple varieties.

Recent studies show that concentrated apple juice presents an aroma of significantly high concentrations in acetaldehyde, *trans*-2-hexenal, 3-methyl- 1-butanol, ethyl acetate, and hexanal characterised by a green fresh estery odour as reported by Nikfardjam & Maier (2011). In contrast, volatile compounds evaluated in unconcentrated juice such as 1-butanol, 2-methyl-1-butanol, ethyl butyrate, and ethyl-2-methylbutyrate presented the highest concentration characterised as fruity, ripe and sweet (Nikfardjam & Maier, 2011). Esters, the most dominant group of volatile compounds reported by Guo *et al*. (2020), comprised concentrations ranging between 3643 to 32143 µg/L, with hexyl acetate and butyl acetate mainly present in

abundance. 1-Butanol and 1-hexanol comprised the highest concentration of total alcohols. Hexanal and *trans*-2-hexenal predominantly comprise the bulk of the aldehydes identified and thus indicates importance in apple aroma (Guo *et al.*, 2020).

2.2.4. Traditional concentration technology

Conventional methods such as distillation, evaporation and solvent extraction are well-established methods used as extraction technology. (López & Echeverría, 2010). These processes show advantages in their processing capacity and easy maintenance and construction costs. However, there are several drawbacks based on product quality. As previously mentioned, distillation and evaporation use harsh conditions (specifically high temperatures) that degrades volatiles that are usually thermally labile (Reverchon & De Marco, 2006). Evaporation is a high energy-intensive process and commonly uses the boiling of water to produce energy. Moreover, the water is boiled by burning coal, and the off-gas produced from the reaction has a detrimental effect on the environment due to air pollution (McCabe *et al*., 1993; López & Echeverría, 2010).

Section 2.3 provides a review of the traditional method applied in the production of apple aroma.

2.3. Traditional method: Evaporation

Evaporation is a conventional method used commercially due to its vast applications; however, it is highly energy-intensive and generally not a standard technique used in the fractionation of aroma due to thermally labile volatiles. The production of fruit concentrate from raw apples recovers diluted apple aroma as a byproduct. Therefore, a review of evaporation techniques follows.

2.3.1. Review of evaporation: Theory and application

During evaporation, a weak, aqueous solution is typically boiled to remove the bulk of the water and produce a more concentrated product. However, with apple aroma as feed, the aroma compounds are co-evaporated, i.e., enriched in the vapour phase (Seader *et al.,* 2011:704). The flow diagram in Figure 2-1**Error! Reference source not found.** illustrates the input and output stream for a basic single-stage evaporation unit:

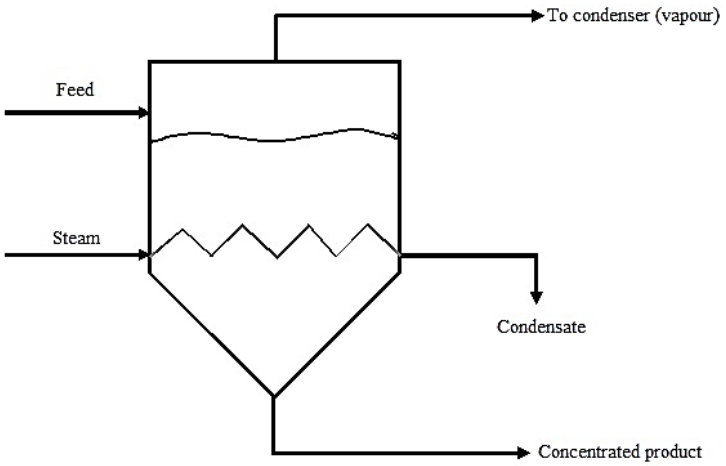

Figure 2-1: Schematic diagram of a simple evaporation unit (Redrawn from Seader et al. (2011:706))

In, the feed supplied at a temperature, T_f and steam at temperature, T_s, evaporate the feed to a temperature of T_1. The solute, enriched in the vapour form (combined with a low fraction of water), are removed, and condensed. If the extraction is successful, the condensate (vapour product) contains a mixture of water and a minimal quantity of the solute. The steam leaves the unit as condensate.

There are numerous types of evaporation units. McCabe *et al.* (1993) provide details of some units, for example, open kettle or pan, horizontal-tube natural circulation evaporator, vertical-type natural circulation evaporator, long-tube vertical-type evaporator, falling-film-type evaporator, forced-circulation evaporator and parallel-feed multiple-effect evaporators (McCabe *et al.*, 1993:465-470).

Typically a tubular falling film multiple-effect evaporator produces apple juice concentrate (Root, 1996). The falling film type evaporator finds use in processes involving a liquid feed with components sensitive to temperature, such as fruit juice (McCabe *et al.*, 1993:465-470). This evaporator consists of extended, vertical, tubular exchangers connected to a liquid-vapour separator. Tubular heat exchanger counter or co-currently fed with steam heats the feed to the required operating temperature. A separating vessel interlinked with the tubular heat exchanger represents a flash for the heated liquid such that the vapour and liquid phase separation occurs. The vapour exits through the top and liquid through the bottom (Geankoplis, 2003). This type of evaporator usually consists of multiple effects and multiple stages. The "stage" refers to the flow of the product (juice) through the evaporator and "effect" to vapour and steam used as a heating medium (Rao, 1989). For the process described in section 2.3.2.1, the first effect would be at the first stage and the same for the rest. The first effect receives steam from the boiler, and the second effect would receive cooler steam from the first effect. The condensate passes through the third effect and is recycled back to the boiler (Rao,

1989). Vaporising 1 kg of water requires 2.256 MJ, indicating that this process is highly energy-intensive (Saravacos *et al.*, 1970).

2.3.2. Extraction of apple aroma by evaporation

Evaporation would generally not be the first option for recovering apple aroma compounds, as it requires a high operating temperature for separation to occur. However, a processing facility produces fruit sugars that recover diluted apple aroma as a byproduct during a triple effect evaporation process. The section to follow describes this process.

2.3.2.1. Description of a typical aroma recovery processing facility

Figure 2-2 illustrates the schematic layout of the general process steps involved in the production of apple juice and sugar concentrate.

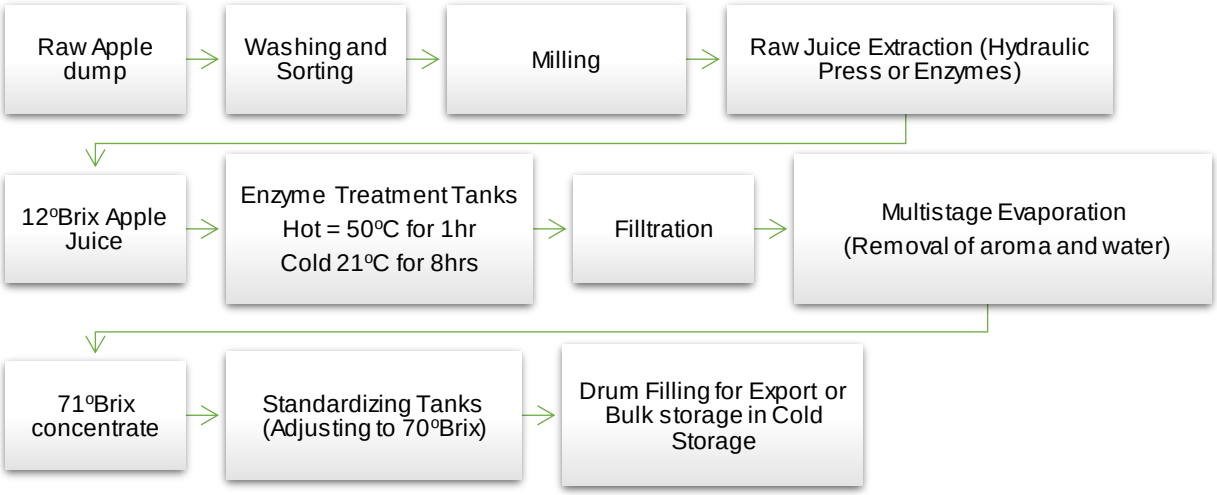

Figure 2-2: Schematic layout for production of apple juice concentrate (Redrawn from Root (1996:14))

The processing sequence starts with apples dumped into a water flume by the bulk truckload or pallet bins to remove dirt or foreign objects. The apples convey onto a sorting table for inspection and removal of any bad fruit. The fruit passes through a disintegrator (hammer or grating mill) to convert it into mash or pulp. There are various types of equipment for the extraction of raw apple juice, and the vertical hydraulic piston press is the most commercially used to separate most solids from the liquid. Enzymes added break down the cell structure to improve the processability. The liquid extracted represents the raw juice, and the remaining solids are disposed of or sold as pomace (Root, 1996).

The second treatment of enzymes to the raw juice remove suspended solid material for a clarified juice and breakdown of pectin. The methods for enzyme treatment include (1) where enzymes are added to 54°C raw apple juice and kept in tanks for 1 to 2 hours (known as hot treatment) and (2) where enzymes are added to room temperature raw juice and kept in tanks

for 6 to 8 hours (known as cold treatment). After the enzyme treatment, the juice passes through a filter to remove suspended solids (as shown in **Error! Reference source not found.**2).

Commercially used filters for these processes are rotary vacuum, pressure leaf, frame, belt, membrane and millipore filters. Centrifugation equipment are used to remove large particles before filtration, if necessary. Apple juice, 20-25°Brix obtained after filtration finds use as a consumable product. Apple juice passes to the next stage to produce concentrated apple juice/ concentrate fruit sugars, preserving fruit juice through pasteurisation.

Heat pasteurisation heats apple juice to 83°C, held for 3 minutes and hermetically sealed. It is filled into containers and cooled to 37°C and held for 1 minute. During the process, a vacuum develops in the container, lowering the oxygen to prevent microbial growth. Apple juice concentrate/sugar production bypasses this process step and enters the muti-effect evaporation unit. The unit comprises falling film evaporators and multi-effect tubular and plate evaporators. The raw juice enters the second stage for recovery of apple aroma (volatile) compounds. In addition, during the process water is removed to obtain a 20-25°Brix concentrate juice because of additional water removed in the process. The juice then passes through a first stage evaporator operating at 100°C for further removal of water which results in a 40-45°Brix concentration. A final stage obtains a product of 50-60°Brix at 45°C. A decrease in temperature to 3-4°C standardises it to 70°Brix before drum filling or bulk storage through condensation (Root, 1996).

The aroma-rich vapour enters a condenser to obtain apple aroma essence. The interest lies in the recovery of volatiles from a product of such because it will fetch a higher value on the market if concentrated in comparison to a synthetic equivalent. However, losses of aromas during evaporation results in a decreased recovery of volatile compounds. In addition, the juices pass through several processing steps that could affect the lability of the volatiles. Therefore, including a processing operation to recover volatiles before exposure to high temperatures could increase the overall concentration of volatiles. Therefore, processing the condensed product by further exposure to temperatures could result in additional degradation in thermal labile volatiles.

2.4. Suggested concentration technology

Extraction of a solute from a solid/liquid/vapour matrix requires a separation process. Examples of these separation processes are distillation, evaporation, absorption, leaching, drying and crystallisation. Newer technologies such as adsorption, chromatography, membrane separation and SFE recently developed could replace the conventional methods due to several drawbacks (Seader *et al*., 2011:2). Recent studies on SFF, described in this

section, indicate feasibility in separation and economic viability on an industrial scale. The section to follow provides a review of the suggested method:

2.4.1. Supercritical Fluid Fractionation (SFF)

In SFF processes, a solvent is used above its critical temperature and pressure to concentrate, fractionate or extract a solute from a mixture (solid or liquid). (Seader *et al*., 2011). Typical solvents include ethylene, carbon dioxide, water, propane, propylene, benzene and toluene (Mukhopadhyay, 2000:4). Solvent selection depends on the solute solubility, the selectivity, and the type of compounds present in the feed (Seader *et al*., 2011)

As previously discussed, apple aroma consists of various volatile compounds, and these compounds are thermally labile. Thus, due to its ability to extract compounds at a low near ambient critical temperature, CO_2 reckons as a suitable solvent for the current investigation.

2.4.1.1. Supercritical CO_2 as a solvent

In general, compression of gas results in a phase change to a liquid. Physical changes to the substance occur with additionally applied pressure and heat. No amount of pressure in combination with heat will cause the gas to change into its liquid form. When fluids reach this temperature and pressure, it is called a supercritical fluid.

The temperature and pressure reach a point known as the supercritical point (see Figure 2-3) at the critical temperature (T_c) and pressure (P_c). The supercritical region of this fluid is above this temperature and pressure as presented in Figure 2-3 (Mukhopadhyay, 2000:2-3).

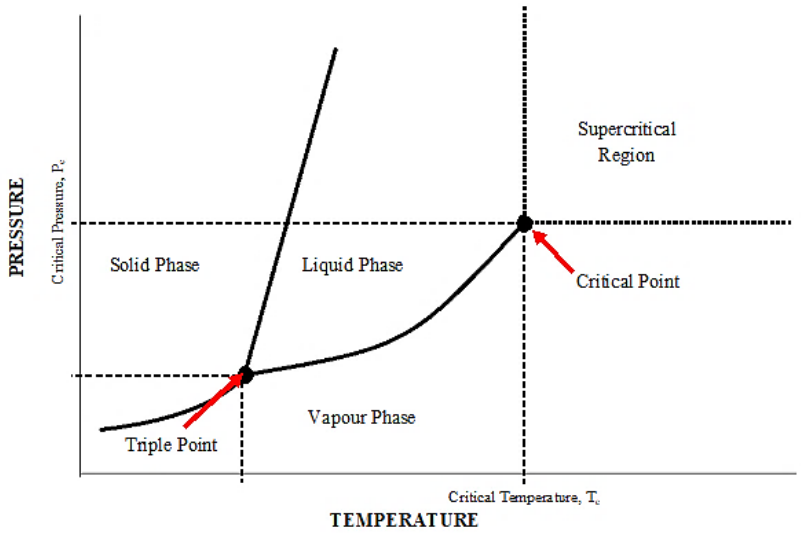

Figure 2-3: Typical phase diagram to illustrate supercritical region (Redrawn from Parhi & Suresh (2013))

Supercritical fluids exert characteristics that represent both a gas and a liquid. It has a low viscosity (like a gas), low surface tension, and a liquid's solvent power and density. The fluid

is also in a region where it has reached its maximum solvent capacity. Due to the low viscosity and surface tension, the supercritical fluid can easily penetrate a solid or liquid matrix from which a solute must be extracted (Mukhopadhyay, 2000:3-4). The density of a supercritical fluid depends on the temperature and pressure and exert liquid and gas-like values. Thus, improving the capability of the fluid to extract or concentrate the solute. It dissolves a solute like a liquid and passes through solid or liquid matrices like a gas (Seader *et al*., 2011:447-449).

The use of $scCO_2$ as a solvent for SFE finds use in processes such as dealcoholisation of alcoholic beverages through the extraction of aromatic compounds from commercially produced brandy using counter current (CC) SFE with $scCO_2$. It results in a higher quality extract using CC-SFE, with an ethanol concentration ranging from 40% to 80% and aroma content close to the original brandy (Señoráns *et al.*, 2001).

Wong *et al.* (2001) investigated the removal of eight target monoterpenes from the Australian tea tree (Melaleuca alternifolia) rehydrated and dried leaves. The extraction occurred at 40, 80 and 110^{o}C; and $scCO_2$ densities of 0.25, 0.4 and 0.6 g/mL. The authors concluded that the optimum conditions resulted in almost complete extraction and recovery of targeted analytes (approximately 95%). The optimum conditions were at 110^{o}C and 0.25 g/mL with complete extraction achieved from the rehydrated whole dried leaves. Results obtained from the whole dried varied insignificantly with the rehydrated whole leave.

Reverchon and De Marco (2006) presented the application of supercritical fluid extraction and the extractions that other authors have studied. The main fields of application are the extraction of essential and seed oils from solid and fluid matrixes, for example, seeds, leaves, fruit and flowers (Reverchon and De Marco, 2006; Catharino *et al.*, 2007; Gañán and Brignole, 2011; Koshima *et al.*, 2015). Most of these processes show technical feasibility, thus making supercritical fluids an applicable separation process in the industry.

2.4.1.2. Properties of supercritical CO_2

CO_2 is considered "generally regarded as safe (GRAS)" solvent for use during the processing of food products, as it is benign. In addition, it exists as a vapour at ambient conditions that results in easy separation from product. With a critical temperature of 304 K (close to ambient) and pressure of 74 bar, it suits the extraction of thermally labile compounds (such as volatiles). Furthermore, it is inert, non-flammable, non-corrosive, inexpensive, non-toxic, and readily available; thus, considered safe for food and pharmaceutical products. In addition, $scCO_2$ has a high critical density that increases solubility as that of a liquid. It has low vapour-like critical viscosities and high molecular diffusivity that results in improved infusion in solid and liquid matrices (Mukhopadhyay, 2000:3-5; Brunner, 2010; Seader *et al*., 2011:449; Peach & Eastoe, 2014).

2.4.1.3. Solubility

The phase behaviour of components in a system governs the separation of volatile organic components from water by selective dissolution in sCO_2. Thus, variations in temperature and pressure determines the solubility at a given point in the process. Ideally, perfect separation is possible if the behaviour of the system was such that the organic components are infinitely soluble in the solvent, $scCO_2$, and the water had zero solubility in the same solvent. Further, the separation would have been easiest had it been that the mass transfer rate of the organic components from the aqueous to the CO_2 phase was so fast as to be irrelevant as a limiting factor. But since both aroma compounds and water have limited solubility in CO_2, the separation is governed by superior solubility of one over the other in CO_2. In this case, one hopes that the organic compounds are significantly more soluble in CO_2 than water and that the mass transfer rate from the aqueous solution to the gas phase is fast enough to be practically feasible in a counter-current column of a reasonable number of stages, i.e. column height (Mukhopadhyay, 2000:17-24). Figure 2-4 illustrates the effect of temperature and pressure on the density of supercritical CO_2.

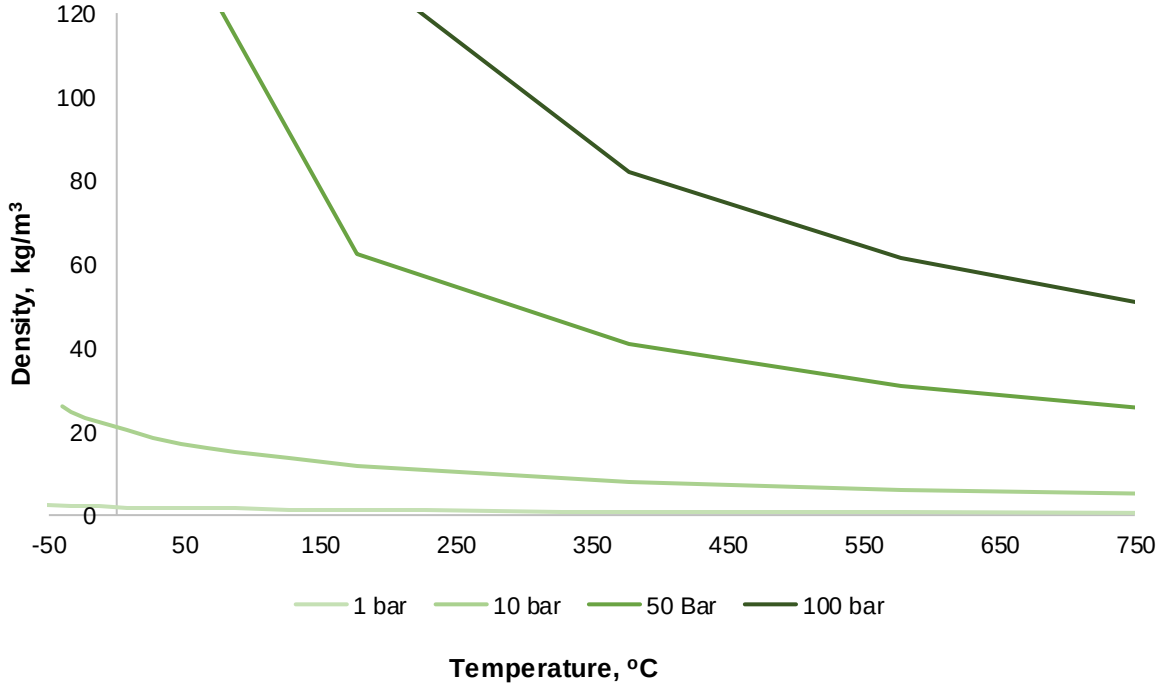

Figure 2-4: Density of CO2 at various temperatures and pressures (Redrawn from Engineeringtoolbox.com (2019))

Figure 2-4 shows that with an increase in temperature, density decreases and with an increase in pressure, density increases. The density increases significantly with increasing pressure, resulting in increased solubility. Density increases faster in the higher-pressure range and settles as the pressure approaches the critical pressure. In addition, the density is maximum at lower operating temperatures. Thus, optimum extraction favours low temperatures and high

pressure due to the higher density at these conditions, consequently increasing the solvent power.

2.4.2. Supercritical fluid fractionation (SFF): Theory and Application

In 1879 Hannay and Hogarth investigated the dissolution of solid matrices with a dense gas at supercritical conditions above the critical temperature and pressure. Through the measurement of pressure, the solid was easily dissolved into the gas and precipitates as 'snow' or 'frost' by reducing pressure. Ethanol used in the process recovered quickly from the potassic iodide by reducing pressure (Hannay & Hogarth, 1879). This process was later called supercritical fluid extraction, supercritical-gas-extraction and most commonly supercritical extraction. By the 1970's William proposed applications of SFE was patented and available in literature (Schultz, 1969). Several researchers followed by doing research on SFE and its application to different processes.

During SFE, a solute is extracted from a liquid or solid mixture using a supercritical solvent. The type of solvent involved in this process is discussed in section 2.5.2. Nonetheless, the process does not rely only on the characteristics of the solvent but also the transport properties of CO_2 and mass transfer between the solvent and the feed.

2.4.2.1. Chemical basis for separation

As previously discussed, CO_2 is the most common fluid used in SFE. However, it is the relevant chemical principles at high pressure that is important for the application of SFE. This chemical basis consists of thermodynamic properties, dielectric properties and transport properties of CO_2 (Schneider *et al.*, 2000:31).

2.4.2.1.1. Thermodynamic properties

The supercritical state of a fluid is thermodynamically in a region above the critical temperature and pressure of the fluid. CO_2 is a nonpolar molecule because it has no net dipole moment, therefore, dissolving nonpolar molecules. The phrase that commonly refers to this is "like dissolves like". However, the quadruple moment allows CO_2 to dissolve slightly polar and polar compounds at high pressures (Mukhopadhyay, 2000:13).

For supercritical fluids, the solvent capacity is density-dependent. Density relies on temperature and pressure, which makes it easy to adjust the solvent capacity. Density can be related to the solvent capacity in terms of isothermal compressibility, defined as (Mukhopadhyay, 2000:14):

$$K_T = -\frac{1}{\rho}\left(\frac{\partial \rho}{\partial P}\right)_T \quad (1)$$

Where ρ is molar density.

Supercritical fluids exert high gas-like compressibility, consequently affecting the solvent capacity. As the system approaches the high-pressure region, the compressibility decreases, resulting in an increased solvent capacity (Schneider *et al*., 2000:32-33).

2.4.2.1.2. Dielectric properties

In general, the CO_2 molecule has a low (non-permanent) dielectric dipole moment due to the intermolecular interactions governed mainly by the Van-der-Waals forces. Thus, CO_2 is a weak solvent due to its ability to extract compounds with a low molar mass and polarity. However, the solvent power of CO_2 is not only governed by the dielectric properties but factors such as temperature, pressure and density (Schneider *et al*., 2000:33-34).

2.4.2.2. Mass transfer

Mass transfer is the transport of components in a mixture from one point to another. In separation processes, it is the transfer between two different interfaces. Fick's first law states that the mass flux is directly proportional to the concentration gradient at steady state, mathematically expressed as in equation (2) (Seader *et al.*, 2011:85-130):

$$J = -D\frac{dc}{dx} \quad (2)$$

Where J is the mass flux, D the diffusion coefficient and $\frac{dc}{dx}$ the concentration gradient. In this case, the concentration gradient is the driving force.

The mass transfer depends on the phase or state of the compounds. For instance, pressure has a significant impact on the mass transfer for gas extraction. Other processes depend on the mass transfer coefficient. With an increasing temperature, the diffusion increases because there is an increase in the motion of the atoms thus increasing intermolecular interactions (Brunner, 2013).

According to Fick's Law, a compound would diffuse from a high to low region across a concentration gradient. For molecular mass transfer in a binary mixture, equation (2) can be written in terms of the molar flux of species A, $N_{A,z}$,relative to length, z:

$$N_{A,z} = -cD_{AB}\frac{dy_A}{dz} + y_A(N_{A,z} + N_{B,z}) \quad (3)$$

For a binary mixture, $D_{AB} = D_{BA}$. $N_{B,z}$ describes the molar flux and c total molar concentration.

For SFF processes, the mass transfer occurs between the CO_2 phase and organic phase. At the same time, the water-rich phase interacts with organics as well. Therefore, mass transfer between organics and CO_2 phases should be favoured to decrease organics enriched in the water-rich phase.

2.4.2.3. Advantages and Disadvantages

Below a list of advantages and disadvantages to SFE are provided:

Advantages

The advantages of SFF is as follow (Reverchon, 1997; Schneider *et al*., 2000; Pourmortazavi & Hajimirsadeghi, 2007; Peach & Eastoe, 2014; Bejarano *et al*., 2016; Manjare & Dhingra, 2019):

- The solvent is easily recovered and recycled. It is also easily removed from the final product.
- The easily adjusted solvent power improves yield and selectivity by changing density (temperature and pressure).
- CO_2 is a cheap, non-toxic, non-flammable and inert solvent.
- It is suitable for thermally labile compounds since CO_2 has a low critical temperature of 31°C.
- The solvent power/capacity is easily adjusted by altering density to control the selectivity and yield of the process.
- Improved mass transfer when compared to liquids because of easier penetration through packing material.

Disadvantages and Limitations

The disadvantages of SFF is as follows (Reverchon, 1997; Schneider *et al*., 2000; Pourmortazavi & Hajimirsadeghi, 2007; Peach & Eastoe, 2014; Bejarano *et al*., 2016; Manjare & Dhingra, 2019):

- High-priced equipment because of high operating pressure
- Expensive purchasing costs
- Complicated phase behaviour signifies that conventional mathematical expressions might not be capable of assisting with VLE calculations.

2.4.3. Studies on supercritical fluid fractionation (SFF)

Over the past century, there have been significant improvements in the application of SFF with a countercurrent liquid feed. Research fields range from the removal of terpenes from essential oils to alcohol from alcoholic beverages. (Reverchon, 1997; Simándi *et al*., 1999; Rodrigues *et al*., 2003; Reverchon & De Marco, 2006; Pourmortazavi & Hajimirsadeghi, 2007; Brunner, 2010; Fornari *et al*., 2012; Knez *et al.*, 2014).

Over 25 volatile compounds were recovered from sugar cane spirits through a CC fractionation column using $scCO_2$ as a solvent. Gracia *et al*. (2007) shows that this extraction process is technically viable as a by-pass during the production of rum for the recovery of valuable aroma compounds. The volatile compounds were extracted at very low operating conditions of 40°C to 50°C (Gracia *et al*., 2007).

Similarly, low conditions were preferable for the optimum extraction yield in isolating citrus essential oil from seed oils at 40°C and 100 bar (Mouahid *et al*., 2017). Near 100% recovery of essential oil was achieved at 30°C. Therefore, this process presents high feasibility at much lower energy requirements to recover valuable volatile compounds in essential oils (Mouahid *et al*., 2017). Low solvent-to-feed (S/F) ratios are required to isolate valuable brandy aroma from alcoholic beverages as presented by Señoŕns *et al*. (2001). In addition, a low operating temperature of 40°C was selected (Señoŕns *et al*., 2001).

It is thus obvious that low operating temperatures are preferred for the recovery of volatile compounds.

2.4.3.1. SFF of apple aroma

Schultz (1969) presented the first process for extracting flavours from materials containing flavours, such as fruit juices and apple essence using liquid CO_2. The extraction method was investigated for Red Delicious apple essence with a 150-fold continuously counter-currently fed at 63 bar and 25°C. The residue obtained after extraction contained a high concentration of flavour compounds free from water, alcohols, sugars, fruit acids and non-flavour compounds, resulting in a product that includes the natural aroma of apple. A starting material containing a high-water concentration will result in an extract containing flavour compounds combined with water (which is typically not more significant than the flavour compounds); however, the oily phase flavour compounds are easily separable from water. The author suggests that temperatures above the critical temperature of CO_2 will improve the solubility of flavour compounds. It does not affect the thermal labile compounds (Schultz, 1969).

Bejarano & del Valle (2017) performed the counter-current fractionation of the key apple aroma components from a model apple aroma solution using supercritical CO_2. The model solution

comprised of hexanal, (E)-2-hexenal, hexanol and water. Figure 2-5 illustrates the results obtained from the experimental work performed by the authors:

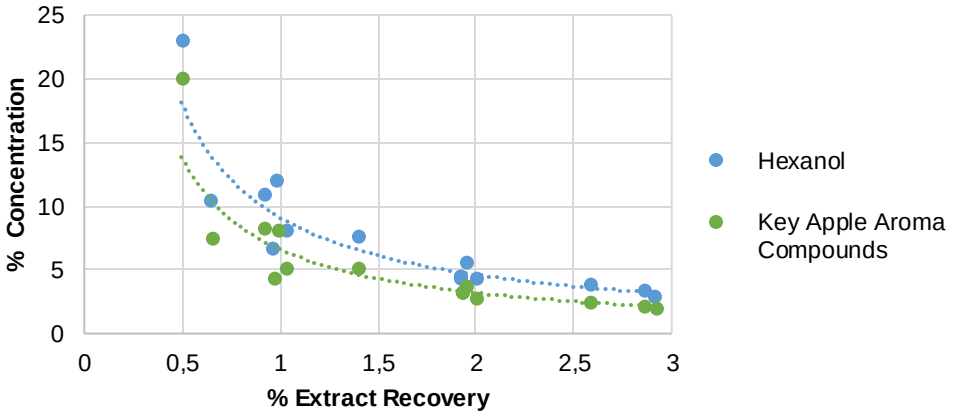

Figure 2-5: Concentration and recovery obtained from Bejarano & Del Valle (2017) for ● hexanol and ● hexanal + (E)-2-hexenal (Redrawn from Bejarano & Del Valle (2017))

Figure 2-5 shows the effect of extract recovery on the concentration of the specific compounds obtained from Bejarano & Del Valle (2017). An increase in the extract recovery results in a decrease in the concentration of the hexanol and the key apple aroma constituents (i.e., hexanal and (E)-2-hexenal). This means that for the conditions investigated, the hexanol and key valuable compounds were not separable. Also, hexanol will always have a higher concentration than the key compounds. It is thus evident that the selected operating conditions were suitable for concentrating the key compounds but not suited for separating the key compounds from the hexanol. Therefore, a high extraction yield is obtained but at the risk of low selectivities. The authors also found the maximum extraction yield at 40°C, 14 MPa and a solvent-to-feed ratio of 5. The highest concentration of the desirable compounds achieved in the extract was 20% w/w with a maximum extraction yield of 95,5%, which means that 95,5% of the desirable compounds in the feed were recovered as extract (Bejarano & Del Valle, 2017).

This paper shows that SFF of key apple aroma constituents will achieve almost perfect organic recoveries with almost no traces presented in the water-rich phase. Phase behaviour indicates that organics separation occurs as a single stage because of polarity differences in feed. Therefore, organics are easily recovered in the vapour phase. Thus, indicating the likelihood of feasibility in terms of its separation.

2.5. Comparison of advantages and disadvantages for the traditional and suggested extraction method

Table 2-5 provides a summary of the mentioned advantages and disadvantages between the conventional evaporation) and suggested (SFF) extraction methods as previously discussed:

Table 2-5 Advantages and disadvantages of the traditional and suggested method

Advantages	Disadvantages
Conventional Method: Evaporation	
• Suitable for small- and large-scale productions • Easily maintained and low construction cost • Simple operation	• High energy-intensive process • Boiling of water not environmentally friendly • High operating temperatures not suitable for thermally labile compounds
Suggested Method: SFF	
• Solvent easily recovered • Solvent power-adjustable improving yield and selectivity • Solvent cheap, non-toxic, non-flammable and inert • Suitable for thermally labile compounds • Improved transport properties	• High operating pressure = High operating costs • High purchasing costs • Unpredictable phase behaviour for complicated mixtures. • Limited processing capacity

2.6. Phase equilibria: Review

In most industrial processes, such as distillation, adsorption, and solvent extraction, two phases are in contact, and mass transfer occurs between these two phases, i.e., the vapour and liquid. The rate and amount of mass transferred depend on the distance between the compounds and whether the system is at equilibrium or not (Varasteh, 2012). Vapour liquid equilibrium data, generally presented in a graphical form, include the representation of vapour and liquid phase concentrations obtained at various process parameters (i.e., temperature and pressure). Evaluating the vapour-liquid equilibrium data enables the comparison of a range of process parameters optimum to enrich the vapour and liquid fractions (McCabe *et al.*, 1993). Data obtained from previous authors for pure component and binary systems, and in some instances ternary systems, are readily available in literature (Elizalde-Solis *et al*., 2003; Secuianu *et al*., 2010; Bejarano *et al*., 2011; Zamudio *et al.*, 2011; Varasteh, 2012; Bejarano *et al.*, 2015; Madzimbamuto *et al*., 2016; Fourie *et al*., 2019). However, the phase equilibrium data is not available for all systems, especially those containing multicomponent mixtures. In this case, a compound of similar binary phase behaviour can assist with the analysis of the behaviour of the unknown compound present in the multicomponent mixture. In certain instances, the phase equilibrium data for a binary system can be used to investigate the

parameters required for fractionation of a multicomponent mixture (Reverchon *et al*., 1995; Núñez *et al*., 2011; Del Valle, 2015; Garcez *et al*., 2017; Lee *et al*., 2018).

With over 300 volatile compounds present in apple aroma, evaluating the multicomponent phase behaviour for each binary system with CO_2 of this system would be time-consuming. Therefore, the multicomponent phase behaviour comprised of volatile apple aroma compounds present in South African produced apple aroma concentrate based on their:

- Contribution to the overall aroma.
- Characteristic apple odour/description.
- Concentration; and
- Presence in different apple variants

The process presented uses CO_2 as the solvent as described in 2.4. The volatile compounds selected comprised of selected compounds identified as adding value to the characteristic apple aroma (desired) and those that don't have any direct resemblance to apple aroma (undesired) and based on their overall concentration and contribution to the odour/scent as described in 2.2.3.

2.6.1. Binary VLE data

Figure 2-6, Figure 2-7 and Figure 2-8 shows the VLE data for the binary system of hexanal and CO_2 (López-Porfiri *et al*., 2017), *trans*-2-hexenal (Villablanca-Ahues *et al.*, 2021) and CO_2, and hexanol and CO_2 (Elizalde-Solis *et al*., 2003; Secuianu *et al*., 2010).

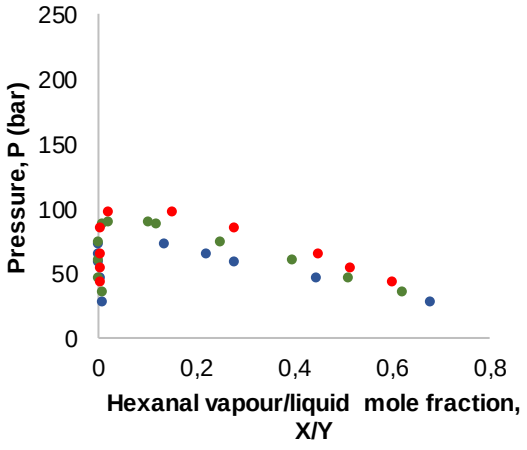

Figure 2-6: Isothermal binary vapour-liquid equilibrium data for hexanal/CO_2 at ● 313,2K; ● 323,2 K; ● 333,2 K (Redrawn from López-Porfiri *et al.* (2017))

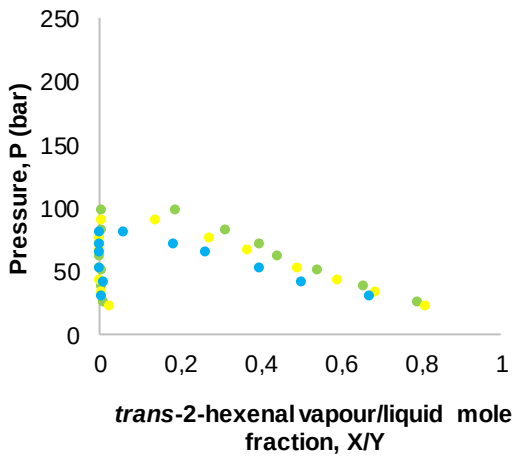

Figure 2-7: Isothermal binary vapour-liquid equilibrium data for *trans*-2-hexenal/CO_2 at ● 313,2K; ● 323,2 K; ● 333,2 K (Redrawn from Villablanca-Ahues *et al.* (2021))

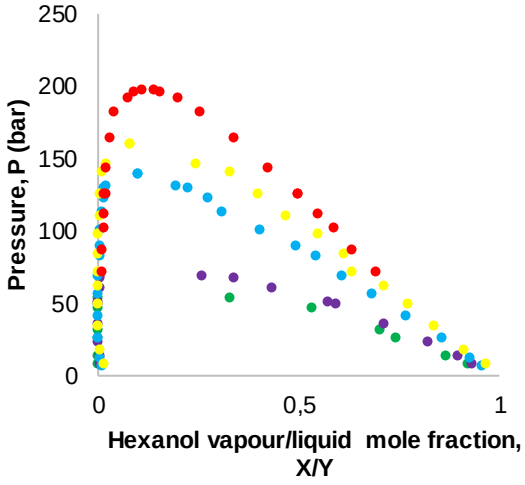

Figure 2-8: Isothermal binary vapour-liquid equilibrium data for hexanal/CO_2 at ● 293,15 K; ● 303,15 K; ● 333,15 K; ● 353,15 K; ●397,78 K (Redrawn from Elizalde-Solis *et al.* (2003) and Secuianu *et al*. (2010))

For Figure 2-6, Figure 2-7, and Figure 2-8, the left-hand side of each graph represents the fraction obtained in the vapour phase, and on the right-hand side, the fraction obtained in the liquid phase. The figures provided presents the binary vapour and liquid equilibrium mole fraction for the volatile compounds present in apple aroma and CO_2 at a given pressure and isothermal conditions. The volatile compounds in each binary system represented those compounds described to have a significant contribution and concentration present in apple aroma described as desired and undesired in section 2.2.3.

Figure 2-6 shows that increasing pressure at a lower constant temperature will decrease the hexanal vapour fraction. In contrast, increasing temperature will result in liquid rich in CO_2, with similar trends presented in Figure 2-7 and Figure 2-8 followed for the binary systems; *trans*-2-hexenal and hexanol. However, a significantly small change in the fraction of vapour enriched at changes in pressure and temperature for all binary systems. Further, increasing the temperature to above 353,2 K results in an increased hexanol vapour fraction and increases significantly as the CO_2 enriches in the vapour phases, as shown in Figure 2-8. An illustration of the separability of the said desired and undesired volatile apple aroma compounds presented in shows the binary vapour-liquid phase equilibrium data for the systems combined at 333 K as represented in Figure 2-9:

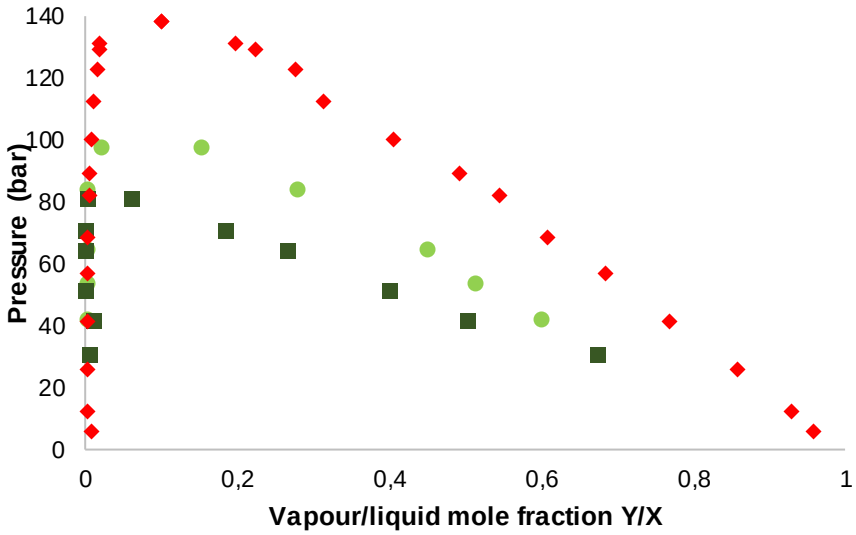

Figure 2-9: Vapour-liquid equilibrium for binary systems ■ *trans*-2-hexenal/CO_2; ● hexanal/CO_2; and ♦ hexanol/CO_2 at 333 K

It is evident in Figure 2-9 that the desirable/valuable hexanal and *trans*-2-hexenal can be enriched in the vapour phase but hexanol will comprise a higher fraction. At the same operating conditions, these compounds follow similar trends thus indicating that these compounds are not separable in the vapour phase but will always coexist. However, further optimisation and fine-tuning conditions such as temperature and pressure can minimise the amount of hexanol enriched in the vapour phase.

At pressures above 100 bar, change in the slope in the vapour phase fraction hexanol can be noted, indicating that the above this pressure at the given temperature the rate at which the hexanol enriched in the vapour. The amount of the desired hexanal and *trans*-2-hexenal enriched in the vapour phase could be maximised at an operating pressure below 100 bar. At the given conditions, the fraction of hexanol enriched in the liquid phase increases with a decrease in pressure, indicating that the liquid enriched can be maximised as well.

The data presented above indicate that desired volatile apple aroma compounds and the undesired hexanol are not entirely separable. However, it is possible to enrich the vapour with a higher fraction of the said desired volatile compounds and the liquid with a higher fraction of the said undesired volatile compounds and water.

2.7. Mathematical models to describe phase behaviour of supercritical systems

Mathematical models can predict the phase behaviour of multicomponent mixtures by correlating a suitable mathematical expression with vapour-liquid equilibrium data of binary systems. The expressions are usually represented in a computational form and are selected based on the dynamics of the process.

2.7.1. Dynamic models used to predict phase equilibria

Thermodynamic modelling combines an appropriate mathematical model to experimental vapour-liquid equilibrium data to correctly describe the behaviour of binary systems. This allows the use of mathematical equations instead of experimental data, such as to test the possibility of post-reactional fractionation (Reverchon & De Marco, 2006). Based on experimental data, the simulator uses this model to predict the vapour-liquid equilibrium data and other physical properties such as density, viscosity, specific volume, etc.

There are various types of equations of state (EoS); the most widely used are Peng-Robinson (PR), Redlich and Kwong (RK) and Soave (SRK) equations of state. The Peng-Robinson equations usually provide similar results to the Soave-Redlich-Kwong (SRK) equation. However, it is better in predicting the density of many components in the liquid phase, especially those that are nonpolar (Peng & Robinson, 1976). The typical activity coefficient model includes the Non-Random Two Liquids (NRTL) model. This model applies to mixtures containing polar compounds (for example, water). The other types of models that are also known are Wilson, UNIFAC, UNIQUAC and Van Laar. These models make use of the activity coefficient of compounds to predict the properties of liquids.

Literature shows that EoS have been most successfully used to model the phase behaviour of SFF systems (Coelho *et al*., 2016). Most used are the Redlich-Kwong and Peng-Robinson family of correlations, with their corresponding mixing rules. Of these, one of the most successfully used EoS is the Redlich-Kwong –Aspen EoS. However, the unique property method describes the organic components in an aqueous solution. Thus, excluding water phase interactions. The use of a simplified EoS, in the same manner, may be inappropriate, as the effect of the highly polar water molecule is likely to have a significant impact on the prediction of the system's phase behaviour (Yazdizadeh *et al*., 2011; López-Porfiri *et al.*, 2017; Jafarian Asl & Niazmand, 2020).

Novella *et al*., (2020) combined the Soave-Redlich Kwong (SRK) thermodynamic model modified by Boston Mathias with the Peng-Robinson-Redlich-Kwong (PRSK) mixing rules and UNIQUAC activity coefficient model (known as the $\varphi - \varphi$ approach: EoS thermodynamic model combined with an activity coefficient model) to describe the thermodynamics for the

fractionation of acetic acid in a counter-current column using supercritical CO_2. A thermodynamic model combined with the activity coefficient model selected governs the polar nature of carboxylic acids and water with high pressure. The mixing rule incorporates excess Gibbs free energy, G^E, and four binary interaction coefficients regressed with experimental data for each binary sub-system predicted the multicomponent phase behaviour. The theoretical stage approach seems inadequate because the simulation overestimated the actual separation performance and the number of stages determined required less than one stage, explained by the low mass transfer rate. Simulation data shows that high solvent-to-feed ratios govern the mass transfer efficiency, i.e., theoretical stages. Simulation data and experimental data could vary due to liquid distribution in the column, ultimately affecting the liquid-fluid exchange area, which explains the poor mass transfer efficiency obtained from experimental data. However, the simulation is still suitable for theoretically predicting the system performances and optimising the system for optimum extraction and the theoretical stages required to obtain the objective (Novella *et al*., 2020).

A dynamic model developed by Fernandes *et al*., (2007) for the fractionation of a binary mixture containing squalene and methyl oleate by supercritical CO_2 showed a good correlation within a reasonable degree of accuracy compared to experimental data and its ability to predict outlet stream composition profiles. The model is developed based on partial differential equations corresponding to the material balance on the column in combination with algebraic equations used to describe mass transfer, biphasic flow hydrodynamics in packing and VLE of the system. Results obtained from the model shows a good representation of supercritical systems and find use in optimising process parameters and control purposes (Fernandes *et al*., 2007)

Using EoS and conventional mixing rules in combination with group contribution G^E models could improve predictability and correlative ability (Boukouvalas *et al*., 1994; Spiliotis *et al.*, 1994).

Two recently proposed models (EoS/G^E), Linear Combination of Vidal and Michelsen (LCVM) and modified Huron-Vidal (MHV2) mixing rules, were compared by Spiliotiis *et al.*, (1994) based on the predictability of the solubility of aromatic hydrocarbons in supercritical CO_2. The LCVM model (Boukouvalas *et al.*, 1994), which is a linear combination of the Vidal and Michelsen mixing rules coupled with UNIFAC and *t*-mPR EoS, results show a better prediction at bubble point pressure than the MHV2 model (Michelsen, 1990; Dahl and Michelsen, 1990; Dahl *et al.*, 1991). The model couples the SRK EoS with modified UNIFAC with the Huron-Vidal mixing rule. However, it does have difficulty in predicting the solubilities VLE for heavy compounds and solids. The MHV2 model gave significant errors in phase equilibrium predictions as the asymmetry increased in size. For most compounds, the two models presented similar results (Dahl and Michelsen, 1990; ; Michelsen, 1990; Dahl *et al.*, 1991; Spiliotis *et al*., 1994)

In the work of Effendi *et al.*, (2013), two semi-empirical density-based models, Chrastil and Del Valle-Aguilera, were used to evaluate experimental solubility data and Peng–Robinson EoS (PR-EoS) with quadratic and Stryjek–Vera mixing rules described phase behaviour of the system. The Chrastil and Del Valle-Aguilera models correlated with experimental solubilities at various temperature and pressures with satisfactory results. The PR-EoS with quadratic and Stryjek-Vera mixing rules interprets phase equilibria well but adjusted binary interaction parameter hardly affected the data. However, the total reaction heat results showed consistent conventional density-based correlations because it reflects stronger interaction forces (Effendi *et al.*, 2013).

Correlation G^E models, such as the UNIFAC class, allow EoS models to become a strictly predictive tool. The UNIFAC/G^E model accounts for low pressure group parameters. However, the EoS/G^E models have difficulty in predicting the phase behaviour of specific compounds. Therefore, the development of EoS/G^E models requires an EoS based expression for the G^E model.

2.7.2. Mathematical models for CO_2-water-hydrocarbon systems

Flexible and predictive EOS models apply to a system with polar components and an activity coefficient model for mixtures containing polar and nonpolar mixtures and low pressures. For this study, the Soave-Redlich-Kwong EOS model was investigated in combination with the Kabadi-Danner (SRK-KD) mixing rules, an improved equilibrium calculation for a mixture containing hydrocarbons and water for phase equilibrium calculations.

The thermodynamic model is a modification of Soave-Redlich-Kwong EOS designed explicitly for a hydrocarbon and water system. The model on its own has been unsuccessful in predicting the phase equilibria for the water-rich liquid phase due to the immiscibility of the hydrocarbon system. The modified SRK EOS is mathematically expressed as (Soave, 1972):

$$P = \frac{RT}{V_m - b} - \frac{a}{V_m(V_m + b)} \tag{4}$$

Where,

$$a = a_0 + a_{KD} \tag{5}$$

And a_0 is described as the standard quadratic mixing term:

$$a_0 = \sum_{i=1}^{n} \sum_{j=1}^{n} x_i\, x_j \sqrt{a_i\, a_j}\,(1 - k_{ij}) \tag{6}$$

Where;

$$k_{ij} = k_{ij}^{(1)} + k_{ij}^{(2)}T + \frac{k_{ij}^{(3)}}{T}$$
$$k_{ij} = k_{ji} \quad (7)$$

a_{KD} is the Kabadi-Danner mixing rule term for water and is determined from (Kabadi & Danner, 1985):

$$a_{KD} = \sum_{i=1}^{n} a''_{wi} x_w^2 x_i \quad (8)$$

Where;

$$a''_{wi} = G_i \left[1 - \left(\frac{T}{T_{cw}}\right)^{c_1}\right] \quad (9)$$

And the term G_i is described as the sum of the group contributions that make up the hydrocarbon molecule and the best fit value obtained for $c_1 = 0.80$, mathematically expressed as:

$$G_i = \sum_l g_l \quad (10)$$

Where g_l is described as the group contribution parameter for the group, including hydrocarbons. Typical values for k_{wj} are represented in Table 2-6.

Table 2-6: Best fit values of k_{wj} for hydrocarbon interactions

Hydrocarbon group	k_{wj}
Alkanes	0.500
Alkenes	0.393
Dialkenes	0.311
Acetylenes	0.348
Napthenes	0.445
Cycloalkenes	0.355
Aromatics	0.315

Considering that the feed presented comprises mainly water, interactions within the organic-rich phase might not be easily predicted by the general EoS or activity coefficient models. The Kabadi-Danner mixing term, therefore, accounts for the hydrophobic interaction of

hydrocarbon molecules and water. This is a result of most organics presenting immiscibility in the water-rich phase (Kabadi & Danner, 1985).

2.8. Economic evaluation: Supercritical fluid extraction (SFE)

Supercritical fluid technology has shown diverse applications in processing industries based on research. However, due to the misconception that the technology is not fully competitive and extortionate compared to conventional or common methods, certain countries have been hesitant to apply this technology in industries (Del Valle, 2015).

Studies show that mathematical models can be used to predict the technical feasibility of SFE processes. However, the interest is in the economic viability of such operations. Applying this technology on a commercial scale shows feasibility in the separation by upscale methods and the economic viability demonstrated as the cost of manufacturing suggested by Turton et al., (1998).

An investigation by Rosa & Meireles (2005) establishes the feasibility in terms of manufacturing cost (shown in the expression below (Turton *et al*., 1998) of the supercritical extracts of clove buds oil (*Eugenia caryophyllus*) and ginger oleoresin (*Zingiber officinale Roscoe*) from experimental data.:

$$COM = 0.304FCI_L + 2.73C_{OL} + 1.23(C_{UT} + C_{WT} + C_{RM}) \quad (11)$$

Where COM is the cost of manufacturing, FCI_L is the fixed capital investment; C_{OL} is the cost of operating labour, C_{UT} is the cost of utilities, C_{WT} is the cost of waste treatment, and C_{RM} is the cost of raw materials (Turton *et al*., 1998).

70 minutes total extraction for the extraction of clove buds determined the manufacturing costs at a clove and ginger extraction rate of 90 and 345 kg/h, respectively. With the total operating hours of 7920 hours per year (Rosa & Meireles, 2005). In addition, clove extractions required a higher CO_2 flow rate than that of the ginger. The study shows that the production of clove oil using SFE is noticeably more economically feasible when compared to ginger oleoresin. Of the total manufacturing cost, the raw material cost comprised 55.67% for clove oil. In ginger oleoresin, the fixed capital investment was 60.59% of the total manufacturing costs and approximately the selling price. The data clearly indicates that SFE does not present feasibility in extracting clove bud oil and ginger oleoresin. Various factors influence the feasibility of a process, and in this case, optimising process parameters longer extraction time results in higher manufacturing costs (Rosa & Meireles, 2005).

In the investigation by Rocha-Uribe *et al*., (2014) the same method as used by Rosa & Meireles (2005) for determining the manufacturing costs demonstrated feasibility in the extraction of

habanero chilli oleoresin and clove bud oil based on experimental data. The Chemical Engineering Plant Cost Index (CEPCI) provided in equation (12) includes the inflation on manufacturing cost as part of the total manufacturing cost (Turton *et al*., 1998):

$$C_2 = C_1 \times \left(\frac{I_2}{I_1}\right) \times \left(\frac{V_2}{V_1}\right) \quad (12)$$

Where C represents the cost, I the index and V the capacity (m^3).

A process simulator validated with experimental data based on SFE extraction of habanero oil evaluated the process's energy requirements obtained at a solvent flow rate, 90.2kg/h of CO_2 to enable the feasibility study. Upscale pilot plant data were used to investigate the economic feasibility for industrial applications. Increasing run time resulted in decreased manufacturing costs. Both habanero chilli and clove extractions presented high manufacturing costs due to raw material costs (approximately 75 – 81 %). Habanero chilli oleoresin SFE extracts fetched a higher market value, thus deemed economically more feasible than clove oil extracts. However, SFE presented positive economic development for both processes in terms of their feasibility. Despite the significantly high manufacturing costs, CO_2 extract fetches a considerably higher value on the market, thus, presenting feasibility (Rocha-Uribe *et al*., 2014).

SFE of peach almond, spearmint leaves and marigold flowers extractions present similar feasibility results. Data obtained from experimental VLE enabled the evaluation of process parameters deemed feasible due to the cost-intensive process. Peach almond and spearmint oils showed that the consumer-ready products for the cosmetics and food industries are attainable from SFE. The SFE of marigold flowers does not measure up to commercial oils shown to be not competitive compared to the commercially produced marigold oleoresin in terms of product quality; however, high raw material cost explains the high manufacturing costs. Once again, the manufacturing cost acquired is not at optimum process parameters, thus influencing the end-result and economic viability for industrial application *(Mezzomo et al.*, 2011). It is, therefore, crucial to compare a process at optimum conditions to fully comprehend the economic viability for industrial applications,

2.9. Conclusion

A thorough assessment of literature revealed that:

1) Apple aroma is currently produced as a byproduct during the production of fruit sugars with triple effect evaporation. The process yields a highly diluted product therefore it requires further processing.
2) Apple juice consists of various volatile compounds, all of which, to a greater or lesser extent, dissolve in supercritical CO_2. The volatile compounds comprise those that add value to the aroma and other organic compounds that have undesired characteristics. *Trans*-2-hexenal shows importance in the characteristic apple aroma. In addition, carbon-6 aldehydes and esters are described to have an apple-like odour. Hexanal and ethyl-2-methyl butyrate are present in significant concentrations in most apple varieties. The alcohols such as hexanol identified have no direct resemblance to apple aroma, thus not adding value to the product.
3) Literature indicates the likelihood of feasibility in the separation of organics, hexanal, *trans*-2-hexenal, and hexanol, and water. The economic analysis of such processes has not been published.
4) Various methods could be used to concentrate apple aroma from apple juice. Thermal labile compounds rule out the use of evaporation and distillation. Solvent extraction poses difficulty in the separation of solvent from the product obtained. On the other hand, supercritical fluid fractionation using CO_2 requires a lower operating temperature and solvent is easily separable from the product.
5) High recovery of total organics obtained through CC-SFF indicates that supercritical CO_2 is a viable solvent, and the product has added value. On the other hand, vapour rich in both desired and undesirable compounds indicate CO_2 might not achieve the partition for these fractions. The process also requires further investigation to reduce water enriched in the vapour phase

The economic viability for the process indicates positive prospects; however, SFE lacks industrial applications due to the misconception that it is more expensive and operational costs are too high compared to other traditional methods. Be that as it may, process presents a significant increase in the product quality and lowered energy consumption. Therefore, feasibility is shown in the product quality and energy consumption when compared to conventional methods.

2.10. Chapter Outcomes

Phase equilibria reviewed in this chapter fulfil the requirements for the first objective in Chapter One. For selected compounds based on the overall contribution to the apple aroma profile show optimum at pressures below 100 bar and low operating temperatures. Mathematical models described show that a modification to the equation of state thermodynamic models is suitable for the extraction of aroma compounds. The mathematical model described correlated with vapour-liquid equilibrium data obtained from literature provides a base for the development of process models using a process simulator. Therefore, fulfilling the requirements for objective one. Thermodynamic models are used by various authors for investigating a limited range of process conditions for multi-component mixtures. The accuracy of these models is improved through correlation with experimental data through computerisation. Thus, formed part of the second objective. Previous research suggests that separation occurs as a single stage for the fractionation of apple aroma. Compounds that add value to apple aroma and those that are undesired will always coexist in the vapour phase therefore product quality is increased by decreased water concentration. This forms part of the considerations made for the process layout consideration thus fulfilling part of the requirements for objective three.

.

CHAPTER THREE

Materials, Methods, and Methodology

3. MATERIALS, METHODS, AND METHODOLOGY

This chapter outlines the materials and methods employed during the experimental work to attain the objectives (1-3) set in Chapter 1. The first objective required the development of a process model. Principally, data by Bejarano & Del Valle (2017) and pilot plant experiments validated the model to investigate the multi-component mixture for the second objective. The model was used to investigate the ideal process layout of a process to concentrate apple aroma. Further, an order of magnitude and simulation energy data based on the best-suited process layout were used to investigate the economic viability to fulfil the requirements for objective three.

3.1. Introduction

Process simulation tools assist with the investigation of a range of process conditions that are not obtainable from experiments or deemed time-consuming. The model's predictability was improved by correlating thermodynamic models with literature obtained phase behaviour data. Further data obtained from such models are generally validated with experimental and literature data to establish the error margin and accuracy of the model. In this investigation, pilot plant experiments performed were used to validate mass balance data for the process model developed.

The process model was investigated for the multicomponent phase behaviour to obtain optimum conditions suitable for the fractionation of apple aroma. Further, the model developed was validated with pilot plant data and results obtained from Bejarano & del Valle, (2017). The model was further developed into process layout scenarios to present the best-suited layout based on product quality, yield, and organics recovery. The economic viability of the process was established based on upscale of pilot plant experiments and energy consumption obtained from the Aspen Plus® process simulator.

3.2. Methodology

Figure 3-1 illustrates the layout of the approach to achieve each of the objectives set in Chapter1. Most of this work was model-based; a computerised process simulator was used to regress a suitable thermodynamic model with literature obtained vapour-liquid equilibrium data. As shown in Figure 3-1, the sequence of activities begins with the model development of phase equilibrium data. This was simulated as a single flash unit using the Gibbs flash algorithm to investigate the separability of the multicomponent mixture. In addition, it served as a base for the development of process layout scenarios. A model feed solution based on South African industry produced apple aroma concentrate, recovered from a multi-staged evaporation process, was investigated to represent fractionation of apple aroma using

supercritical CO_2. Process route layout scenarios developed based on the previous model were investigated to retrofit a fabricated apple concentrate production facility. The best-suited process layout scenario was selected by comparing the product quality, organic compounds recovery, product yield, and energy requirements. The best process layout scenario was presented. The economic viability for the best layout was represented through an order of magnitude evaluation based on pilot plant data and simulation energy consumption.

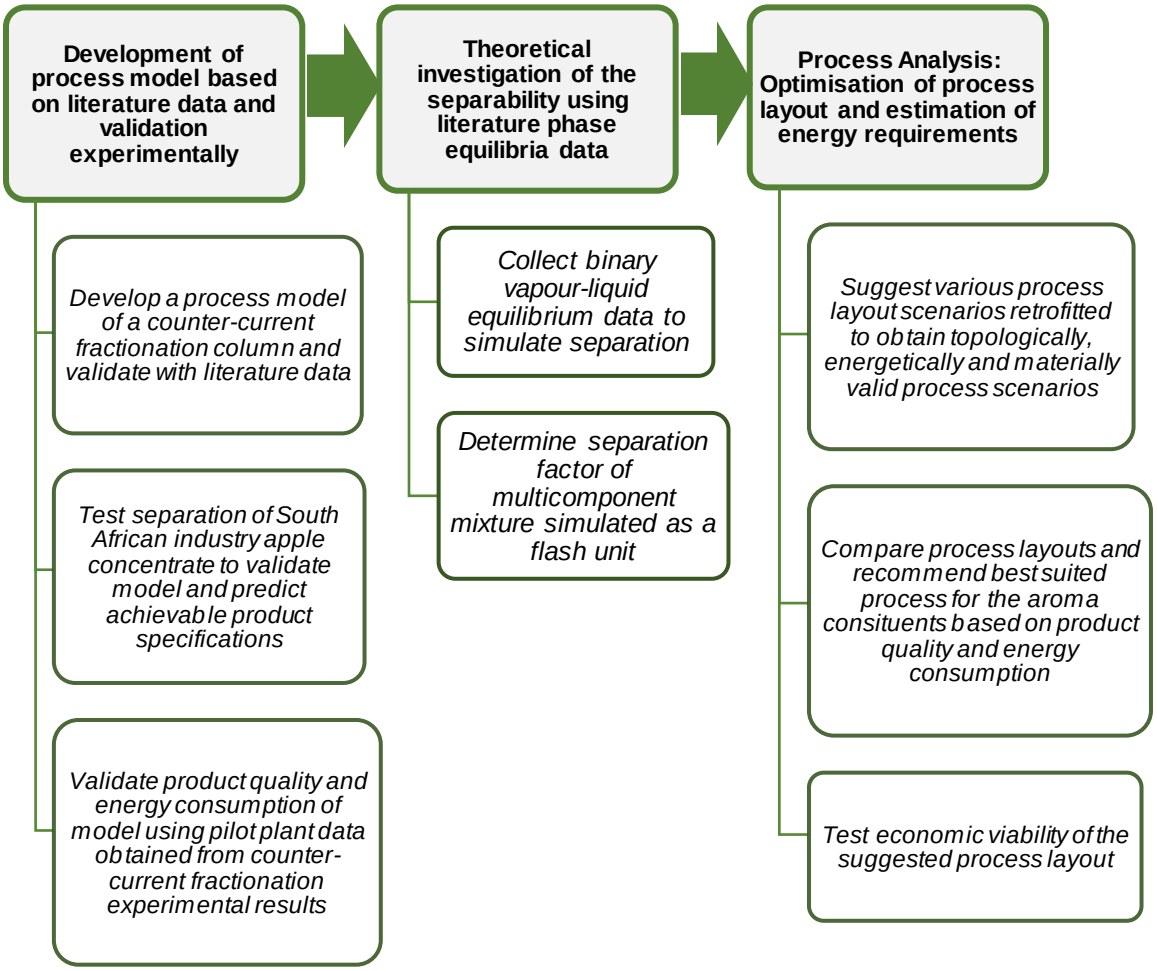

Figure 3-1: Approach to experimental work

The proposed method uses gas absorption at high pressure using supercritical CO_2. A model solution was investigated to represent apple aroma obtained from the South African industry. The model solution comprised of key apple aroma compounds was investigated to fractionate valuable apple aroma compounds i.e., total aromas (hexenal and *trans*-2-hexenal) from undesired compounds (hexanol and water). Product quality obtained from experimental work were used to validate computer-simulated process models.

Whenever possible, scientific investigations can be assisted with correlation models that enable the feasibility of a process to be determined. This saves resources in terms of the costs and time incurred. In the current investigation, a process model was developed based on the existing process. It was validated using the analysis results of the products obtained from the

pilot plant discussed in this chapter. The energy and material data obtained from the process model was then adjusted to fit pilot plant data to improve the predictive accuracy of the product quality.

Knowledge of the phase behaviour of the relevant system enables the prediction of the feasibility of the proposed process. The phase behaviour data can be obtained from literature through vapour-liquid equilibrium (VLE) data. There are numerous mathematical models (or equations) that can be used to predict phase behaviour. These mathematical models are known as thermodynamic models. Each thermodynamic model has its specific applications, and most models can be used to accurately predict a specific compound's phase behaviour. However, the accuracy of these models is improved by regressing the model with vapour-liquid equilibrium data obtained from the literature. Furthermore, the regressed thermodynamic model was used to predict the phase behaviour of the compounds for the development of the process model.

The process model was regenerated into process route scenarios to represent the fractionation column retrofitted to a fabricated industrial process. The process layout scenarios were investigated based on the process topology, energy requirements and product quality and compared to obtain the best-suited process layout for concentrating the apple aroma compounds. The mass fraction of water enriched in the vapour phase, obtained from the process simulator, was used to establish the product quality; as the water fraction increases, the product quality decreases. Product yield was established from the feed and enriched vapour fractions. Each layout presented was based on scenarios for the fractionation column. Other major units, such as heaters, coolers, pumps, etc., were not considered because material and energy data remain constant throughout those units. Products obtained from pilot plant experiments were used to validate the results of the process model developed. Experimental data obtained from pilot plant experiments were used to validate the process model developed.

The economic viability of the proposed process layout was illustrated through an order of magnitude economic feasibility study based on a scale-up of the pilot plant used to investigate the counter-current fractionation of apple aroma. Energy consumption obtained from the Aspen Plus® process simulator validated energy of the CO_2 recycle process.

In the sections to follow, a detailed description of the activities labelled in Figure 3-1 is described.

3.3. Development of process models

Process models are mathematical representations used to describe a process. Typically, they consist of interconnected process units, each represented by their characteristic process

model written in mathematical form. They have an input entered by the user or adopted from the preceding unit. The output of the system represents the process output. Process models are typically used to perform mass and energy balances and predict stream and product compositions. Process models land themselves to computerisation since they typically involve iterative computations. In this age of ubiquitous computational facilities, process models are almost exclusively used in computer applications and software packages. They vary in complexity. The most sophisticated include thermodynamic and economic modules capable of predicting physical properties, vapour-liquid equilibria calculations and can source the latest physical and economic data from online resources.

The Aspen Plus® v10 process simulator, part of the AspenOne package by AspenTech®, was used in this work. It is primarily a steady-state process simulator, although v10 has incorporated the modelling of batch processes. The main advantage of using a computer package is its ability to rapidly perform many iterative calculation cycles that enable several process parameters to be investigated.

The general procedure for developing a process model using the Aspen Plus ® process simulator is described below:

(1) The "properties" mode under the **Properties** option on the start-up provided chemical components that were retrieved from the databank and retained in the active memory of the programme.

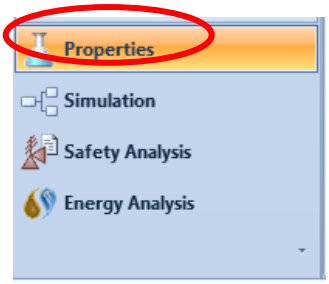

a. Components were specified under the **Component Specifications** in the list box:

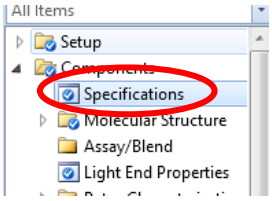

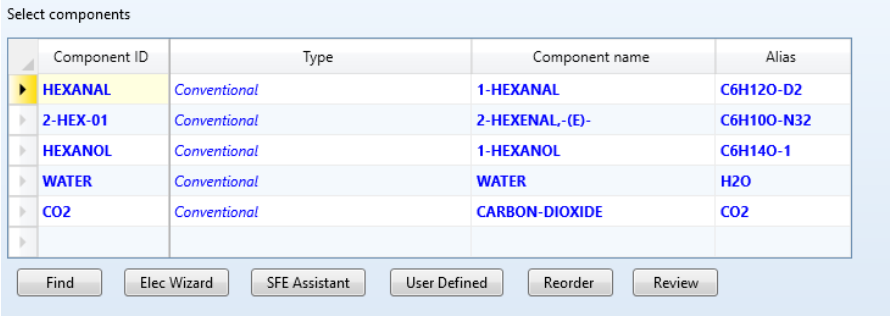

b. The thermodynamic model was specified under the **Methods Specifications** in the list box. The Soave-Redlich-Kwong Eos in combination with the Kabadi-Danner (**SRKKD**) method was selected:

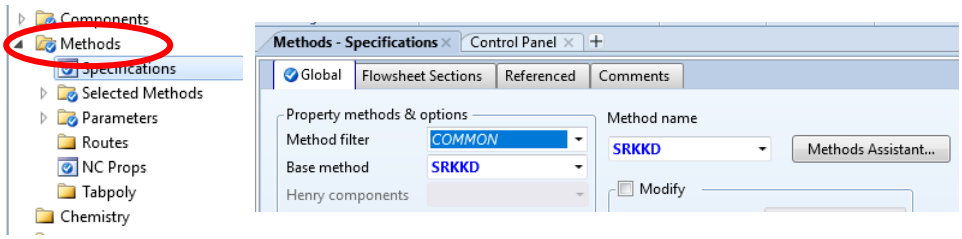

(2) The properties module were run to retrieve property data and to calculate additional properties for the selected components,

a. Experimental isothermal binary-liquid phase equilibrium data were retrieved from the Aspen Plus® database and input under **Data** in the list box.

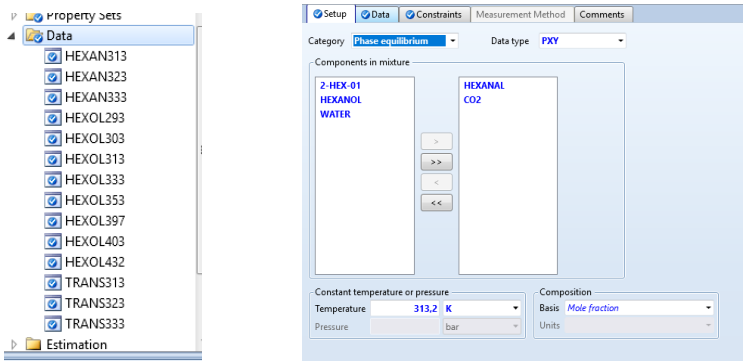

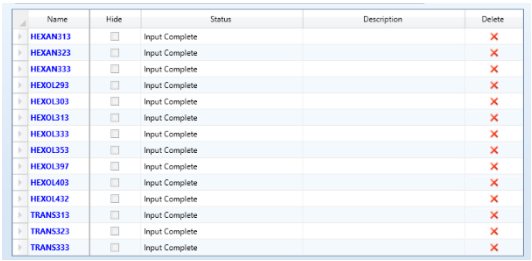

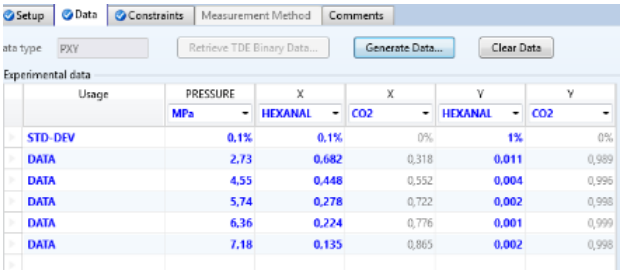

b. Experimental data for pure components were entered in the **Properties Data PURE-COMP** form

c. In the Run Type list box, the **Regression** option was selected in the **Run Type** list box to set up the correlation to simulate the experimental binary phase equilibrium data entered in **Properties Data MIXTURE** form

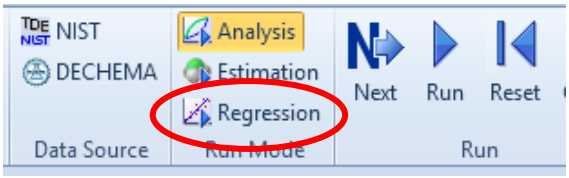

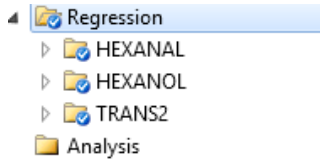

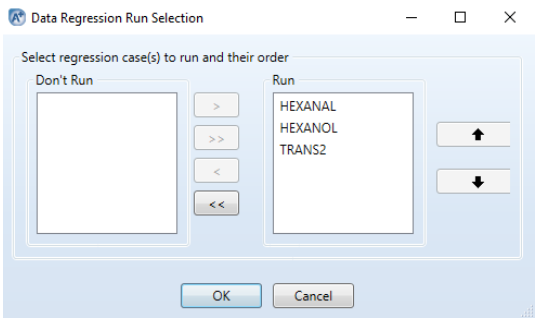

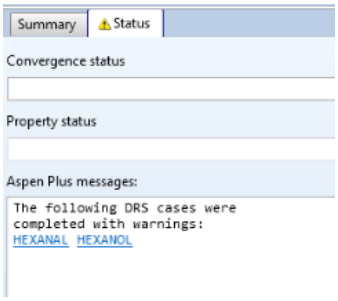

(3) In the simulation option of the package, a flowsheet was built by sequentially placing the icons representing each process unit on the "canvas" in the flowsheet tab of the graphical interface,

a. Process streams link the units,

(4) The properties, such as pressure, temperature, flow rate and compositions, of each stream, were entered into all feed streams,

(5) the parameters, such as pressure, temperature, and other parameters of each process unit, were entered into the entry tab for each unit,

(6) Once all required parameters were entered, the **RUN** option was selected to simulate and perform phase equilibria calculations

(7) Mass and energy balance for the entire flowsheet was obtained from the **Results Analysis.**

(8) The multicomponent phase behaviour of the system was modelled using the Gibbs flash algorithm simulated as a flash drum (simulated as a FLASH2 unit) in the Aspen Plus® process simulator based on the correlated experimental binary phase equilibrium and pure component data. The Gibbs flash algorithm is used to calculate vapour and liquid mole fraction in equilibrium at a given temperature and pressure.

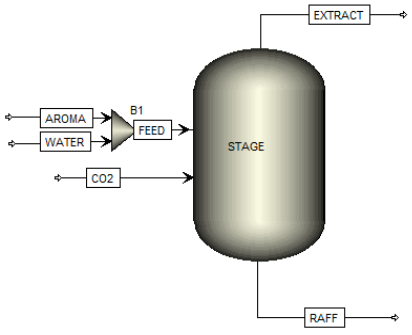

(9) In addition, the process model analysis tool, **Sensitivity Model Analysis**, assisted with the evaluation of process operating conditions effect on the product quality, product yield and organics recovery.

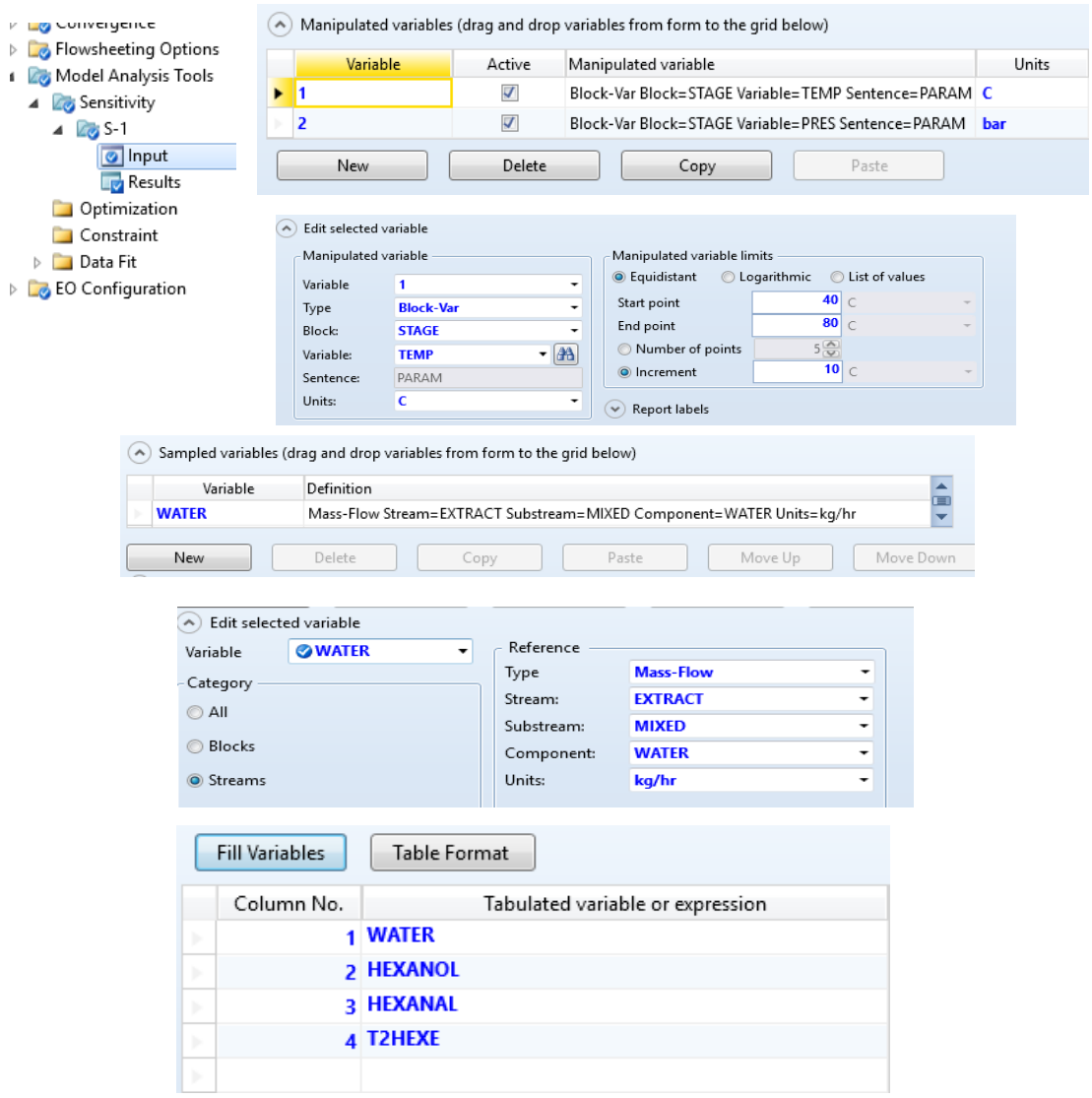

3.3.1. Thermodynamic Models

In this work, thermodynamic models were used to predict the phase behaviour of the relevant systems to estimate the distribution of each component in the different phases using computational tools such as spreadsheets or process simulators. A more in-depth treatment of thermodynamic models is provided in Chapter 2.

Under the thermodynamic property model, thermodynamic models provided in the Aspen Plus® process simulator include activity coefficient models, equation of state models, solids, and electrolyte models. Equation-of-state property methods suggested for hydrocarbons at high pressure by the Aspen Plus® programme are Benedict-Webb-Rubin-Starling (BWRS), Benedict-Webb-Rubin-Lee-Starling (BWR-LS), Lee-Kesler-Plöcker (LK-PLOCK), Peng-

Robinson-Boston-Mathias (PR-BM) and Redlich-Kwong-Soave-Boston-Mathias (RKS-BM). However, flexible, and predictive EOS models apply to a system with polar components and an activity coefficient model for mixtures containing polar and nonpolar mixtures and low pressures. For this study, the Soave-Redlich-Kwong EOS model was investigated in combination with the Kabadi-Danner (SRK-KD) mixing rules, an improved equilibrium calculation for a mixture containing hydrocarbons and water for phase equilibrium calculations described in Chapter 2.

Through correlation with literature VLE data, the model predicts binary interaction parameters to describe the phase behaviour of the mixture. These parameters are usually temperature dependant.

The "regression" function in the Aspen Plus® database utilizes experimental correlated data to determine the selected parameters for the specific thermodynamic model. The regression of the binary parameters, the Britt-Luecke algorithm were implemented to estimate the objective function presented in (13):

$$Q = \sum_i \left(\frac{T^{exp} - T^{calc}}{\sigma_T}\right)^2 + \sum_i \left(\frac{P^{exp} - P^{calc}}{\sigma_T}\right)^2 + \sum_i \left(\frac{x^{exp} - x^{calc}}{\sigma_T}\right)^2 + \sum_i \left(\frac{y^{exp} - y^{calc}}{\sigma_T}\right)^2 \quad (13)$$

where, T and P refer to the temperature and pressure, x and y to the liquid and vapour phase composition of each component, σ the standard deviation and the superscripts exp and $calc$ refer to the experimental/measured and calculated values, respectively. The quality of the data was evaluated based on the average absolute deviation (AAD) as presented in equation (14):

$$AAD\ (\%) = \frac{1}{N}\sum_{k=1}^{N} |e_k| \times 100\% \quad (14)$$

where, e_k is the error between the experimental and calculated values and N is the number of data points.

3.3.2. Validation of process model with literature and experimental data

Process modelling assisted tools enabled the investigation of process parameters required to fulfil objectives due to limited experimental work. The process simulator uses this model to predict the vapour-liquid equilibrium data and other physical properties such as density, viscosity, specific volume, etc. The model's accuracy was improved by the correlation of experimental VLE data with a selected thermodynamic model. Pilot plant experiments validate

data obtained from the process model. Process models perform calculations, and the number of iterations determines the accuracy of the results; therefore, the model cannot replicate results obtained from pilot plant data. The FLASH2 unit previously described employs the Runge-Kutta method to relate the activity coefficient minimisation of Gibbs free energy shown in equation (15) to an EoS.

$$G_{exc} = RT\left[ln\delta_i - \sum_i x_i ln\delta_i\right] \quad (15)$$

A minimum number of 30 iterations and an error tolerance of 0.0001 was selected.

Approach to fractionation experiments

The following objectives were set for the fractionation experiments with respect to the objectives set in Chapter 1:

1. To obtain optimum operating conditions, extraction yield and selectivity for the theoretical model solution characterised by industry:
    a. By performing fractionation 4 experiments using column C42 at optimum conditions reported:
    b. By performing fraction experiments on the following optimum conditions obtained from the Gibbs flash calculation:
    c. Determine energy requirement for the fractionation and product quality of the extract obtained from the theoretical model solution
2. To validate the process model
3. To validate the best-suited process layout.
4. To provide pilot plant material and energy data that will enable the economic evaluation.

Equipment described in 3.7 enabled the investigation of the proposed method. Since the aroma compounds and water have limited solubility in CO_2, separation depends on the superior solubility over the other in CO_2. In this case, the organic compounds are significantly more soluble in CO_2 than water, and almost all compounds have limited miscibility in water. The mass transfer rate from the aqueous solution to the gas phase is efficient enough to be practically feasible in a counter-current column of a reasonable number of stages, i.e., column height. The optimum range of operating conditions to maximise product quality, organics recovery, and yield for the process was investigated through a sensitivity analysis using the Aspen Plus® process simulator. Analysis of product samples obtained from pilot plant experiments validates data obtained from the process simulator; therefore, experiments were investigated at conditions (i.e., temperature, pressure, and S/F ratio) optimum for the process.

A comparison of mass flow rate and composition obtained from the simulated model and pilot plant experiments establishes the error margin for the process simulator. Once validated, the model for the continuous process was optimised and used to generate process route layout scenarios.

3.4. Generation of process layout scenarios: Process Synthesis

When a mixture of compounds (products, byproduct, raw material) coexists in one stream, separation units assist in splitting these mixtures into desirable final products. Counter-current fractionation obtains concentrated apple aroma constituents from a diluted mixture at high product recovery.

Mixers and splitters are the basic separation units considered. A mixing operation is only introduced when necessary, and splitting is accomplished in the piping. As the number of separation operations increases, the difference in required product specifications decreases. Therefore, the criteria for selecting separation methods are (1) the separating method; (2) energy of mass separating agents; (3) separation equipment, (4) optimal arrangement of sequencing of equipment; and (5) optimal operating conditions. The procedure involved in the general design procedure is (Turton *et al*., 1998; Sinnott, 2005; Seader *et al*., 2011):

1. The selection of a solvent
2. The column diameter, D, to obtain gas velocity
3. Length/height, H, of the vessel, contracting trays/packing
4. Optimum solvent circulation
5. The temperature of inlet and outlet streams
6. Pressure
7. Mechanical design

In general, these steps are followed in the design of a unit of operation. However, for the current investigation, a fabricated process is retrofitted with a sub-process for further processing apple aroma concentrate recovered as a byproduct from multi-effect evaporation. For the process described, a process design was considered, and therefore, process route layout scenarios were developed to establish the best-suited layout scenario. The process layout scenarios only included optimising the fractionation column. Other major process units (heat exchangers, pumps, valves, separating vessels) were not included in the investigation process layout scenarios. Material and energy data is constant for those units; therefore, it was disregarded. It was included in the economic evaluation.

The best-suited process layout scenario was obtained by comparing various scenarios based on CC-SFF. It consists of a basic stripping process in a packed column using a mass transfer operation (or mass exchanger network). The separation in a packed column is generally

treated as a staged process, and the mode of operation is selected as stripping, reflux, batch/semi-batch and continuous. For design purposes, a flash drum used to separate feed mixture containing two phases, vapour and liquid, are assumed to be in equilibrium (Seader *et al.*, 2011).

Apple aroma recovered as a byproduct during the production of fruit sugars, and the process layout scenarios presented were to be retrofitted to the current process layout in the industry presented in the literature. The process synthesising steps involved and considered in process layouts suggested are (1) distribution of chemicals, (2) eliminating differences in composition, (3) energy consumption, and (4) process topology. The process layouts were synthesised to configure a reliable, safe, and economically feasible process with high product quality and minimal waste (Turton *et al*., 1998). The process layout scenarios were developed using the Aspen Plus® process simulator based on a control model to compare the product quality, recovery, yield, and energy consumed. The best-suited process model was obtained.

Water mass fraction enriched in the vapour phase was used to establish the product quality. Where possible, the operating conditions were investigated such that the undesired compound, hexanol, was enriched in the liquid phase, ultimately increasing the product quality. Optimum conditions for each layout were obtained by investigating operating temperature, pressure, and solvent-to-feed ratio and, when necessary, near-critical conditions.

3.5. Economic evaluation

Economic evaluation is the systematic identification, measurement and valuation of the inputs and outcomes of alternative activities. These activities are subsequently analytically compared. It also helps plan the project's success, knowing when the production will start making a profit. The types of economic evaluations include; benefit-cost analysis (BCA), Cost-effectiveness analysis (CEA), cost-utility analysis (CUA) and equivalent annual operating cost (EAOC).

An upscale of pilot plant data enabled the economic evaluation based on an order of magnitude study in terms of energy unit per product yield. Material balance obtained from pilot plant experiments evaluated the yield and gas-chromatography analysis the product quality. Heat duty obtained from the process model was used as energy consumption for the economic evaluation.

3.6. Materials

The chemicals used during this experiment are listed in Table 3-1:

Table 3-1 Chemicals used during experimental work

Chemical Name	Supplier	Purity	CAS Number
Carbon Dioxide	Air Liquide (Pty) Ltd	99,9%	124-38-9
Hexanal	Kimix	98%	66-25-1
***Trans*-2-hexenal**	Kimix	98%	6728-26-3
Hexanol	Kimix	98%	111-27-3
Distilled Water			

Table 3-2 shows the list of compounds obtained from Gas-Chromatography Mass-Spectroscopy analysis using a Thermo TSQ 8000 coupled to a Thermo Trace 1300 GC provided by Elgin Fruit Juices (Pty) Ltd. The compounds comprise apple aroma recovered as a byproduct during evaporation in the production facility of the local company. 1000 µl was diluted into a CTC headspace vial to a final volume of 10 ml with MQ water. 2.5 ml of a 20% salt chloride solution was added. Anisole d* was added as internal standard. The mixture vortexed for 30 seconds. The headspace of the sample was analysed with a PDMS/DVB/Carboxen SPME fibre (grey).

Table 3-2 Analysis of apple aroma obtained from Elgin Fruit Juices (Pty) Ltd

Compound	Apple Aroma AA18/156 (standard) Concentration (mg/l)	Apple Aroma AA18/157 (05/06/2018) Concentration (mg/l)
1-Butanol	273,55	253,11
Hexanal	7,77	7,39
Ethylbutanoate (Ethylbutyrate)	9,55	8,85
Butylacetate	46,56	46,4
ethyl-2-methylbutanoate	1,65	1,75
trans-2-hexenal / E-2-hexenal	30,49	25,01
Hexanol	2581,49	2476,46
2-methylbutyl acetate	10,37	9,52
(3-Methylbutyl acetate) Isoamylacetate	1,32	1,2
Benzaldehyde	8,31	7,73
Hexylacetate	3,36	3,24

A model solution was comprised of selected compounds identified in the apple aroma obtained from the analysis in Table 3-2. The model solution comprised of a 5% total organics concentration for analysis purposes solution as shown in Table 3-3.

Table 3-3: Model solution composition

Compound	Mass Fraction in aroma concentrate	Mass fraction in 5% solution
Hexanal	9.01E-04	1.47E-02
Trans-2-hexenal	3.56E-03	5.82E-02
Hexanol	3.02E-01	4.93
Distilled water	99.7	95

The model solution comprised 5% organics due to the low concentration of organics in the aroma concentrate (0.3%) and for analysis purposes. The 5% concentration were made up of the same organic ratio as in the 0.3% feed. This fraction comprised 0.3% hexanal, 1.2% *trans*-2-hexenal and 98.5% hexanol. Hence, only the total organics fraction increased

3.7. Experimental Methods: Supercritical fluid fractionation (SFF)

The experiment was performed using the process illustrated in Figure 3-2 part of a combined extraction unit purchased from Separex. Table 3-4 describes all equipment in the pilot plant located in the High-Pressure Laboratory at the Cape Peninsula University of Technology.

Table 3-4: Main equipment description for Pilot plant

Main Component (As labelled on the plant)	Description	Operating range
CO_2 high-pressure pump, P200	Piston pump with adjustable flow rate. Equipped with frequency drive, mass flow meter and its controller to automatically control flow rate.	100 − 300 g/min at max 700 bar and 0/5^{o}C
Two liquid pumps: P210/P400	P210: Dosing co-solvent and feeding the extraction column. P400: Feeding reflux line to top of column.	0.01 − 50 ml/min at max 700 bar
Two high-pressure extraction vessels, A40/A41	5L vessel equipped with a basket and hand-operated screw lids. Surrounded by heated jacket to control temperature.	ID = 131 mm 0 − 1150 bar +20 − +250^{o}C
Counter-current extraction column, C42	1L pall ring packed column equipped with heated jackets and sapphire windows at the bottom of the column for viewing of liquid.	H = 4 m 0 – 350 bar +20 – 200^{o}C
Three separators, S50/S51/S52	0.6L vessels to separate and fractionate vapour and co-solvent from expanding CO2 at different temperatures and pressures	0 – 200 bar +20 − +120^{o}C
Filter, F53	0.6L vessel to remove fine particles and volatile substances from CO_2 before recycling.	0 – 200 bar +20 − +120^{o}C

Condenser, CE2000	Condenses CO_2 before pump with a refrigerant mixture supplied by chiller C2000. Additional in-line double pipe cooler ensures CO_2 is maintained in a liquid state located between condenser and pump.
Heater, HE3000	Aluminium block with CO_2 channels on the inside, heated through an element. Located after the pump for heating CO_2 to required operating temperature (usually above the critical temperature, 31,1°C).

For this investigation, the high-pressure vessels A40 and A41 were not in operation and therefore excluded as part of the process description.

3.7.1. Process flow description

The main component of the experimental apparatus was the column (C42), with a height of 4m and an internal diameter of 28mm. The operating conditions (temperature and pressure) for the operation of the column (C42) were selected based on the binary phase equilibrium data described in Chapter 2. The column is equipped with four heating jackets to maintain the operating temperature inside the column. The pressure inside the column is controlled and maintained by ARV400. For increased mass transfer, the column is randomly packed with pall rings.

Pure CO_2 (99.99% purity), in its vapour form, was fed to the system (from the cylinder in Figure 3-2). This line is connected to a recycle stream (controlled by a manual valve MV100) from the filter (F53) containing pure CO_2. This valve is usually flared to the atmosphere before the plant's start-up to avoid impurities entering the feed stream. The CO_2 from the feed stream entered through the condenser (CE2000), condensing the CO_2 down to below 10°C (its liquid form). It then passed through the cooler to ensure that the CO_2 is liquid when passing through the piston pump (P200). The pump controls the CO_2 flow rate and establishes flow through the system as well. The CO_2 then passes through a heater (HE3000), which heats it to the required operating temperature, usually above its critical temperature, 31°C, to ensure that it is in its supercritical state before entering the column. The CO_2 entered the bottom of the column (C42), operating at the desired pressure, temperature, and solvent flow rate. The pressure, temperature and CO_2 flow rate are measured and controlled by Laboratory Virtual Instrument Engineering Workbench (Lab View). The liquid level of the column was viewed through the sight glass, located on the samp of the column, to ensure that the column was not flooded. For

the continuous mode of operation, the model apple aroma solution was fed through piston pump (P400) at the 3rd feed entry point of the column (C42) through MV423. This prevented entrainment from occurring and extended contact time between the solvent and model solution (McCabe *et al*., 1993). In addition, this enabled counter-current flow in the column. The solvent-to-feed ratio(S/F) was established from the mass flow rate of feed recorded. The CO_2 combined with compounds enriched in vapour phase exited the top of the column through MV425 and passed through ARV400. Separation vessels (S50-52) operated at a pressure of ~50 bar, which reduces the solvent power of CO_2, and consequently separating enriched compounds. The CO_2 passes through a filter (F53) to remove any solid particles or other impurities and recycles then back to the process via MV500. The operating conditions for experiments are shown in Table 3-5.

Table 3-5: Operating conditions investigated during experimental work

Experiment	T (°C)	P (bar)	CO_2 flow rate (kg/hr)	Feed Pump rate rpm	Description
1	40	70	5	500	Validate process model optimum
2	50	100	5	500	Effect of increasing temperature
3	40	70	10	200	Effect of increasing S/F ratio
4	40	140	5	500	Bejarano & Dell Valle (2018) optimum findings
5	40	70	5	500	Replica (not for analysis)

Due to variations in feed densities, the feed pump (P210 in Figure 3-2) does not measure flow rate. However, the flow rate was adjustable by its rotating speed or rate per min (rpm), hence the variations in feed pump rpm in Table 3-5. Mass recorded over time established the mass flow rate. A high pump rate and low solvent flow rate enabled the investigation of a low S/F ratio (i.e., solvent bubbling in liquid). Decreasing pump rate and increasing the solvent flow rate increases solvent to feed ratio (i.e., liquid trickling down, higher solvent capacity). Literature obtained optimum conditions was also validated using the fractionation column C42. A replica of one of the previous runs signifies the reproducibility of the experimental data.

Based on the phase behaviour described for the binary systems in 2.6.1, the process was investigated at 40 – 60°C, 80 – 140 bar and a S/F ratio of 5 – 15. This established the effect of temperature, pressure, and S/F ratio on the multicomponent system. The conditions of the experiments were selected to validate the process model developed. Bejarano & Del Valle (2017) performed an extensive range of experiments. Since this work was also used to validate the process model, it was not necessary for all parameters to be investigated. Hence, experiments were investigated at the selected operating conditions as presented in Table 3-5.

The first experiment validated the optimum fractionation conditions obtained from the process model developed. Increasing the temperature and S/F ratio established the accuracy in model trend predictions. An experiment at the optimum from Bejarano & Del Valle (2017) investigated enabled the comparison of the phase behaviour for the different compositions of the model solutions. In addition, it validated the effect of increasing pressure from the process model.

Limited capacity in the column increased the chance of the column flooding with the feed; therefore, sampling times were set as follow:

- Mass of feed was recorded every 5 minutes by weighing feed on a balance to establish a steady feed rate.
- Raffinate was discharged through DAV420 and DMRV420 every 15 minutes and drained entirely (for approx. 20 seconds) and recorded. Once the **steady-state operation** has been established a collective sample of raffinate was collected at the end of each run for analysis. Additionally, flooding was monitored through sight glass located at the bottom of the column (the samp) presented in Figure 3-2.
- The extract was collected at the end of each run and collective samples were sent for analysis.

The steady-state operation was established in terms of:

i. Mechanical operation: Steady pumps rate and control systems measurements (pressure) recorded on Lab View
ii. Thermal equipment: Achieved setpoint temperatures and steady thermal measurements recorded on Lab View
iii. Hydrodynamic: Steady feed, raffinate and solvent flow rate established from mass recorded.
iv. Chemical: Composition of raffinate and extract unchanging over time. This was only established after experimental runs through analysis of samples.

Based on the experiments performed by Bejarano & del Valle, (2017) an extraction time of 2 hours was selected to establish steady-state operation based on the compositions of hexanal, *trans*-2-hexenal (or (E)-2-hexenal as referred by the authors) and hexanol in the raffinate. Aroma losses due to the solvent were accounted for during the first hour of operation. The following hour of operation was used for the observation of component mass balances. After 100 minutes, hexanol achieved a steady composition in the raffinate and trans-2-hexenal after 110 minutes. The composition of hexanal remains constant (Bejarano & Del Valle, 2017). For this investigation, an extraction time of 2 hours (as suggested by Bejarano & del Valle (2017)) was selected initially after establishing steady-state operation.

During the start-up for the third experiment, a leak on the liquid feed pump occurred which affected the feed rate to the column recorded and ultimately affecting mass balance calculations. Upon further evaluation, the pump was diagnosed with a broken seal. In addition, a significant leak on a bolt at the bottom of the column during experiment 3 prevented the investigation of all experimental conditions set in Table 3-5. Thus, experiments were limited to the following conditions presented in Table 3-6.

Table 3-6: Conditions investigated after equipment failure

Experiment	T (^{o}C)	P (bar)	Solvent Flow (kg/hr)	Feed Pump rate, rpm
1	40	70	5	500
2	50	100	5	500

Nonetheless, these conditions validated the process model for the feed used in this work. The viability of the process model was shown through the validation with data obtained from Bejarano & del Valle (2017).

Figure 3-2 illustrates the schematic diagram of the equipment used to perform the experimental work.

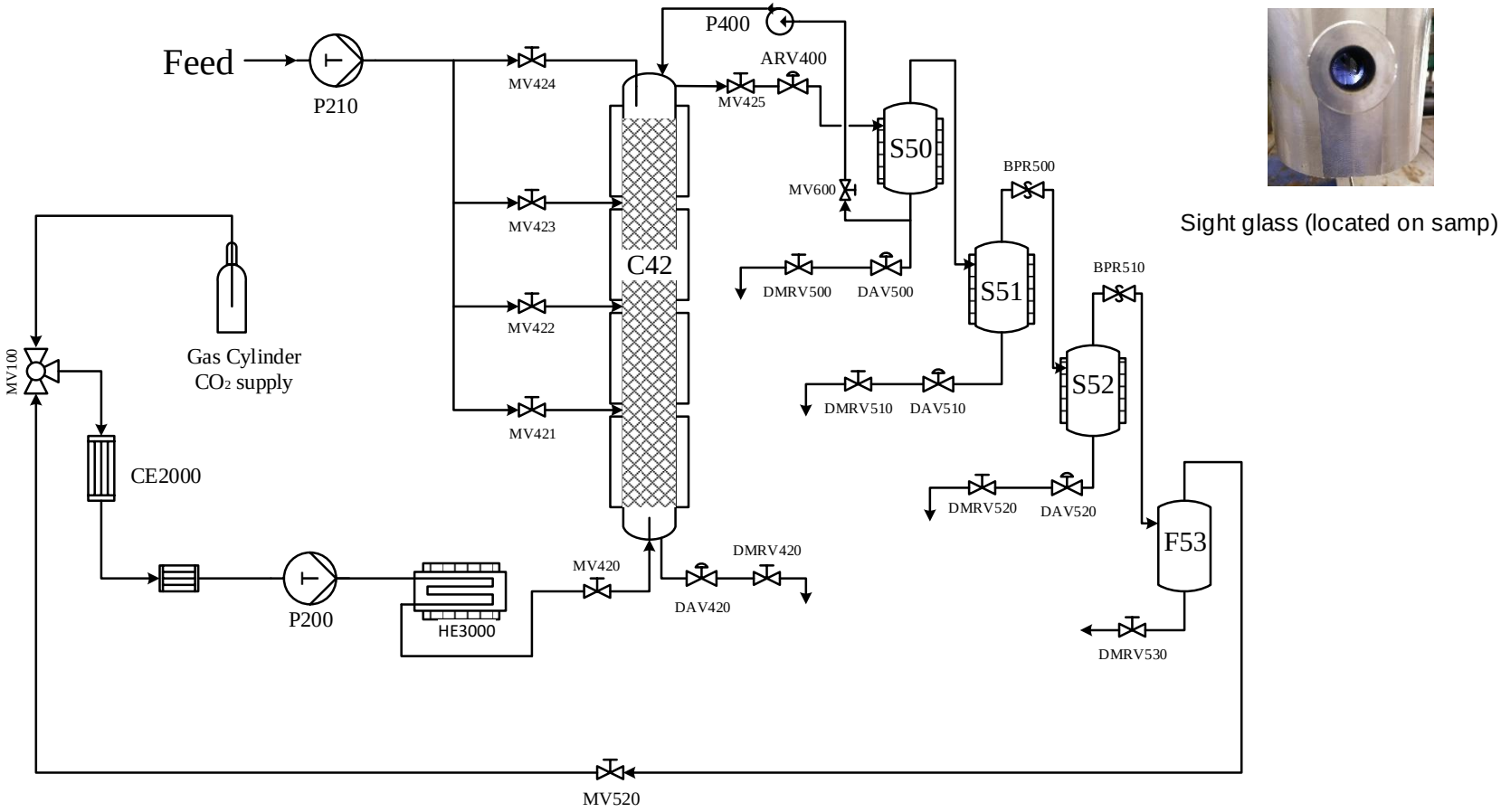

Sight glass (located on samp)

Figure 3-2 Schematic Diagram of Fractionation Column (C42), Condenser (CE2000) followed by the in-line Cooler, CO_2 supply pump (P200), Heater (HE3000), Liquid feed pump (P210) Reflux pump, (P400), Separation vessels (S50-52) and Liquid filter (F53)

3.8. Sample Analysis

Gas Chromatography coupled with mass spectroscopy (GC-MS) analysed the samples collected from experiments for the identification of volatile compounds. The GC uses a Thermo TSQ 8000 coupled to a Thermo Trace 1300 GC. The headspace of the samples were analysed with a PDMS/DVB/Carboxen SPME fibre (grey)

3.8.1. Sample Analysis

Samples of the feed, raffinate and extract were analysed for the concentration hexanal, *trans*-2-hexenal and hexanol. One sample of the model solution was analysed to enable mass balance calculations. The samples were analysed to determine the effect of temperature, pressure, and CO_2 flow rate on key apple aroma constituents and concentration fractionation. The following analyses were considered:

3.8.1.1. Gas Chromatography (GC) Analysis

The analysis was done as follow:

- For hexanal – 200 µl of the sample was pipetted into 5 ml MQ water and then extracted with 2 ml diethyl ether.
- For *trans*-2-hexenal – 20 µl of the sample for samples 01, 02 and Feed was pipetted into 5 ml MQ water and then extracted with 2 ml diethyl ether. While samples 03-08, 200 ul of the sample was pipetted into 5 ml MQ water.
- The results for hexanol – 20 µl of the sample-for samples 01, 02 and Feed was pipetted into 5 ml MQ water and then extracted with 2 ml diethyl ether. While samples 03-08, 200 µl of the sample was pipetted into 5 ml MQ water.

Sample numbers are shown in Table 3-7.

Table 3-7: Sample number descriptions

Sample	Description
01	Extract from run 1
02	Extract from run 2
03	Total raffinate run 1
04	Total raffinate run 2
05	Steady-state evaluation of raffinate at 30 minutes run 1
06	Steady-state evaluation of raffinate at 45 minutes run 1
07	Steady-state evaluation of raffinate at 60 minutes run 1
08	Steady-state evaluation of raffinate at 75 minutes run 1

3.9. Chapter outcomes

This chapter provided the material and methods used to attain the objectives of the current investigation. The process model described in this chapter fulfilled objective 1. Phase equilibria data obtained from literature was regressed with a thermodynamic model using the Aspen Plus® process simulator. The process model was developed using a flash unit (FLASH2) to simulate the phase behaviour for the apple aroma feed with supercritical CO_2 based on the Gibbs flash algorithm. The multicomponent phase behaviour and separability were investigated using the sensitivity analysis. This was validated with data obtained from Bejarano & del Valle, (2017) and pilot plant experiments performed, thus satisfying objective 2. Process layout scenarios were developed based on the previously validated model to obtain product quality, yield and organics recovery, and energy consumption. Objective 3 was thus accomplished by the comparison of the previously mentioned factors such as to obtain the best-suited process layout scenario. Pilot plant mass and energy balances recorded during experiments were used to perform an order of magnitude economic evaluation (in Chapters 4 and 5) to fulfil objective 3.

CHAPTER FOUR

Results

4. RESULTS

The section presents the results obtained from pilot plant experiments and process simulator in pursuit of the objectives stated in Chapter 1. Mass balances were performed to evaluate the product yield and quality, and energy consumption was evaluated based on the process model developed.

4.1. Introduction

Pilot plant experiments were performed at the given range of operating conditions presented in Chapter three. Mass recorded (of feed, raffinate, and extract) and thermal measurements enabled the evaluation of steady-state operation, and mass and energy balances to validate the process model developed to fulfil the requirements for the first objective.

Literature vapour-liquid equilibrium data were regressed with the Soave-Redlich-Kwong equation of state in combination with the Kabadi-Danner mixing rules (SRKKD) using the Aspen Plus® process simulator. Differences between pressure estimated by the thermodynamic model and literature measured data evaluated established the accuracy for the regression. In addition, the multicomponent mixture simulated as a single two-phase flash unit model (FLASH2) evaluated the phase behaviour for objective 2. This established an optimum range for the separability of the model solution. The process model was then validated with experimental data from Bejarano & del Valle, (2017) and pilot plant experiments.

Based on this model, objective 3 was attained through the development of process layout scenarios for the best-suited process layout based on product quality, yield, and organics recovery. The sensitivity analysis tool in the Aspen Plus® process simulator assisted with the evaluation of optimum process parameters for each scenario. Experimental composition data and an order of magnitude economic evaluation established the economic viability of the process based on energy consumption.

4.2. Experimental Results

Experiments included the evaluation of steady state operation for the pilot plant in terms of thermal, mechanical, and hydrodynamic measurements during operation. The product yield was determined from data recorded of feed and raffinate, and validated process model. Results obtained from gas chromatography mass spectroscopy (GC-MS) analysis of raffinate chemical composition steady state. Further, the extract analysis enabled the validation of product quality and organics recovery for process model (objective 1). Due to equipment malfunctioning, 2 experiments as shown in Table 3-6, Chapter 3.

4.2.1. Steady-state operation

For the pilot plant presented in Chapter Three, steady-state operation was required for validation of the process model developed for objective 1. The process model comprised of a FLASH2 unit (as described in Chapter three) that simulates the Gibbs flash algorithm at equilibrium. This required pilot plant experiments to be performed at steady state for the system to remain at equilibrium for the validation of the process model. The following monitored measurements established steady state operation:

- Thermal measurements – column temperature remained unchanged at the required operating temperature for each experiment and separators temperatures below 60°C (to prevent degradation of thermally labile compounds)
- Mechanical measurements – CO_2 pump flow rate and column pressure remained unchanged over time. Separator pressures were maintained at 50 bar.
- Hydrodynamic measurements – feed and raffinate flow rate measurements remained unchanged over time.
- Chemical composition measurements – chemical composition of compounds remained unchanged over time. This was evaluated based on GC-MS analysis results presented in 4.2.2.

In Table 4-1, Table 4-2, Table 4-3, and Table 4-4 the average, standard deviation and standard error were determined from the following equations to establish the accuracy in the data measured.

$$Average, \bar{X} = \frac{\sum X_i}{n} \tag{16}$$

Where, $\sum X_i$ is defined as the sum of all variables and n the total number of variables and the standard deviation:

$$standard\ deviation, \sigma = \sqrt{\frac{\sum (x_i - \bar{X})^2}{n}} \tag{17}$$

And,

$$standard\ error, SE = \frac{\sigma}{n} \tag{18}$$

Where the standard deviation shows the accuracy in the data measured and the standard error shows the precision in the data.

Thermal and mechanical measurements

Data presented in Figure 4-1, Figure 4-2, Figure 4-3, and Figure 4-4 shows data obtained from the Laboratory Virtual Instrument Engineering Workbench (LabView). This is coupled with the supercritical pilot plant. Data were recorded from start-up for each process controller to completion of the experiment, every 1-second interval. Each experiment was performed based on the Pilot Plant Standard Operating Procedure.

The pressure presented in Figure 4-1 shows the data recorded of column pressure (by PI420) for experiments 1 and 2. During the experiments, thermal measurements of CO_2 entering the column (by TI300), column heating jacket temperatures (by TI420, TI421, TI422, and TI423), and separators (by TI500. TI510, TI520) were monitored to evaluate the achievement of setpoint temperatures and steady-state operation. The column temperature was kept at a temperature to account for heat losses caused by the ambient aroma feed entering. Data obtained from temperature recorded of the vapour exiting the column (by TI423) are presented in Figure 4-2. Figure 4-3 shows data recorded for the temperature of vapour leaving the first separator (by TI500), as most of the extract was collected from the first separator for both experiments. The temperature was to be maintained below 60^{o}C to prevent loss/degradation of aromas. Data presented in Figure 4-4 shows the mass flow rate of CO_2 recorded during the operation of experiments 1 and 2.

The data in Figure 4-1 shows that the system achieved the required column pressure at an increased rate (as indicated by the inclined slope of the graph) within a short-time interval. This is explained by the small volume of the column. Therefore, requiring less time to build pressure in the column. After an initial overshoot, column pressure was well maintained within a reasonable range during operation for both experiments. This is a normal response in controllers. Minor fluctuations were a result of solvent feed pump and ARV400 controllers keeping the operating pressure maintained. A pressure drop of 1 bar occurred over 30 seconds of discharge every 15 minutes. This implies that the system could maintain column pressure well within the given time range during discharge. The temperature in Figure 4-2 took much longer to reach the required operating temperature. In contrast, it presented a larger overshoot in Figure 4-1.

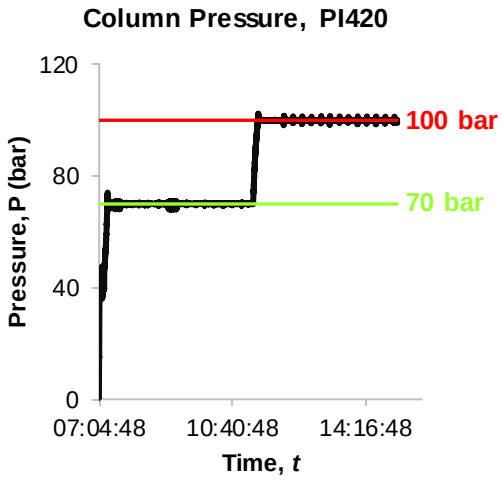

Figure 4-1: Column **pressure** recorded during experiments

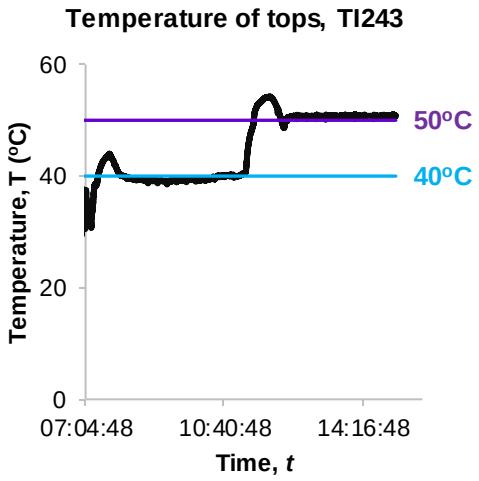

Figure 4-2: Column **temperature** recorded during experiments

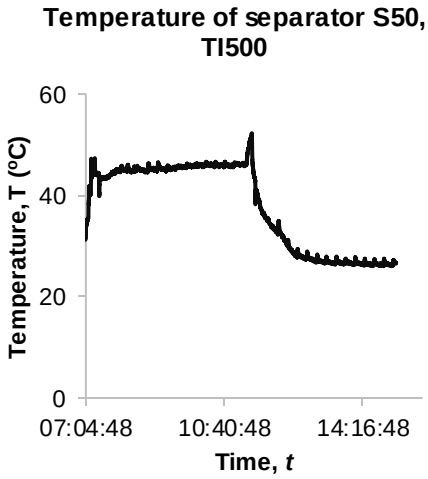

Figure 4-3: Separator **temperature** recorded during experiments

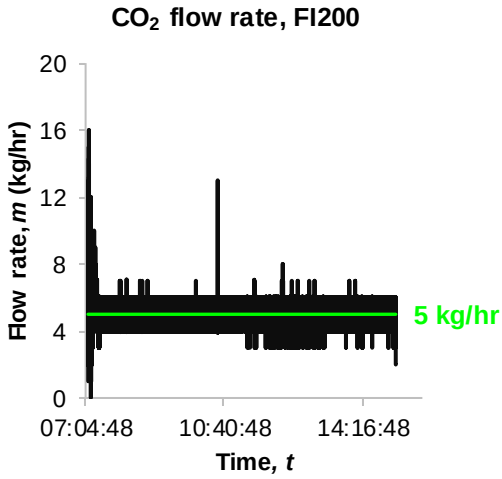

Figure 4-4: CO_2 pump flow rate recorded during experiments

The heat exchanger (HE3000) consists of an aluminium block heated by an element. CO_2 lines pass through the heat exchanger. Thus, a delay in the heat exchanger's response was expected as the controller takes time to respond to changes in temperature. First, the element heats up through an electric signal which then adds heat to the aluminium block. This then transfers heat to the CO_2 in the lines. In contrast, PI420 is maintained by the automated valve ARV400 that requires less steps for the controller to take effect. However, after the achievement of the required operating temperature, the controller maintained temperature with little variance, < 1°C. The temperature of the first separator after ARV400 maintained a temperature well below 60°C. On the other hand, temperature was not maintained at steady-state during both experiments. However, in the separators the enriched vapour is separated from CO_2 by the reduction of pressure.

There is a significant change in pressure drop between the fractionation column and separators (S50 – 51). Therefore, the first separator experiences the largest amount of thermal stress due to the Joule-Thompson effect. Generally, described by the change in temperature that accounts for the expansion of gases. Thus, a decrease in pressure results in a decrease in temperature. Therefore, the heating jacket surrounding the separator has a greater temperature loss to account for. In addition, the maximum temperature is limited to 100°C. Thus, operating at much lower temperatures than the second (S51) and third (S52) separators. Which usually operates above the 50°C operating line. Therefore, the unsteady temperature was expected. However, it was well maintained the maximum temperature of 60°C.

Figure 4-4 shows a large variance in the flow rate measured by the feed pump. The pump clearly had difficulty in maintaining a steady constant solvent flow rate for both experiments. The risk of vapour entering the pump could explain the erratic behaviour. A pump is designed to process liquids only. In addition, water enriched in the solvent cycle could result in freezing in the lines. The low freezing point of water is easily affected by the Joule Thompson effect experienced in the pump. During the experiment, a malfunction of the solvent pump occurred. However, after diagnosis, a leak was noted on a line leaving one of the valves located on the pump. After several minutes of operating, it was concluded that the leak had no significant impact on the pressure maintained in the column. Thus, the experiments were completed. However, the leak on the pump could explain the unsteady solvent flow rate recorded. In contrast, an average solvent flow rate was maintained at 4,97 kg/hr for experiment 1 and 5,04 kg/hr for experiment 2 as shown in Table 4-1 and Table 4-2, respectively.

Table 4-1: Experiment 1 error in measurements

	P, PI420 (bar)	T of top outlets, TI423 (°C)	T of first separator, TI500 (°C)	CO_2 flow rate, FI200 (kg/hr)
Average measurement	70.00	39.54	45.55	4.97
Standard deviation	0.24	0.44	0.48	0.78
Standard error	1.95E-05	3.64E-05	3.98E-05	6.30E-05

As expected, the standard deviation for the solvent flow rate showed a large variance. In comparison, temperature and pressure measurements presented the least deviations. A standard deviation of almost 1 was obtained for both experiments. This indicates that a steady pump rate was never achieved with a great fluctuation in the measured rate. However, in contrast, the standard error for temperature is within a reasonably small, almost insignificant, range ($\times 10^{-5}$) for this data and corresponds well with the standard errors obtained for the other measurements. This shows that the process was able to maintain the CO_2 flow rate within 4 to 6 kg/hr, on average approximately 5 kg/hr. It presented little to no variation from that range but remained quite well within that range. Overall, an average rate was well maintained when

compared to the required flow rate. It is thus obvious that steady-state was achieved in terms of thermal measurements. For mechanical operation, the pressure was well maintained. However, the flow rate remained fluctuating. Therefore, steady-state was not completely achieved and should be noted for validation with the simulation equilibrium process model. The average pressure measured was well maintained at 70 bar for experiment 1 and 100 bar for experiment 2, based on data presented in Table 4-1 and Table 4-2. The pressures had low standard deviations and standard error for both runs indicating the low variance in the pressure measurements. The system was quite steady in terms of pressure.

Table 4-2: Experiment 2 error in measurements

	P, PI420 (bar)	T of top outlets, TI423 (°C)	T of first separator, TI500 (°C)	CO_2 flow rate, FI200 (kg/hr)
Average measurement	100.00	50.87	27.76	5.04
Standard deviation	0.24	0.72	2.08	0.83
Standard error	2.05E-05	6.10E-05	1.77E-04	7.07E-05

For the first experiment, the average outlet temperature was below the required 40°C. However, an average overall temperature for the column (TI420, TI421, TI422, TI423) of 40.79°C was maintained during operation. Indicating that the temperature operates above the required in the column. Similarly, for experiment 2 the outlet temperature was 50.87°C and an overall average column temperature was 50.8°C. The required temperature was at 50°C.

Albeit, the top outlet and overall column temperature deviations, it does not vary significantly from the required operating temperature for both experiments (by 1°C). A 1°C difference does not significantly impact the overall phase behaviour of the process and mass transfer. Therefore, it can be assumed that process temperature was well maintained at the required set points. This is also justified by the low standard errors obtained, which shows the little variance in the measured data.

Variations in data obtained for the temperature of the first separator temperature is explained by the thermal stress experienced by the heating jacket to account for the significant pressure drop previously described (the Joule-Thompson effect). The pressure in the column is maintained by ARV400 and responds to the solvent pump rate at which CO_2 is fed to the column. As a result of the inconsistent solvent pump rate, the ARV400 had to account for the fluctuations by releasing pressure to the separators. Ultimately, influencing the temperature maintained. It was thus expected that the temperature controller would not be able to maintain temperature steady.

Hydrodynamic measurements

After the thermal and mechanical steady state was established, the hydrodynamic behaviour of the process was evaluated. Data recorded from feed to the column and raffinate discharged enabled mass balances to be performed. The aromas enriched in the vapour phase and lost due to the solvent cycle was determined from the mass balance. Feed and raffinate data were recorded for 2 hours over 10 minute intervals as presented in Figure 4-5. This prevented a significant pressure drop to maintain steady-state operation because during discharge column was emptied through raffinate. Frequent discharging time intervals results in too many unsteady data points in data and ultimately increasing standard deviation.

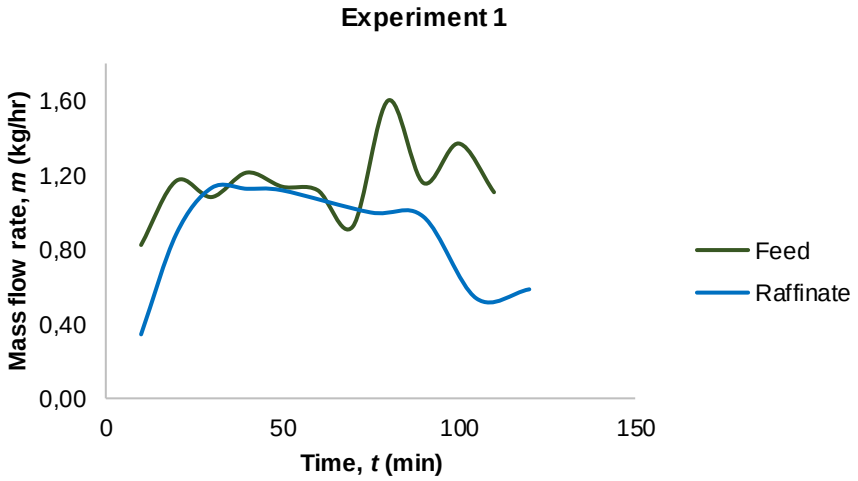

Figure 4-5: Feed and raffinate mass flow rate measured during experiment 1

The first experiment established hydrodynamic steady state within 45 minutes. The raffinate discharge rate was steadier than the feed rate based on the data presented in Figure 4-5. Both feed and raffinate data evaluation occurred every 10 minutes and the feed rate remained within a reasonable range was steady after 30 minutes. For an additional 90 minutes, mass flow rate data was recorded to start data collection for chemical composition steady state. After 75 minutes of feeding, the feed rate changed significantly and varies at a higher range. The raffinate rate remained steady for the first 90 minutes of operation, followed by a sudden decline.

The possibility of inconsistent pump rate (from feed pump P210) could have resulted in the erratic feed rate recorded. In addition, the line to the pump is exposed to air, thus, a sudden decline in the feed rate could be because of air entering the system, especially during changing of the feed bottle. Erratic behaviour of pumps was also noted. In addition, the pump was pumping against the pressure in the column and as previously observed. Column pressure was steady overall but showed deviation based on the pressure recorded for a certain time interval. Therefore, explaining the inconsistent feed rates. However, rate fluctuations fall within

a reasonable range for mass flow rates. This was confirmed with the low standard deviations obtained from the feed and raffinate data presented in Table 4-3. The standard error indicated that variance in feed data was within a reasonable range.

Raffinate data indicated that there was variance in the mass flow rates but is still within an acceptable range. Accumulation and hold up in the column could result in not all fluid reaching the bottom to evaluate the mass balance. Due to column packing, it is likely that accumulation and hold up would occur. Therefore, it takes time for the fluid to pass through the packing to reach the bottom. In addition, the packing is random. Therefore, an inconsistent discharge rate should be expected. However, the deviation was 33%. This affected the mass balance for the following reading as fluid accumulated in the column could be discharged at any point. Therefore, there are instances where the raffinate mass recorded was greater than the feed flow rate.

Table 4-3: Standard error for experiment 1 mass flow rate data

	Mass flow rate (kg/hr)	
	Feed	**Raffinate**
Average	1.14	0.86
Standard deviation	0.30	0.29
Standard error	0.08	0.10

An average rate of 1,14kg/hr was maintained during the first experiment as presented in Table 4-3. A standard deviation of 0,3 was obtained, which means that the data deviates within a ~26% range from the average. This is within an acceptable range. Steady-state operation is usually not maintained during industrial applications. Similarly, a standard deviation of 0,29 was obtained for the raffinate data, showing a variance of ~33%. This was a result of the decline in the raffinate flow rate after 90 minutes of operation.

Mass flow rates recorded for experiment 2 shows a large variance for the feed data measured at different time intervals. The raffinate flow rate remained quite steady within a reasonable range after 50 minutes. After 100 minutes the flow rate increased to above the steady line between 50 and 90 minutes. Experiment 2 clearly shows a larger deviation in the feed data in comparison to experiment 1.

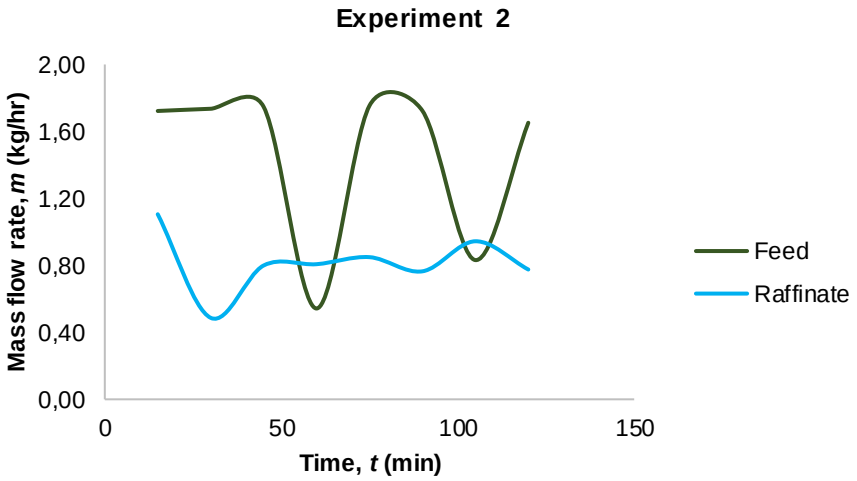

Figure 4-6: Feed and raffinate mass flow rate measured during experiment 1

A higher average feed rate was obtained at 1,46 kg/hr with a similar average raffinate discharging rate as presented in Table 4-4. As expected, the data showed a larger standard deviation in mass flow rates recorded for the feed. The raffinate feed data recorded had a lower standard deviation as steady flow rates were achieved within 60 minutes. It is thus obvious that it took the system approximately 60 minutes to establish a hydrodynamic steady-state for both experiments.

Table 4-4: Standard error for experiment 2 mass flow rate data

	Mass flow rate (kg/hr)	
	Feed	**Raffinate**
Average	1,46	0,82
Standard deviation	0,49	0,17
Standard error	0,17	0,06

The increased pressure had an impact on process controllers' ability to maintain steady state. This is due to the backpressure of the column that the liquid feed pump (PI210) experiences during feeding. The feed pump is pumping the feed from ambient conditions to a pressure of 100 bar. Changes in pressure during operation creates a pressure pulse and could translate to increased vibrations that the pump experiences (Sinnott, 2005). In addition, the ARV400 was able to maintain pressure in the column. However, minor fluctuations measured by PI420 creates fluctuations in the backpressure experienced by the feed pump. Therefore, the feed pump experiences vibrations that could explain the inconsistent feed rate. Overall, the process maintained steady-state operation within a reasonable range with variations in terms of thermal, mechanical, and hydrodynamic behaviour of the process. The process shows that it can reach a set point and keep it well maintained considering the pumps operation.

Chemical measurements

Chemical measurements were evaluated based on the composition of the organics in the raffinate. After 1 hour of establishing hydrodynamic steady-state, samples were recorded every 15-minute interval. Data presented in Figure 4-7 shows mass fractions of organics obtained from GC-MS analysis. Data are presented from a sampling time 60 minutes.

An absence of *trans*-2-hexenal in raffinate samples collected indicated that complete enrichment of the compound into the vapour phase occurs before feed reaches the bottom of the column. This implies that it is possible to completely extract *trans*-2-hexenal from the aqueous feed. All samples from sampling time 60 to 105 presented consistency in the presence of *trans*-2-hexenal in the raffinate. Thus, based on the observations mentioned above the concentration of *trans*-2-hexenal established a steady concentration within the given timeframe by remaining absent in the raffinate.

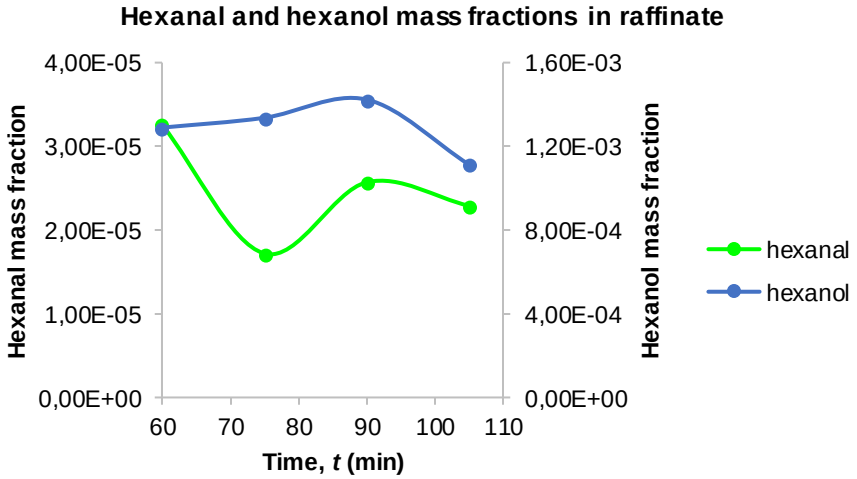

Figure 4-7: Establishment of **steady state** in terms of **chemical composition** from **experiment 1**

Contrastingly, the concentrations of hexanal and hexanol remained fluctuating within the timeframe presented in Figure 4-7. This indicated that the concentration for these compounds did not establish steady state. The concentration for hexanal changed significantly between 60 and 90 minutes. A decreased slope after 90 minutes indicated that the concentration started to settle. However, a validation point after 105 minutes are required to validate this.

In contrast, the concentration for hexanol remained steadily between 60 and 75 minutes and reduces rapidly after 90 minutes. Between 75 and 105 minutes the concentrations for hexanal and hexanol follows the same phase behaviour. Both increases then decreases. Thus, it could be that the compounds mentioned have a relation in terms of their concentrations. In other words, the concentrations of hexanal and hexanol coexists in the liquid phase. Thus, showing that the said organic phases are inseparable. The similar phase behaviour trends indicated

that process established steady state even during the introduction of process disturbances. Which is clear from the concentrations obtained. In addition, both concentrations data presented low standard deviations for hexanal at 6.40×10^{-3} $(max \pm 37\%)$ and hexanol 0.13 $(max \pm 12\%)$. The low deviation for hexanol suggested that the concentration of hexanol presented a steady behaviour, therefore fluctuations resulted from another source.

Process disturbances during operation interferes with the steady behaviour of the process unit operations. Process control systems responds to these disturbances thus changing the steady state for the process unit. Therefore, the process established a new steady state following this disturbance. In this case, previous inconsistent feed rates could have altered the steady state behaviour of the process. This could have affected the thermal and mechanical behaviour of the process. Irregular pump behaviour was significant contributors in this case. However, as previously mentioned, the hydrodynamics and mechanics operated within a stable region with considering the pump behaviour.

To validate the process model developed, the concentrations had to remain stable over a certain period. Hexanal had a larger deviation range but the decreased slope between 90 and 105 minutes shows the mass fraction starts to reach a stable range. The expected low deviation obtained for hexanol resulted from the stable concentration between 60 and 90 minutes. Additionally, hexanol operated in a much stable range in comparison to hexanal. This indicates that it might require longer time to establish a stable concentration for hexanal.

Trans-2-hexenal achieved a steady concentration since the raffinate samples contained no traces thereof. Thus, based on the concentrations of hexanol and *trans*-2-hexenal, the system achieved a steady concentration before 60 minutes of chemical evaluation considering the process disturbances. However, the concentration of hexanal takes longer to reach a steady concentration. Additionally, unavoidable process disturbances disrupt the steady behaviour of the system. In response, the system changes process controllers to maintain system at steady state. Therefore, it establishes a new steady state operation line and it might be difficult to establish an exact concentration for the compounds selected. Overall, the concentration remained quite steady after 45 minutes from the recorded sampling time (minute 105). Indicating that within 2 hours of operating at hydrodynamic steady state the pilot plant established steady state. Therefore 2 hours was selected for the second experiment as the run time for each experiment. The additional 60 minutes would be sufficient to allow hexanal to achieve a steady concentration.

4.2.2. Product yield evaluation based on mass balance from pilot plant

The mass balance around the column was performed to establish the mass flow rate of the extract and compounds lost due to the solvent cycle. The mass balance data was used to validate the process model as part of objective 1. Energy balance calculations were performed based on process model data with mass balance data obtained from pilot plant experiments. Since no reaction occurs, the general mass balance equation used in this section is described as:

$$Accumulation = Input - Output \tag{19}$$

Which is mathematically expressed in terms of mass with respect to time:

$$\frac{d\dot{m}}{dt} = \dot{m}_i - \dot{m}_f \tag{20}$$

Where, $\frac{d\dot{m}}{dt}$ refers to mass accumulation rate, $\dot{m}_i$ the total mass rate of input streams and $\dot{m}_f$ the total mass rate of output streams. For the mass balance the following assumptions were made:

- The system was operating at steady, therefore no accumulation in the column
- Feed mixture was well mixed before entering column, therefore equal mixing
- Constant overall density over time.
- Volume was constant.
- Equal density for a similar compound
- Nonreactive process
- Temperature and pressure remained constant throughout the column

Thus, the mass balance in equation (20) becomes;

$$\dot{m}_i = \dot{m}_f \tag{21}$$

Inputs to the column was the CO_2 feed and liquid aroma feed. Output product streams were the raffinate (liquid) and extract (extract). The mass balance for the column was as follows:

$$\dot{m}_{extract} + \dot{m}_{raffinate} = \dot{m}_{feed} + \dot{m}_{solvent} \tag{22}$$

Results of extract and compounds lost to solvent cycle – Mass balance

The mass flow rate of the extract was determined from raffinate, feed and solvent flow rate during experiments shown in Figure 4-8 and Figure 4-9. Calculations were done on a solvent-

free basis The fluctuation in the extract flow rate shown in Figure 4-8 and Figure 4-9 was because of inconsistent feed and raffinate flow rates recorded during experiments. For experiment 1 an average extract flow rate of 0,29 kg/hr was obtained and 0,65 kg/hr for experiment 2. However, the average value includes the total extract and compounds lost to the solvent cycle. Therefore, it should be noted that the actual extract obtained in separators could vary from the average value calculated. Nonetheless, the value will not have a significant difference as accumulation in the column is generally considered as 0 for steady-state processes.

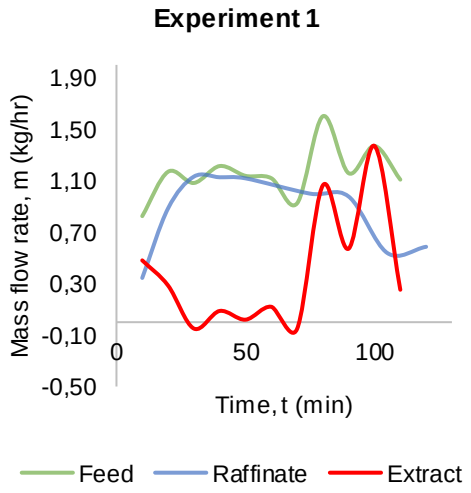

Figure 4-8: Mass balance obtained for extract (vapour phase) for experiment 1

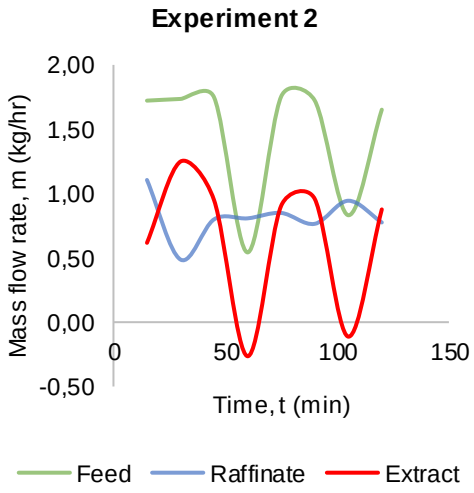

Figure 4-9: Mass balance obtained for extract (vapour phase) for experiment 2

Almost 25% of feed was enriched in the vapour phase for experiment 1 and 44% for experiment 2. This indicates that the product yield increased from the first to the second experiment. It could be because of the increased temperature and pressure in experiment 2. However, even though the product yield has increased, this does not indicate that the product quality has improved. The increased product yield could therefore be because of increased water enriched in the vapour phase (i.e., extract) thus decreasing the concentration of organics enriched and ultimately reducing product quality. By the evaluation of the extract using gas-chromatography analysis, the product quality was established for the extract obtained from both experiments. The results are presented in 4.2.3.

4.2.3. Product quality- physical and chemical analysis

This section presents data obtained from gas chromatography coupled with mass spectrometry. Samples collected from experiments 1 and 2 as described in Chapter Three were analysed. The raffinate and extract for both runs were evaluated for product quality and separability of valuable apple aroma compounds. Product quality from pilot plant experiments validated the model developed in 4.3.2.

The extract samples from experiment 1 had a stronger apple odour in comparison to experiment 2 based on the physical characteristics. In both experiments, the raffinate samples had a significantly reduced apple odour. Extract from experiment 1 had a strong alcohol and fruity odour in comparison to the feed. Which indicated a high concentration of hexanol. Samples from experiment 2 had a reduced odour in comparison to experiment 1. Thus, indicating that samples from experiment 2 had a higher concentration of water due to the reduced odour. On the other hand, the strong fruity-apple odour noted from the sample indicated a high recovery of valuable apple aroma compounds. Both extract samples had a distinct water and organics phase as shown in Figure 4-10. The golden colour represented water with obvious impurities dissolved in the water phase. However, the impurities in the process did not influence the result of this investigation due to the model solution feed prepared and analysis was conducted for the compounds in the model solution. The milky white liquid comprised of the organics (i.e., hexanal, *trans*-2-hexenal and hexanol). This showed the miscibility of the organics in water. Additionally, it is also possible to further increase product quality of the extract obtained. Organics and water phase can be separated through simple processes such as a separation funnel. Therefore, it is possible to obtain a 100% organics recovery in the product.

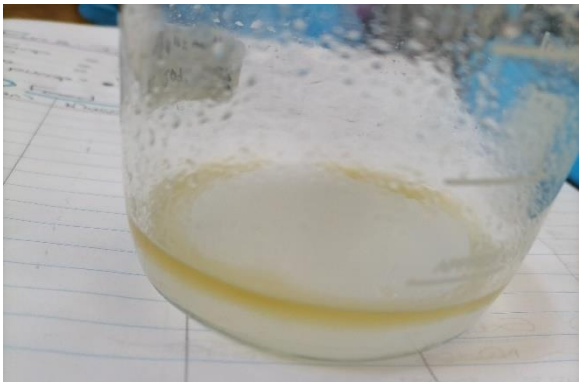

Figure 4-10: Extract collected from separators S50 – 52

For the data presented in Table 4-5, experiment 1 was performed at 40^{o}C, 70 bar and experiment 2 at 50^{o}C and 100 bar. Both experiments were performed at a S/F ratio of 5. The extract comprised of samples collected from separators S50, S51 and S52. No extract was obtained from the filter, F53, for both runs. The raffinate comprised of a combined sample of the total raffinate collected from minute 30 to minute 105.

Table 4-5: Product quality from pilot plant experiments 1 and 2

Sample	Description	Hexanal	*trans*-2-hexenal	Hexanol	Water
		Mass fractions			
	FEED	8.34E-05	1.63E-03	4.30E-02	0.96
1	ext run 1	1.97E-03	6.01E-02	0.93	8.42E-03
2	ext run 2	4.65E-04	2.80E-03	5.64E-02	0.94
3	Total raff run 1	3.55E-05	7.62E-05	4.66E-03	1.00
4	Total raff run 2	1.56E-05	-	1.23E-03	1.00

ext = extract, raff = raffinate

The extract obtained from experiment 1 to experiment 2 showed a significant change in total organics recovered. For experiment 1 the concentration for hexanal, *trans*-2-hexenal and hexanol increased by 24, 37 and 22 times, respectively. For experiment 2 the concentrations increased by 5, 2 and 1 times. It is thus obvious that experiment 1 presented a much greater recovery of organic compounds in the extract. The ratio for organics achieved in the extract for experiment 1 was 1:2:1 and experiment 2 at 5:2:1. For experiment 2, hexanal achieved a greater fold in the extract. The ratio of *trans*-2-hexanal and hexanol remained the same. However, the increased water concentration decreases the product quality significantly. Therefore, experiment 1 achieved much higher product qualities. For experiment 2, greater recovery was achieved for valuable aroma compounds at a lowered product quality. In addition, the extract obtained from experiment 2 had more of an apple-like odour in comparison to experiment 1. Thus, it is obvious that extract from experiment 2 showed an improved overall quality in terms of the recovery of organics that add value (represented by hexanal and *trans*-2-hexenal) and enriching liquid phase with the undesired aroma fraction (represented by hexanol).

In the total combined raffinate for experiment 2, no *trans*-2-hexenal was present in comparison to experiment 1. This means that for experiment 2, *trans*-2-hexenal was completely enriched in the vapour phase before sampling minute 30. *Trans*-2-hexenal is therefore easily separated from the water. In addition, chemical measurements in 4.2.1 show no presence of *trans*-2-hexenal in the raffinate. This indicates that the experiment doesn't need to run to completion to extract the valuable apple aroma compound. However, not all hexanal was extracted. The fact that hexanol comprises significant traces in the raffinate indicated that it might be possible to completely recover all the desired compounds (hexanal and *trans*-2-hexenal). However, the similar phase behaviour for organics clearly shows that these two phases are not separable. Therefore, organics concentration in both liquid and vapour phases will always coexist. (Villablanca-Ahues *et al.*, 2021; López-Porfiri *et al*., 2017; Secuianu *et al*., 2010).

On the other hand, *trans*-2-hexenal presents separability in the liquid phase. In addition, hexanal shows much greater recovery in the vapour phase in comparison to hexanol. Thus, all valuable compounds are possibly separable from water but not from hexanol. The fact that *trans*-2-hexenal and hexanal presented much lower concentrations in the raffinate indicates that these compounds achieved a greater recovery in the vapour phase. Therefore, this process might not be able to separate the organic phases from water. However, a higher recovery of valuable aroma compounds could be achieved. Raffinate also comprises a combined sample, therefore the mass fractions do not represent the actual final concentrations. However, based on 4.2.1, the concentration for hexanol and hexanal at minute 105 does not differ significantly from the combined raffinate. This implies that the system achieved steady-state within the given time frame.

From experiments 1 to 2, the water fraction enriched in the vapour phase significantly increases. Therefore, a higher product quality was obtained from experiment 1. In experiment 2, a lower fraction of organics was obtained. Nearly 16 times lower than that obtained from experiment 1 and similar for the valuable apple aroma fraction. This shows a significant shift in the fractionation of the process. CO_2 density changes significantly between these two conditions. Therefore, the solubility also changes. But higher CO_2 densities do not favour the fractionation of apple aroma compounds. However, this requires validation.

4.3. Process model development

A process model was developed using the Aspen Plus® process simulation to accomplish objective 1. Literature vapour-liquid equilibrium data were regressed with a thermodynamic model to obtain binary interaction parameters for computation of the phase behaviour. A two-phase outlet flash drum using the global minimisation of the total Gibbs free energy simulated as a FLASH2 unit was selected to represent the fractionation column. The model was used to investigate conditions such as to validate with literature and pilot plant experiments. This fulfilled the requirements of objective 1. The phase behaviour of the multicomponent mixture was described to attain objective 2.

4.3.1. Data obtained from correlation with a thermodynamic model

A thermodynamic model was selected to correlate with experimental VLE data for the development of a process model to attain objective 1. The binary data for each compound with CO_2 was obtained from literature (Elizalde-Solis *et al*., 2003; López-Porfiri *et al*., 2017; Secuianu *et al*., 2010; Villablanca-Ahues *et al*., 2021). The Aspen Plus® process simulator uses the correlated thermodynamic model to predict phase behaviour for a process model under the Simulation tool option. Binary vapour liquid equilibrium (VLE) data for hexanal, hexanol and *trans*-2-hexenal with CO_2, respectively, obtained from literature data was

regressed with the Soave-Redlich-Kwong (SRK) equation of state in combination with the Kabadi-Danner mixing rules using the Aspen Plus® process simulator with the method described in Chapter 2.

Thermodynamic and transport properties (the fugacity coefficient, enthalpy, entropy, Gibb's free energy, viscosity, thermal conductivity, diffusion coefficient, surface tension, critical volume, temperature and pressure, heat of fusion, specific gravity, and heat of formation) were obtained from literature data and using the NIST database in the Aspen Plus® process simulator. Data added to the pure components data improved the predictability of the thermodynamic model. The process simulator estimated the parameters not available.

The results of the regression of the phase behaviour for the binary system hexanal/CO_2 are shown in Figure 4-11. The source of the data used in the correlation is shown together with the sets of data. On the left-hand side vapour and liquid phases are shown in combination and the right-hand side shows the vapour phase correlation. Similarly for the data presented in Figure 4-12 and Figure 4-13.

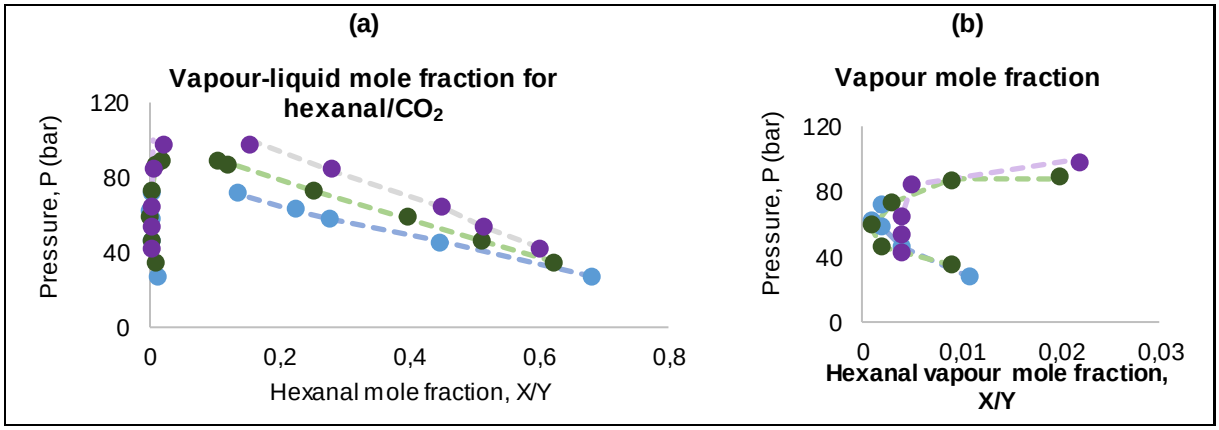

Figure 4-11: SRK-KD correlation with literature obtained VLE for binary system hexanal/CO_2 ● **40°C** (López-Porfiri *et al*., 2017); ● **50°C** (López-Porfiri *et al*., 2017); ● **60°C** (López-Porfiri *et al*., 2017); – – – **SRKKD correlation**

The mole fraction of hexanal/CO2 in vapour and liquid phases measured at variations in pressures experimentally was obtained from literature (López-Porfiri *et al.*, 2017). The SRKKD thermodynamic model regressed with little variance in the estimated pressure from the measured value. The percentage difference was determined from equation (23):

$$Difference\,(\%) = \frac{P_{measured} - P_{estimated}}{P_{measured}} \qquad (23)$$

Equation (18) was used to determine the percentage difference for binary data of *trans*-2-hexanal and hexanol. The results of the simulation for the binary system *trans*-2-hexenal/CO2 are shown in Figure 4-12.

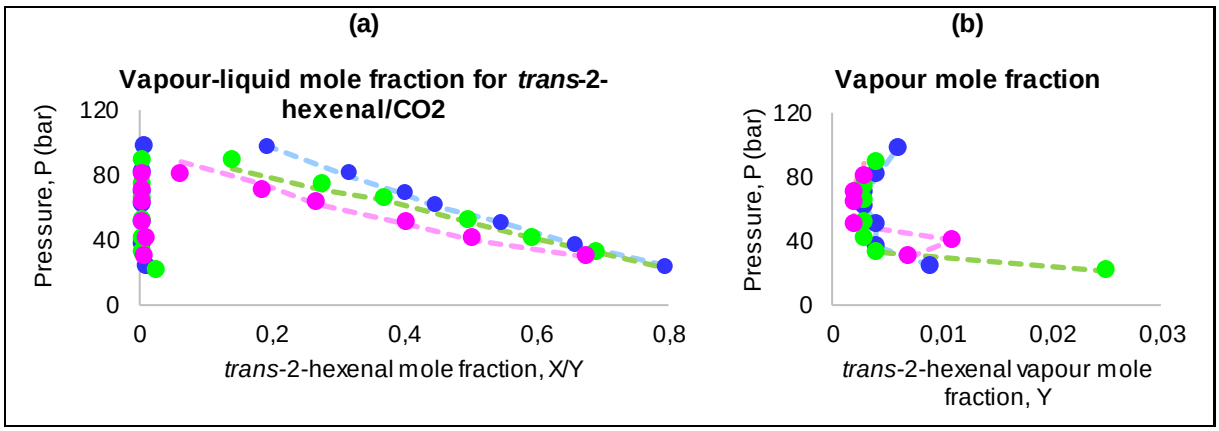

Figure 4-12: SRK-KD correlation with literature obtained VLE for binary system *trans*-2-hexenal/CO_2

● **40°C** (Villablanca-Ahues *et al*., 2021); ● **50°C** (Villablanca-Ahues *et al*., 2021); ● **60°C** (Villablanca-Ahues *et al*., 2021)**;** – – –**SRKKD correlation**

Correlation results corresponded to that obtained for hexanol/CO_2 regression. Figure 4-11 and Figure 4-12 suggests that the SRKKD model does not fit well with experimentally measured pressure obtained from literature in the vapour phase. The results of the simulation for the binary system hexanol/CO_2 are shown in Figure 4-13 (Secuianu *et al.*, 2010; Elizalde-Solis *et al.,* 2003).

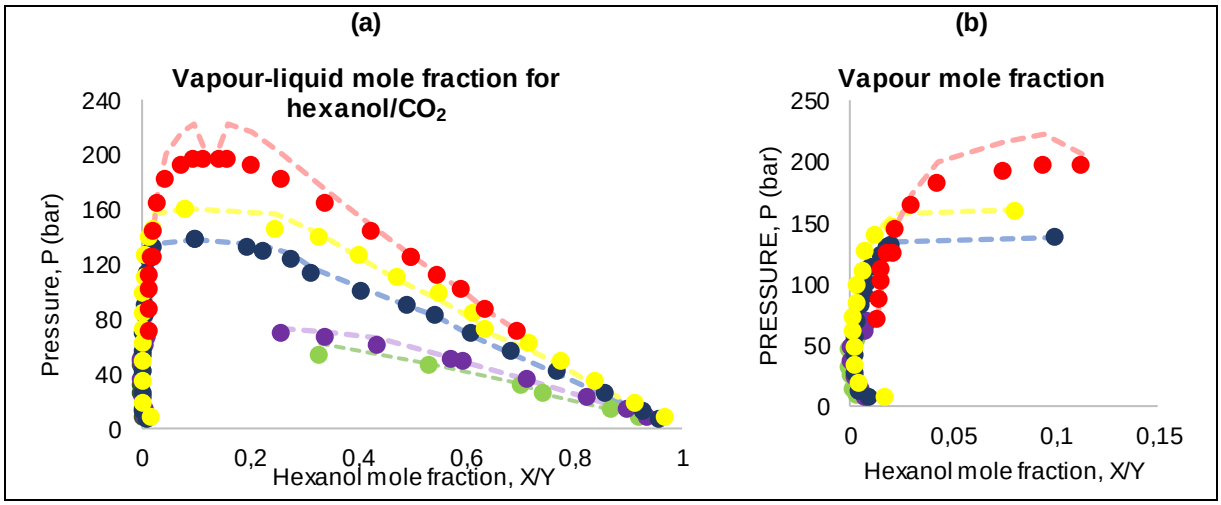

Figure 4-13: SRK-KD correlation with literature obtained VLE for binary system **hexanol/CO2**

● **20°C** (Secuianu *et al.*, 2010); ● **30°C** (Secuianu *et al.*, 2010); ● **60°C** (Secuianu *et al.*, 2010); ● **80°C** (Secuianu *et al.*, 2010); ● **124,63°C** (Elizalde-Solis *et al.,* 2003)**;**– – – **SRRKKD correlation**

The data presented in Figure 4-11, Figure 4-12, and Figure 4-13 show the binary data for the regressed Soave-Redlich-Kwong EoS with the Kabadi-Danner mixing rules (SRKKD) thermodynamic model (the lines) with experimentally obtained phase behaviour (the dots). All correlation data obtained from the process simulator for the SRKKD thermodynamic model showed difficulty in predicting the vapour composition, specifically in the critical region of CO_2.

The SRKKD model could predict liquid fractions within an acceptable range for hexanal and *trans*-2-hexenal. However, for hexanol, above 60°C the model seems to overestimate the liquid

fraction as it approaches higher pressure (greater than 150 bar), with an even larger variance in the critical region. In most cases, the model overestimated the vapour and liquid fraction for hexanol.

The hexanal correlation data varied between -3 to 2% from experimental data. *Trans*-2-hexenal varied between -10 and 6%, with mostly overestimated data points. Hexanol varied between -16 to 12%. Both hexanal and *trans*-2-hexenal presented the best correlation at 40°C. At 60°C, the model correlated well with experimentally measured data for hexanol. However, the process presents feasibility in the lower temperature ranges (Bejarano & Del Valle, 2017). In addition, the conditions investigated in 4.3.2 is well below the 150 bar mark. Seeing that the model predictability decreases at higher temperatures, the model's behaviour was only investigated at temperatures below 60°C. Therefore, based on the correlation data presented in Figure 4-11, Figure 4-12 and Figure 4-13 the SRKKD model was capable of predicting experimental measured data below 160 bar and 60°C within a reasonable range of accuracy. Using this thermodynamic model to investigate above the parameters said, would result in inaccurate phase behaviour predictions. Table 4-6 shows the regression results obtained for the temperature-dependent binary parameters for SRKKD thermodynamic model obtained from the ASPEN PLUS® process simulator:

Table 4-6 Regression results of binary parameters for the SRKKD thermodynamic model

Component i	Component j	Binary interaction parameter	
		SRKKIJ/1	SRKKIJ/2
Hexanal	CO_2	-0,4246 $\sigma^* = 0{,}0167$	0,0014 $\sigma^* = 0{,}0001$
Trans-2-hexenal	CO_2	4,6545 $\sigma^* = 0{,}9331$	-0,0143 $\sigma^* = 0{,}0029$
Hexanol	CO_2	0,2196 $\sigma^* = 0{,}0590$	-0,0003 $\sigma^* = 1{,}76E\text{-}05$

*σ = standard deviation

In Table 4-6 the regressed parameters for the binary mixture hexanal/CO_2 both the first and second element is close to zero, and in that case, the binary interaction parameter for this regression case can be regarded as insignificant due to its overall contribution. The low standard deviation for both elements shown in Table 4-6 indicates that the results from the regression converged with very little variations in the data, which shows accuracy in the model's prediction.

For the regression of the binary mixture *trans*-2-hexenal/CO_2, it can be deduced that the first element for the binary interaction parameters has a greater significance when compared to the second element and shows a negative value. Therefore, it can the temperature-dependent parameter can be neglected in this case due to its insignificance to the first element. The

standard deviation also shows the little variance in data, which shows consistency with that obtained from the regression of hexanal/CO_2. The regression for the binary mixture hexanol/CO_2 shows similar results to that obtained from the regression of the binary mixture hexanal/CO_2. The process simulator presented warnings during the regression for the binary mixtures of hexanal/CO_2 and hexanol/CO_2. However, the data presented in Table 4-6 shows consistency in the regression results obtained for all regressions. Also, the regression for both the hexanal/CO_2 mixture and hexanol/CO_2 mixture converged within 5 iterations. On the other hand, the *trans*-2-hexenal/CO_2 regression converged within 14 iterations without presenting any warnings from the process simulator. The model also indicated that the regression for hexanal and hexanol was not tightly satisfied therefore this was noted when investigating the phase behaviour of the multicomponent mixture. In summary, based on the data presented in Figure 4-11, Figure 4-12, Figure 4-13 the SRKKD thermodynamic model was a capable fit to experimental measured data between 40°C and 60°C for up to 150 bar. Therefore, for the investigation of the phase behaviour for the process model, conditions were set within the given range.

4.3.2. Multicomponent phase behaviour and separability

The phase behaviour for the multi-component mixture was simulated with the model presented in Figure 4-14 in Aspen Plus®. Literature VLE was correlated with the SRKKD thermodynamic model. Binary interaction parameters obtained from the regression was used to simulate the multicomponent mixture through a two-phase outlet flash drum. Vapour and liquid phases were calculated by minimisation of the total Gibbs energy. The model was validated with experimental pilot plant and literature data such as to completely attain objective 1. In addition, results for the multicomponent mixture and the separability described in this section fulfilled the requirements for objective 2.

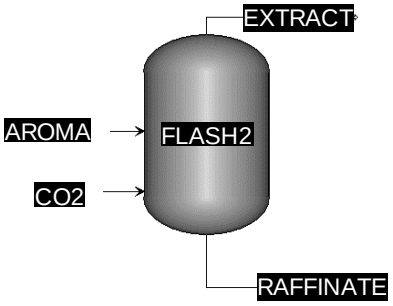

Figure 4-14: FLASH2 unit in Aspen Plus®

For calculation purposes, a basis of 100 kg/hr was selected. In Figure 4-14 the **AROMA** feed comprised of selected compounds presented in Table 4-7, also used for the model solution. The **CO2** flow rate was set to the required solvent-to-feed ratio. **EXTRACT** represented

compounds enriched in the vapour phase and **RAFFINATE** compounds enriched in the liquid phase.

Table 4-7: Mass fraction of organics and water in apple aroma

Compound	Mass Fraction in aroma concentrate from industry	Mass fraction in 5% solution
Hexanal	9,01E-04	1,47E-02
Trans-2-hexenal	3,56E-03	5,82E-02
Hexanol	3,02E-01	4,93
Distilled water	99,7	95

The 5% concentration model solution comprised of the same fraction for the organics as presented in the 0,3% concentration apple aroma concentrate as obtained from industry produced apple aroma concentrate. The organic fraction comprised of 0.3% hexanal, 1.2% *trans*-2-hexenal and 98.5% hexanol. Thus, only the water fraction and total organics fractions changed.

4.3.2.1. Validation of model phase behaviour

The model was validated with experimental literature and pilot plant data. A flash drum was selected to model the phase behaviour of the process. The model was investigated at the process conditions obtained from literature and pilot plant experiments. For experimental work, a model solution of 5% organics was prepared due to the low fraction of organic compounds comprised in industry produced apple aroma. The 5% organics concentration was based on the fraction of the compounds presented in Table 4-7. Therefore, for validation, the model was investigated at the 5% total organics concentration. Literature data comprised of a 0,175% concentration organics. The water, total organics (hexanal + *trans*-2-hexenal + hexanol) and total aromas (hexanal+ *trans*-2-hexenal) vapour fractions obtained from the model are presented in combination with the experimental measured data. The accuracy of the model was shown with the correction factors obtained from the difference in experimental measured data and model data.

Validation with literature experimental data

The model solution and conditions investigated by Bejarano & del Valle (2017) were investigated with the process model to obtain the data presented in Figure 4-15, Figure 4-16, Figure 4-17, Figure 4-18, Figure 4-19 and, Figure 4-20. To validate the model the enriched vapour fractions for water and the total organics obtained from the process model were compared with experimental data. A correction factor was obtained for the results using equation (24) to show model results with experimental data as presented in Chapter 5.

Similarly, the phase behaviour for the 5% organic concentration model solution was investigated at the conditions selected in Chapter 3 obtained from the data described in 3.7.

$$Correction\ factor, CF = \frac{\sum(y_{i,\ exp} - y_{i,\ est})}{n} \quad (24)$$

To show the predictability of the model, feed concentrations of 0.175%, 1.75% and 17.5% at the given CO_2 densities and solvent-to-feed (S/F) ratio. The model predicted vapour content obtained for water are presented in Figure 4-15, Figure 4-16, and Figure 4-17 in combination with experimental measured data points to show overall trends obtained from the model. Similarly for the total organics (hexanal, *trans*-2-hexenal and hexanol) presented in Figure 4-18, Figure 4-19 and, Figure 4-20. 0.175%, 1.75% and 17.5% feed concentrations were investigated using the model as it was noted that the overall prediction trend for the model increased with increasing feed concentrations. However, this results an increased correction factor because of increasing differences between experimental and model feed concentration. Feed concentrations were fluctuated by increasing overall total organics concentration and reducing water concentration in the feed. Therefore, organic concentrations fraction within the total organics remained constant.

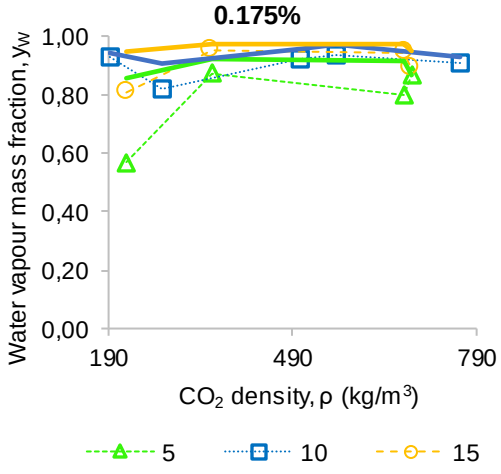

Figure 4-15: Variation of enriched vapour **water content** (mass fraction) for **0.175% organics** with CO_2 density and S/F ratio.

The dotted symbols (–Δ–, ··□··, --○--) represent experimentally measured data and straight lines (—, —, —) model estimated data at S/F ratios 5, 10 and 15

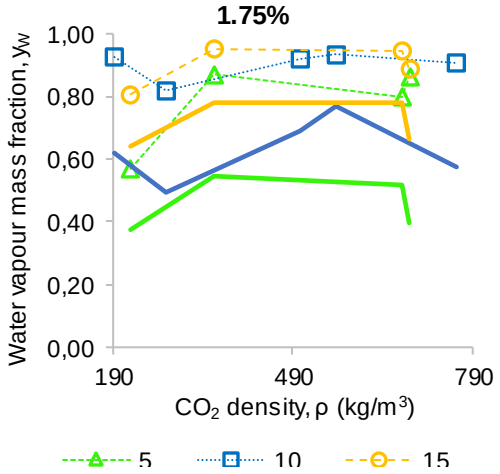

Figure 4-16: Variation of enriched vapour **water content** (mass fraction) for **1.75% organics** with CO_2 density and S/F ratio.

The dotted symbols (–Δ–, ··□··, --○--) represent experimentally measured data and straight lines (—, —, —) model estimated data at S/F ratios 5, 10 and 15

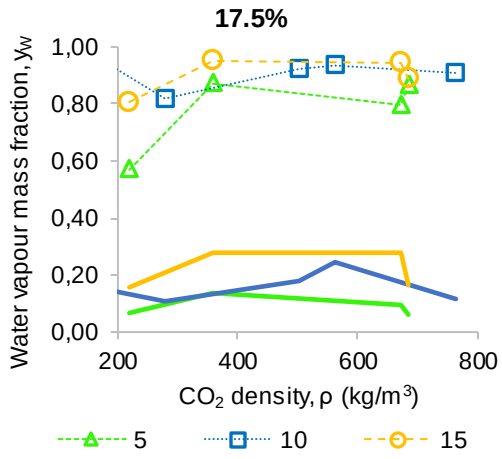

Figure 4-17: Variation of enriched vapour **water content** (mass fraction) for **17.5% organics** with CO_2 density and S/F ratio.

The dotted symbols (–Δ–, ··□··, --○--) represent experimentally measured data and straight lines (—, —, —) model estimated data at S/F ratios 5, 10 and 15

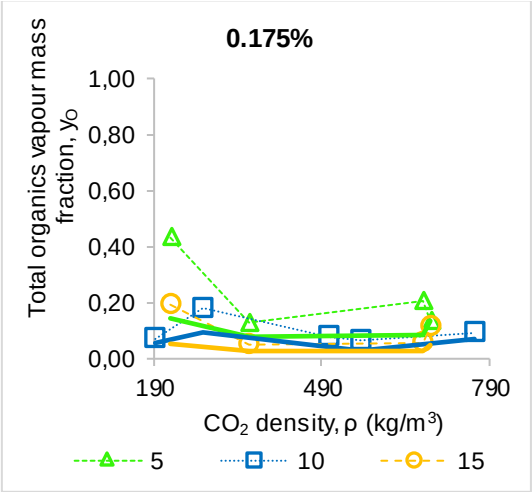

Figure 4-18: Variation of enriched vapour **total organics content** (mass fraction of hexanal, *trans*-2-hexenal and hexanol) for **0.175% organics** with CO_2 density and S/F ratio.

The dotted symbols (–Δ–, ··□··, --○--) represent experimentally measured data and straight lines (—, —, —) model estimated data at S/F ratios 5, 10 and 15

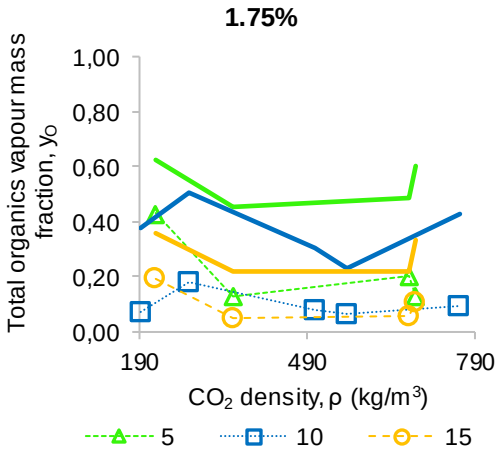

Figure 4-19: Variation of enriched vapour **total organics content** (mass fraction of hexanal, *trans*-2-hexenal and hexanol) for **1.75% organics** with CO_2 density and S/F ratio.

The dotted symbols (–Δ–, ··□··, --○--) represent experimentally measured data and straight lines (—, —, —) model estimated data at S/F ratios 5, 10 and 15

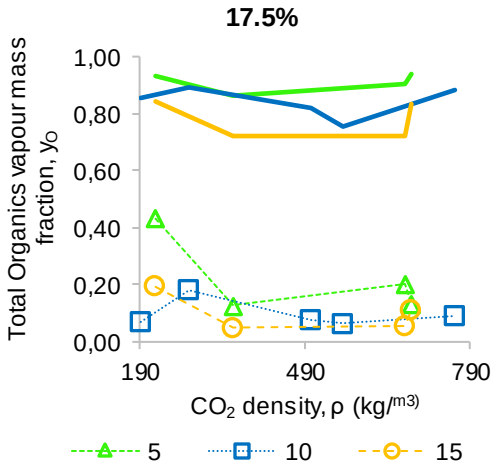

Figure 4-20: Variation of enriched vapour **total organics content** (mass fraction of hexanal, *trans*-2-hexenal and hexanol) for **17.5% organics** with CO_2 density and S/F ratio.

The dotted symbols (–Δ–, ··□··, --○--) represent experimentally measured data and straight lines (—, —, —) model estimated data at S/F ratios 5, 10 and 15

So ultimately, the ratio of hexanal, *trans*-2-hexenal, and hexanol remained constant. Thus, indicating that the model's accuracy in predicting overall phase behaviour trends are adequate by investigating the feed at a concentration 10^2 times the initial concentration. However, this is only viable above a S/F ratio for 10 and above, as shown in the previous figures. Below a S/F

of 10, the model's predicted vapour contents had a greater overall average percentage difference.

At a S/F of 5, the predictability of the model remained the same and well above the literature experimental measured data after applying the correction factors. The average percentage difference remained unchanging with increasing feed concentrations. At a S/F ratio of 10, the model presented the least variations with experimental data. The most deviations were presented at 0.175% feed concentration regardless of increasing feed concentrations. At a 1.75% feed concentration, the standard deviation for the overall data indicates a slight accuracy when compared to 0.175% and 17.5% concentrations. Overall water concentration predictions were the most accurate out of all the data. Almost all data points were equivalent to experimentally measured vapour concentrations. In addition, with increasing CO_2 density the model's accuracy decreases but not significantly. For the organic compounds, the average % differences were similar. The average % difference was determined from equation (25).

$$\%\, difference = \frac{y_{i,\ est} + CF}{y_{i,\ exp}} \tag{25}$$

Data in Table 4-8 presented the overall average percentage difference at increasing solvent-to-feed ratios for each feed organics concentration. It does not show the effect of the CO_2 density. 100% average difference means no deviation from experimental value.

Table 4-8: Model's predictability accuracy for Bejarano & del Valle (2017)

Compound	S/F ratio					
	5		10		15	
	Average % difference	Standard deviation	Average % difference	Standard deviation	Average % difference	Standard deviation
			0.175%			
Hexanal	137%	59%	106%	29%	126%	50%
Trans-2-hexenal	128%	49%	109%	25%	130%	61%
Hexanol	118%	41%	106%	21%	124%	55%
Water	103%	20%	100%	3%	100%	6%
			1.75%			
Hexanal	129%	22%	82%	137%	87%	62%
Trans-2-hexenal	124%	24%	86%	89%	98%	25%
Hexanol	114%	14%	86%	90%	95%	28%
Water	102%	12%	100%	8%	100%	3%
			17.5%			
Hexanal	137%	53%	99%	81%	92%	59%
Trans-2-hexenal	128%	45%	102%	53%	102%	25%

Hexanol	118%	35%	101%	53%	98%	27%
Water	103%	21%	100%	5%	100%	4%

At a S/F of 5, the predictability of the model remained the same and well above the literature experimental measured data after applying the correction factors. The average percentage difference remained unchanging with increasing feed concentrations. At a S/F ratio of 10, the model presented the least variations with experimental data. The most deviations were presented at 0.175% feed concentration regardless of increasing feed concentrations. At a 1.75% feed concentration, the standard deviation for the overall data indicates a slight accuracy when compared to 0.175% and 17.5% concentrations. Overall water concentration predictions were the most accurate out of all the data, with almost all data points being equivalent (100%) to experimentally measured vapour concentrations. For the organic compounds, the average % differences were similar.

Above a S/F of 5 and feed concentration of 1.75% (10^1 times initial organics concentration in feed), the model seems to be capable of predicting the phase behaviour of experimental data points presented with deviations. Even better phase behaviour is predicted at 10^2 times the initial feed organics concentration. The correction factor obtained for a 17,5 % feed concentration on average is presented in Table 4-9. The average was determined over a range of CO_2 densities and are shown in combination with the standard deviation obtained from equation (17). The correction factors obtained for 17,5% is presented as it shows the best correlation with literature phase behaviour.

Table 4-9: Correction factors for 17,5% feed concentration

	S/F ratio	Hexanal	*trans*-2-hexenal	Hexanol	Water
CF	5	-0.10	-0.19	-0.39	0.69
σ_i		0.02	0.04	0.06	0.11
CF	10	-0.11	-0.21	-0.42	0.74
σ_i		5.70E-03	1.13E-02	0.02	0.04
CF	15	-0.10	-0.19	-0.39	0.68
σ_i		4.83E-03	0.01	0.01	0.03

Data presented in Table 4-9 confirmed that the accuracy of the model is improved with increasing S/F ratios. Standard deviations decrease with increasing S/F ratios. The correction factor for water and hexanol is also greater than that obtained for hexanal and *trans*-2-hexenal. Hexanol and water fractions yield higher concentrations in the vapour phase, thus it is expected that the correction factors will be higher as it is in terms of mass. The negative values indicate that the model over-estimated the fractions enriched in the vapour phase. Overall, the CF doesn't change significantly with variations in the S/F ratio for each compound but the standard deviations i.e., accuracy reduces. Therefore, the best correction factor was obtained at a S/F

ratio of 15 and thus this is ultimately the correction factor to adjust vapour fractions obtained from the model.

Validation with pilot plant experiments

The 5% organics concentration feed was investigated using the process model developed in 4.3.2. The model was investigated at the same conditions (i.e., temperature, pressure, and S/F ratio) used in experiments 1 and 2. Product quality and yield are compared to validate the model. Data obtained from the model, in combination with pilot plant data, are shown in Table 4-10. It presented the mass fraction of organics enriched in the extract/vapour phase. For the first experiment, the conditions were at 40°C and 70 bar. Experiment 2 was set at 50°C and 100 bar.

Table 4-10: Model's predictability for vapour phase (extract) pilot plant data

	Experiment 1 40°C, 70 bar		**Experiment 2 50°C, 100bar**	
	Pilot plant	**Model**	**Pilot plant**	**Model**
Total organics (*mass fraction*)	0.99	0.88	5.96E-02	0.73
Hexanal	1.97E-03	2.58E-03	4.65E-04	2.15E-03
Trans-2-hexenal	6.01E-02	1.02E-02	2.80E-03	8.51E-03
Hexanol	0.93	0.86	5.64E-02	0.72
Water concentration	8.42E-03	0.12	0.94	0.27
Total yield	25%	6%	33%	7%

For experiment 1, the model underpredicted the phase behaviour of total organics and over predicted the water's concentration. Contrarily, the model overpredicted for organics and under predicted the water's concentration. The trends from model estimations for experiment 2 corresponds with process model validation data of Bejarano & del Valle (2017). In addition, the model presented consistency in the overall predictions at a 0.175% feed concentration. On the other hand, the model presented larger deviations for experiment 2 as shown in Table 4-10. The range of deviation between model estimated and pilot plant data corresponds with the small range of deviation obtained for the 0.175% feed concentration of Bejarano & del Valle (2017). Which indicated that the large deviation in experiment 2 resulted from a possible error in the data collected. Nonetheless, the feed compositions in this work varied from that in the work of Bejarano & del Valle (2017). Therefore, the interactions of organics and difference in concentrations could have influenced the estimated model data.

The model showed accuracy in the estimation of hexanol enriched in the vapour phase for experiment 1. *Trans-2-hexenal* showed the highest deviation at nearly -500% at these conditions. This shows that the model was not capable of predicting the phase behaviour of

trans-2-hexenal. For both hexanol and *trans*-2-hexenal, the model underestimated vapour fractions. However, it overestimated water and hexanal fractions. The total organics fraction was well underestimated by 13%. Thus, as a result, water enriched in vapour would be underestimated. For experiment 2, the organics fraction was overestimated by 92%. This was mainly contributed by the overestimated hexanol fraction. In this case, *trans*-2-hexenal presented the least deviation from experimentally measured data. Estimated water enriched was completely underestimated by 250%. So even though, the model overestimated the organics fraction, water's concentration still varied significantly.

Data obtained from the process model completely underpredicted total product yield. The model data was based on a 100 kg/hr feed rate. As a result, product yield might not be accurate. However, differences between the two conditions are by 1%. Whereas experiments showed a difference of 8% in the product yield obtained. The process model data showed a significant deviation from experiment 2, greater than 65% for all compounds. Water concentration deviated the most. However, there is a clear shift in the overall concentrations between the two experiments. Therefore, it could be that the model does not accurately account for this change.

4.3.2.2. Multicomponent phase behaviour

An investigation of the effect of temperature, pressure and solvent-to-feed ratio on the mole fraction enriched in liquid and vapour phases established a range of conditions that benefits the separation as presented in Figure 4-21, Figure 4-22, Figure 4-23, Figure 4-24, Figure 4-25, and Figure 4-26. To establish the distribution of a component between the vapour and liquid phases for a multicomponent mixture, the distribution coefficient was determined from the following equation:

$$K_i = \frac{y_i}{x_i} \tag{26}$$

And the separation factor:

$$SF_{ij} = \frac{K_i}{K_j} \tag{27}$$

Liquid and vapour fractions were determined by using the FLASH2 unit at the given operating conditions i.e., temperature and pressure. The range of operating conditions suggested by literature was investigated to determine their effect on the separability of the following pairs such as to increase the product quality:

I. Hexanol (undesired key apple aroma compound) /water
II. Hexanal & *trans*-2-hexenal (valuable key apple aroma compounds)/water
III. Hexanal & trans-2-hexenal/hexanol

The feed comprised of 0,3% selected apple aroma compounds and the concentrations depended on the concentration identified in South African produced apple aroma, presented in 4.3.2.1. The feed solution was investigated at a range of 40 – 60°C, 80 – 140 bar and S/F ratios 5 – 15 as shown in Figure 4-21, Figure 4-22, Figure 4-23, Figure 4-24, Figure 4-25, and Figure 4-26.

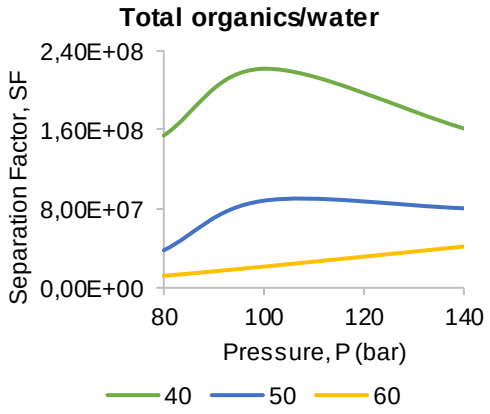

Figure 4-21: Variation of separation factor for **total organics/water** with temperature (°C) and pressure (bar)

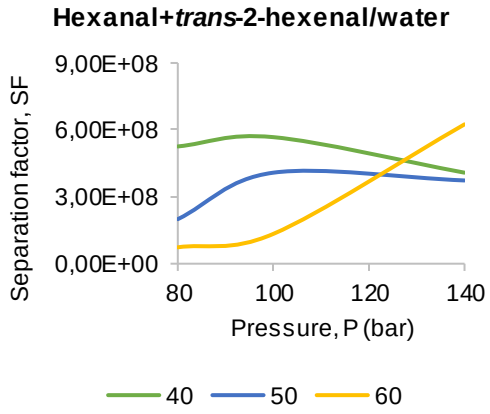

Figure 4-22: Variation of separation factor for **hexanal+*trans*-2-hexenal/water** with temperature (°C) and pressure (bar)

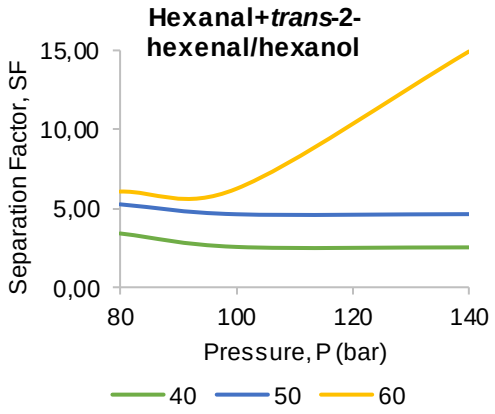

Figure 4-23: Variation of separation factor for **hexanal+*trans*-2-hexenal/hexanol** with temperature (°C) and pressure (bar)

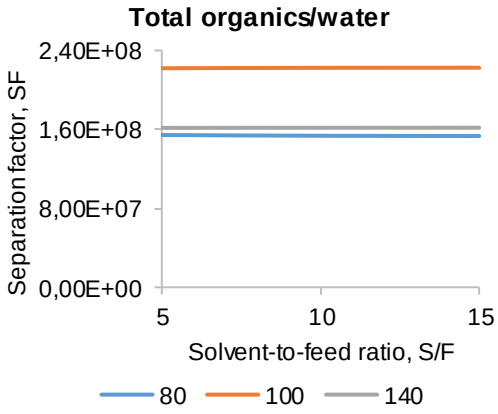

Figure 4-24: Variation of separation factor for **total organics/water** with pressure (bar) and S/F ratio

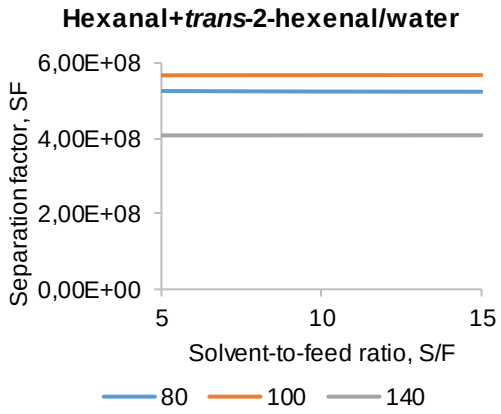

Figure 4-25: Variation of separation factor for **hexanal+*trans*-2-hexenal/water** with pressure (bar) and S/F ratio

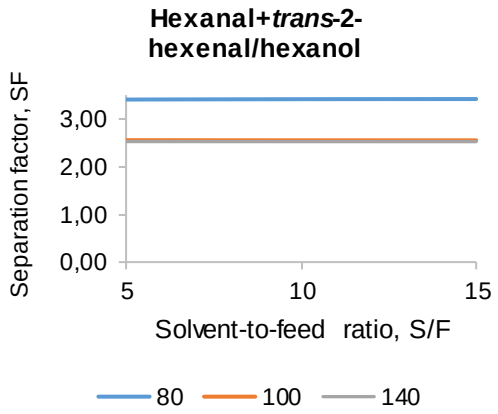

Figure 4-26: Variation of separation factor for **hexanal+*trans*-2-hexenal/hexanol** pressure (bar) and S/F ratio

Generally, a separation factor >2 indicates that the separation of the selected compounds is achievable and that it is possible to enrich the vapour phase with these said compounds. Figure 4-21, Figure 4-22, Figure 4-24, Figure 4-25 show very large separation factors for the total organics (i.e., hexanal, *trans*-2-hexenal and hexanol) and hexanal+*trans*-2-hexenal separation from water, which indicates that the separation is over-achieved.

This suggests that for the range of operating conditions investigated the organic compounds are almost completely enriched in the vapour phase and water enriched in the liquid phase. For both the separation pairs, total organics/water and hexanal+*trans*-2-hexenal/water, the separation factors followed a similar trend. The valuable aroma/water presented much higher values than that obtained for the total organics/water separation. This is evidence that the separation for the hexanal+*trans*-2-hexenal/water pair is easily attained when compared to the total organics/water separation.

At constant pressure, the separation factors for both separation pairs decrease with increasing temperature, with a substantial decline between 40 and 50°C as shown in Figure 4-21 and Figure 4-22. This applied to a pressure range between 80 and 120 bar. At constant temperature, between 80 and 100 bar, the total organics enriched in the vapour phase increases for 40°C and 50°C and reaches its peak at 100 bar. After 100 bar, the separability is decreased and at 50°C it remained almost constant with increasing pressure.

On the other hand, at 60°C the separability increased. While conversely, at increasing S/F ratio, the separability for the total organics/water pair remained unchanging at constant pressure as shown in Figure 4-24. The highest separation factor was obtained at 100 bar. Between 80 and 140 bar the total organics enriched in the vapour phase remained constant, indicating that 100 bar could achieve the best separation when taking the effect temperature into consideration. Operating at a pressure above 100 bar would result in decreased

separability, thus obtaining water-rich vapour and consequently reducing the product quality of the vapour phase.

Similarly, 100 bar seems to favour the hexenal+*trans*-2-hexenal/water separation as shown in Figure 4-25. At 80 bar the separation is slightly decreased and further lowered at 140 bar. Figure 4-22 indicates that hexenal+*trans*-2-hexenal enriched in the vapour phase rapidly increases above 100 bar at 60°C. However, below 100 bar, the separation favours lower temperatures. This indicates that the same separability could be achieved at lower operating conditions. It is thus best to operate at a lower temperature to reduce energy requirements of the process if the higher operating temperature would result the same product quality.

Separation factors obtained for the separation of hexanal+*trans*-2-hexenal/hexanol presents significantly lower values than those obtained for the total organics/water and hexanal+*trans*-2-hexenal/water separation pairs. Thus, the valuable aroma and hexanol are not as easily separable. On the other hand, the separation is achievable as indicated by the separation factors obtained between 2.5 and 15 (which is greater than 2) more likely in the higher operating conditions range. Figure 4-22 indicates that an increase in temperature at constant pressure would result in a significant increase in separability. However, operating at a temperature below 50°C would not affect the separability much. Increasing pressure has very little impact on the separability of hexanal+*trans*-2-hexenal and hexanol at 40°C and 50°C. Contrastingly, at 60°C the separability significantly increases above 100 bar. The solvent-to-feed ratio has a very low effect on the separability (between 2.5 and 3.5) as shown in Figure 4-26. The low separation factors obtained in Figure 4-26 shows the separability is not much influenced by changes in pressure at constant S/F ratio. However, a drop between 80 and 100 bar at 60°C indicates that the separability reduces with increasing pressure. Above 100 bar, increasing pressure in combination with the S/F ratio has no impact on the separability of hexanal+*trans*-2-hexenal and hexanol. It is thus clear that having a lower solvent-to-feed ratio would be preferable and feasible for the separation of hexenal+*trans*-2-hexenal/hexanol.

It is thus obvious that the total organics/water and hexanal+*trans*-2-hexenal/water separation pairs are easily separable as indicated by the significantly high separation factors. In contrast, separating hexanal+*trans*-2-hexenal and hexanol would require an additional processing step as the range of conditions tested indicates that these compounds are separable but in a limited range only. The goal was to increase the product quality by enriching vapour with not only total organic compounds but valuable apple aroma compounds (i.e., hexanal and *trans*-2-hexenal) and enrich the liquid phase with water. Based on the data presented total organics and water are easily separable, thus product quality can be significantly increased.

4.4. Retrofitting of CC $scCO_2$ fractionation column to current process layout

Process route layout considerations were based on the process described in Chapter 2, as shown in Figure 4-27.

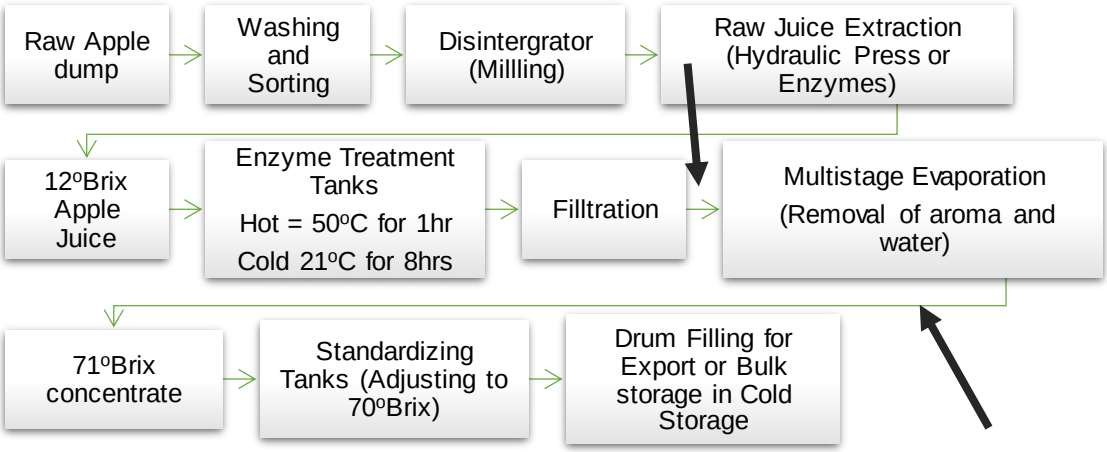

Figure 4-27: Industrial layout of apple concentrate production facility

The CC-fractionation column was to be retrofitted to the process layout presented in Figure 4-27 such as to save resources, production delays and costs for fractioning apple aroma constituents. Literature reveals that this process usually consists of a 3-stage evaporation process and it is at the second stage where the apple aroma compounds are removed at 90°C and vacuum. The following locations for the CC-fractionation column in the process was considered:

1. Before the multistage evaporation after filtration
2. After the second stage of the multistage evaporator.

Ideally, retrofitting the CC-fractionation to the process before the multistage evaporation could result in higher product quality because the compounds have not been exposed to any high temperatures thus preserving thermal labile compounds. However, the feed at this point contains a variety of compounds mainly water, carbohydrates, proteins, sugars, and organic compounds and could contain some solid particles. This poses several difficulties in the CC-fractionation such as the build-up of products in pipelines and column (due to column packing), regular cleaning of equipment, separation efficiency, etc. However, after the multistage evaporation, only apple aroma and water are obtained. This means that separation will require less energy due to a less complex feed. After the considerations above, it was decided to retrofit the CC fractionation column to after the multistage evaporation process.

Multi-component phase behaviour data indicates that a near perfect separation of total aroma compounds and water can be achieved with the proposed method. But further optimization to

the current validated developed process model was required to further increase product quality i.e., reduce water enriched in the vapour phase. Due to the low allowable operating temperature range, the system consumes way less energy than its counter industrialised processes. The model investigated in 4.3.2 was used as a basis for the development of each process layout and as a base of comparison. Other major units (such as heat exchangers, pump, and valves) and vessels (separators) that form part of the process remains the same for each process route layout scenario considered and the operating conditions were kept constant for each layout, therefore it was not included as part of the process model.

4.4.1. Process layout considerations

The control layout presented in Table 4-11 was based on the model developed in 4.3.2 to investigate the multicomponent phase behaviour for the proposed method of fractionation. The Aspen Plus® process simulator was used to develop the process model and to simulate the phase behaviour of the process using binary phase equilibrium data correlated with the SRKKD thermodynamic model. The correlation was performed under the **Properties** data menu option in the Aspen Plus® process simulator and the SRKKD thermodynamic model was selected to simulate the phase behaviour of the process under the **Methods Specification** in the **Properties Methods** in the list box. The model was developed in the **Simulation** option in the data menu and comprised of a separating vessel (labelled as **FLASH2** in the Aspen Plus® process simulator) with two inlet streams, AROMA and CO_2, and two outlet streams, RAFF and EXTRACT, that represented the streams to and from the pilot plant CC fractionation column. The FLASH2 model was selected as it performs vapour liquid calculations at equilibrium. Which is not always the case for industrial applications but for comparative purposes, steady-state operation was assumed.

A model feed based on commercially produced apple aroma represented the AROMA stream. It comprised water and selected apple aroma compounds. The CO_2 flow rate was set at a solvent-to-feed ratio of 5. Multicomponent phase behaviour data indicated that low S/F ratios are optimum for the separability of the total organic compounds present and water. Thus, the best product quality would be obtained. The conditions of the process model were optimised to obtain the optimum conditions by varying key operating and design variables using the **Sensitivity Analysis** tool in the **Data** menu under the **Model Analysis Tools**. In addition, this tool was used to optimise each layout.

The layouts presented in Table 4-11 were investigated to obtain the best-suited process layout for the proposed process. Considerations that presented no separability or significantly decreased product quality were not included such as the recycle of the liquid phase (RAFF). The following design variables were considered for the process layouts presented:

i. Optimum operating conditions for the fractionation process (i.e. pressure, temperature, and S/F ratio).
ii. The purge of key apple aroma compounds enriched in the liquid phase.
iii. Purity of product.
iv. Recovery of key apple aroma compounds enriched in the liquid phase.
v. Recycle of extract
vi. Process energy requirements

Table 4-11: Description of process layout considerations

Process layout consideration	Consideration	Description/Objective
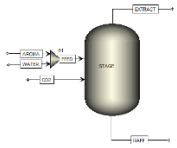 *Control*	*Base of comparison*	Gibbs flash algorithm simulated as a single flash drum used as a base of comparison for the investigation of a process layout consideration.
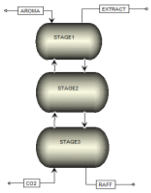 *1*	*Counter-current Multistage fractionation*	Investigation of CC multistage fractionation with *n* number of stages compared based on product quality, feed concentration, energy requirements and yield.
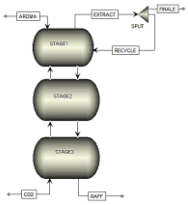 *2*	*CC Multi-stage fractionation with recycling of extract.*	Investigation of a multistage CC-fractionation column including a recycle stream of the extract obtained from the fractionation column based on the split fraction.

The AROMA stream feed comprised of 0.3% organics (hexanal, *trans*-2-hexenal, hexanol) and water. Both the feed streams were kept at the same conditions as the separating vessel to evaluate the unit only. Therefore, the energy of the process obtained from the Aspen Plus® process simulator showed a low value (approx. 33 W), which could be a result of energy required for the separation to occur and not heat duty required. Thus, regarded as insignificant. The first process layout considered presented in Table 4-11 was CC multi-stage fractionation with *n* number of stages. This process layout aimed to obtain a solute-free raffinate and a product of higher percentage key apple aroma compounds. Therefore, improving product quality. In addition, each additional stage was optimised to obtain the optimum conditions for fractionation at each stage. The optimum number of stages was established by investigating each additional based on product quality, feed concentrations, and yield. The second process layout scenario presented in Table 4-11 comprised of the best layout obtained from the CC

multi-stage fractionation with a recycle stream. This process aimed to investigate the recycling of the extract to minimise the vapour fraction of the water such that most water is enriched in the liquid phase. The split fraction was investigated based on the product quality, organics recovery and yield to establish the optimum split fraction.

4.4.1.1. Process layout: Consideration 1

Results from 4.3.2 indicate that a single staged process at equilibrium will be able to enrich most of the water into the liquid phase. However, it is likely that not all key apple aroma compounds present in the aroma concentrate feed were recovered. Generally, CC fractionation columns are designed as packed columns with a mass transfer agent (CO_2), with the packing ultimately increasing the mass transfer rate in the column (Brunner, 2009). The separation in a packed column occurs as a staged process. Thus, an addition of *n* number of stages was considered in counter-current mode for the recovery of all key aroma compounds. Further investigation included the enrichment of hexanol (described as undesired to the characteristic apple aroma scent/odour) and water in the liquid phase.

For the process layout scenarios presented in this section; CC-multistage fractionation of apple aroma concentrate with the addition of *n* number of stages was investigated. Each stage added to the base case was represented by a separating vessel (FLASH2) interlinked counter-currently to achieve the desired separation at the operating conditions inputted. To establish the number of stages/flash units required to fractionate the model feed solution (i.e., apple aroma concentrate), the process was investigated at a range of solvent-to-feed (S/F) ratios at low operating conditions, 40°C and 80 bar, as represented in Figure 4-28. The S/F ratio was investigated as it had no significant impact on the separability using a single flash unit as presented in Figure 4-28, Figure 4-29, Figure 4-30, and Figure 4-31. Therefore, if fractions changed it was considered a result of an additional flash unit.

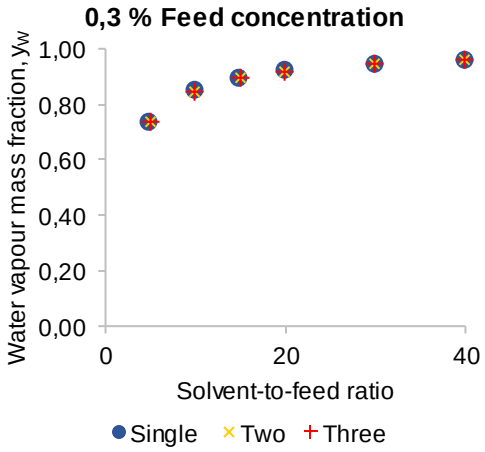

Figure 4-28: Variation of **water content** in the vapour phase with **S/F ratio** and ***n* number of stages** for 0,3% feed conc.

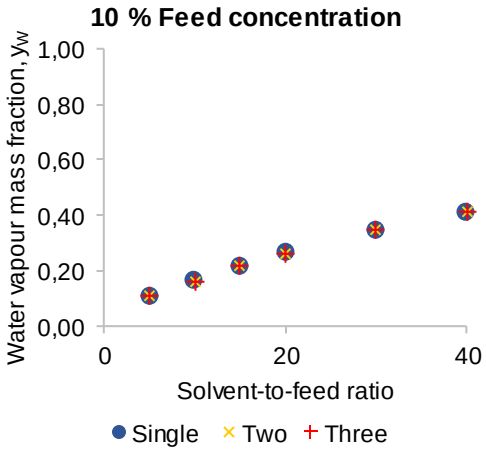

Figure 4-29: Variation of **water content** in the vapour phase with **S/F ratio** and ***n* number of stages** for 10% feed conc.

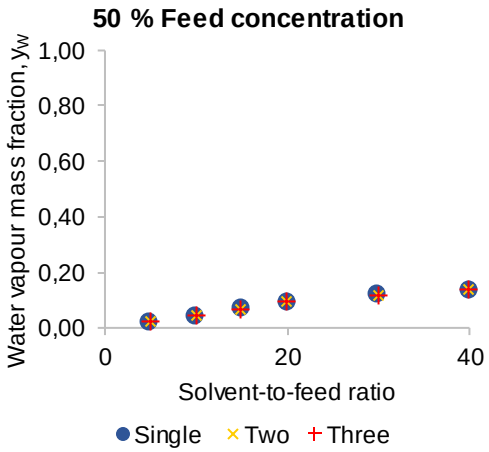

Figure 4-30: Variation of **water content** in the vapour phase with **S/F ratio** and ***n*** **number of stages** for 50% feed conc.

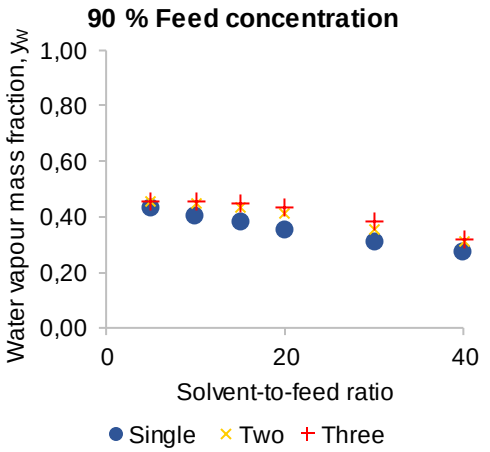

Figure 4-31: Variation of **water content** in the vapour phase with **S/F ratio** and ***n*** **number of stages** for 90% feed conc.

A further investigation established whether the number of stages influenced the product quality and yield obtained from the process. Product quality was established based on enriched vapour water content. Data presented in Figure 4-28 indicated that water enriched in the vapour phase increased with increasing S/F ratios but remained unchanging after a S/F ratio of 20. The data revealed that an additional stage would result in no changes in the phase behaviour of the process. Thus, indicating that the separation occurs as a single stage. Therefore, to further establish the addition of *n* number of stages, reintroducing feed at a higher concentration (i.e., the product obtained from Figure 4-28) was investigated. Results of variation in enriched vapour water content are presented in Figure 4-29, Figure 4-30, and Figure 4-31. The feed concentrations investigated was from 10 to 90% and results were obtained at 40°C and 80 bar.

As the water flow rate increased, the yield increased. Thus, the higher yields were obtained at a lower product quality with a near 100% recovery for all organics. The organics recovery remained the same, regardless of the number of stages or feed concentration, except for concentrations exceeding 90%. Note that the model does not represent actual stages, but a flash unit was added to simulate the phase behaviour of the compounds. It does not include the mass transfer of the process. Therefore, experimental data might vary from these findings. Nonetheless, a single flash unit is just as good as a three-staged flash interlinked counter-currently in terms of product quality and recovery.

It is thus obvious that increasing the number of stages does not influence the product quality and product yield below a 50% organics feed concentration. Reintroducing a feed at 90% organics, clearly indicates that enriched vapour water content increases with the increasing number of stages. In addition, overall, the water content has significantly increased from 10% to ~40% in the vapour phase as shown in Figure 4-31. The content then decreases with increasing S/F ratios. This simply means that a changeover of the product stream occurs above

a 50% feed concentration. Therefore, in that case, the product would be obtained in the liquid phase and not the vapour phase. However, a higher product quality than the feed will not be obtained. The percentage yield obtained from equation (28) is presented in Figure 4-32, Figure 4-33, and Figure 4-34.

$$\%\, product\ yield = \frac{\dot{m}_{vapour}}{\dot{m}_{feed}} \tag{28}$$

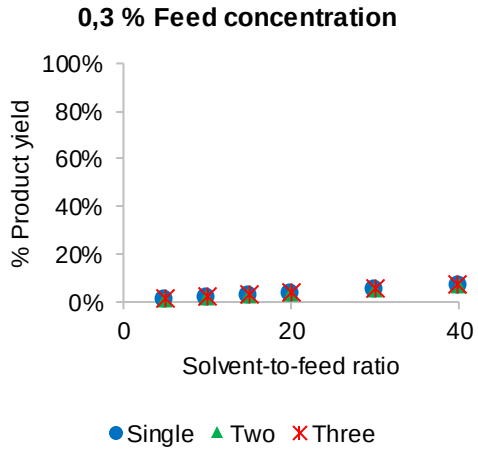

Figure 4-32: Variation of **% product yield** in the vapour phase with **S/F ratio** and ***n*** **number of stages** for 0,3% feed conc.

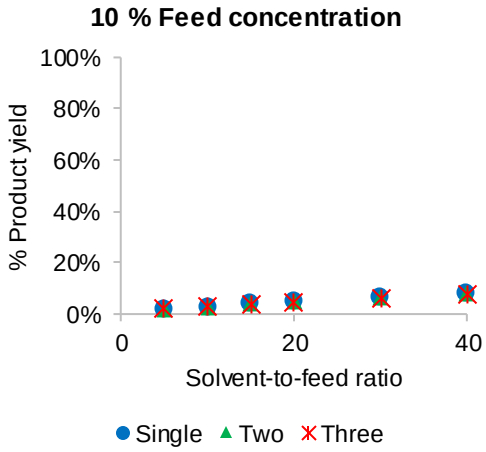

Figure 4-33: Variation of **% product yield** in the vapour phase with **S/F ratio** and ***n*** **number of stages** for 10% feed conc

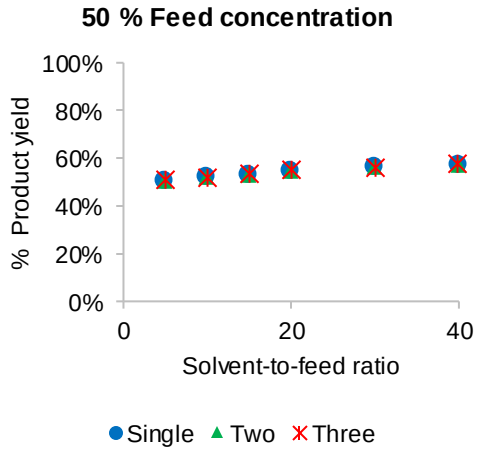

Figure 4-34: Variation of **% product yield** in the vapour phase with **S/F ratio** and ***n*** **number of stages** for 50% feed conc

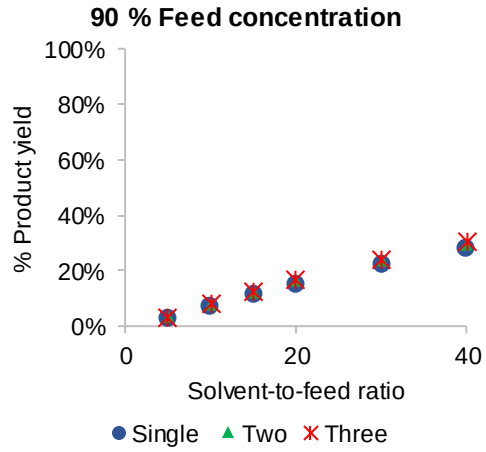

Figure 4-35: Variation of **% product yield** in the vapour phase with **S/F ratio** and ***n*** **number of stages** for 90% feed conc

Similarly, the percentage product yield obtained indicates that yield increases with increasing S/F ratios. It remained constant with an increasing number of stages. Overall, the percentage yield increases at a much lower rate (remains almost unchanged) for feed concentrations 0.3 to 50%. In contrast, the percentage yield increases significantly with increasing solvent-to-feed ratios for 90%. However, increased yields were a result of increased water enriched in the vapour phase. In addition, there were very few changes in percentage product between 0.3 and 10% organics. But there is a significant difference between the water enriched in the

vapour phase shown in Figure 4-28 and Figure 4-29. Therefore, reintroducing a feed of 10% organics would result in a smaller product yield at much higher product qualities. Which indicates that product obtained from first fractionation, will have to be reintroduced to significantly improve product quality.

A sensitivity analysis performed using the Aspen Plus® process simulator (explained in Chapter 3) assisted with establishing the effect of temperature and pressure (i.e., density) on the concentration of water, hexanol, hexanal and *trans*-2-hexenal enriched in the vapour phase. This enabled optimum conditions to be selected to maximise the solvent power. The temperature was investigated at a range of 40 to 70°C, pressure at 70 to 110 bar with a low S/F ratio of 5. Data obtained from the sensitivity analysis are presented in Figure 4-36, Figure 4-37, Figure 4-38, Figure 4-39, Figure 4-40, and Figure 4-41:

From Figure 4-36 it is obvious that the water enriched in the vapour phase increased with increasing temperatures and pressures. At 40°C water content rapidly increases and then steadily decreases with increasing pressure. It remained constant at 100 bar from 40 to 50°C. Above 50°C and 100 bar it is obvious that there is a point at which water enriched in vapour would remain constant. At 40°C a vapour product rich in much lower concentrations of water are produced when compared to higher temperatures below 90 bar. The lowest water fraction was obtained at 40°C and 70 bar.

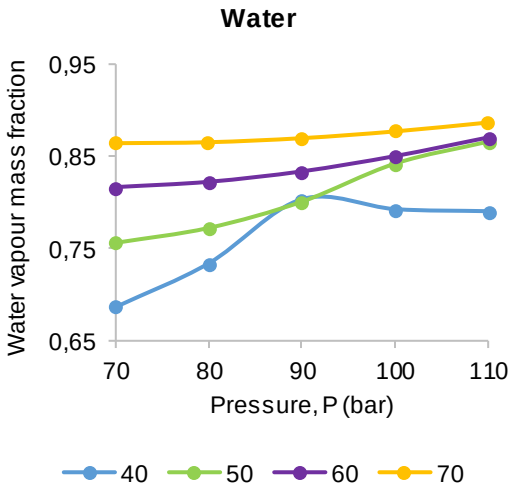

Figure 4-36: Variation of enriched **vapour mass fraction** for **water** with T and P

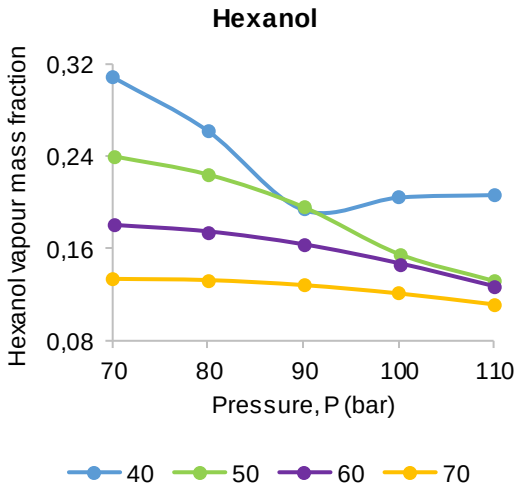

Figure 4-37: Variation of enriched **vapour mass fraction** for **hexanol** with T and P

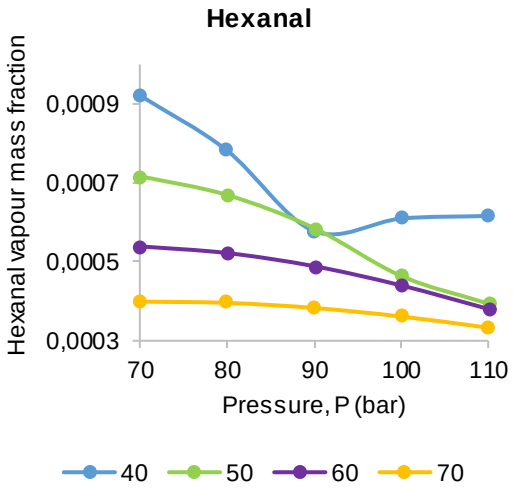

Figure 4-38: Variation of enriched **vapour mass fraction** for **hexanal** with T and P

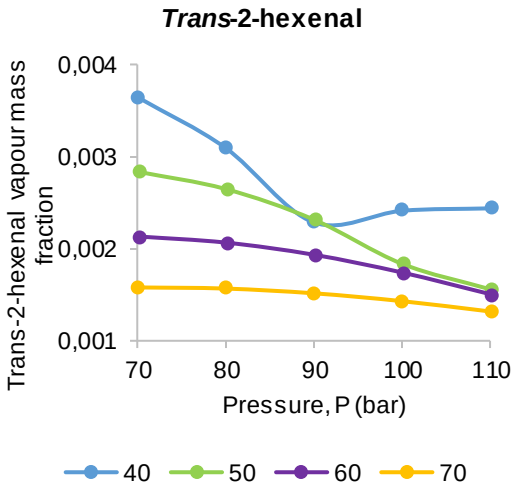

Figure 4-39: Variation of enriched **vapour mass fraction** for ***trans*-2-hexenal** with T and P

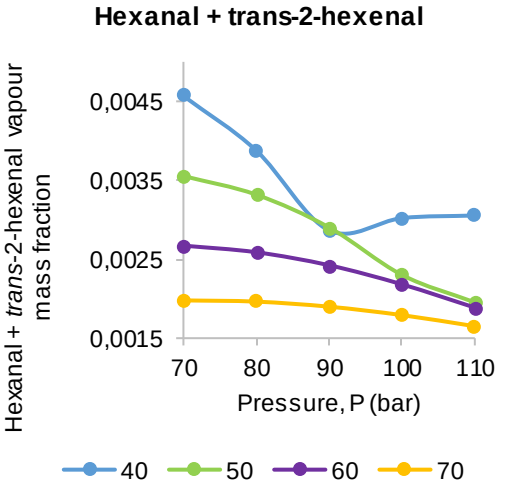

Figure 4-40: Variation of enriched **vapour mass fraction** for **valuable aromas** (hexanal + *trans*-2-hexenal) with T and P

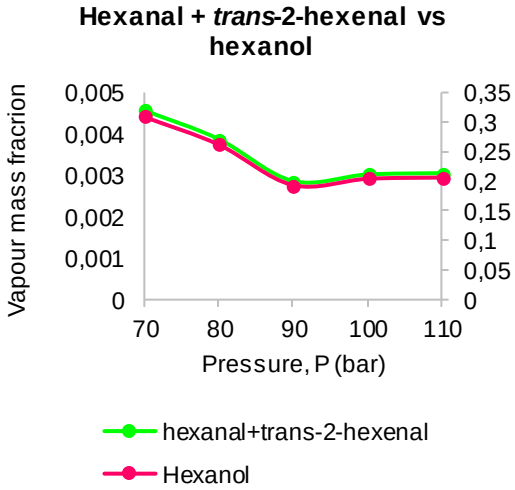

Figure 4-41: Variation of enriched **vapour mass fraction** for **valuable aromas** (hexanal + trans-2-hexenal - **left**) and **hexanol** (**right**) with P at 40°C.

The enriched vapour fraction for hexanol, hexanal and *trans*-2-hexenal follow similar trends with changing temperature and pressure as shown in Figure 4-37, Figure 4-38, and Figure 4-39. As expected, the enriched vapour phases decrease in content with increasing temperature. This was because of increased water fractions. At 40°C and 90 bar, the vapour phase exhibits the same phase behaviour as at 50°C and 90 bar. Therefore, increasing temperature at this point would not be feasible because product quality remains constant and it will increase the energy consumption of the process. Above 100 bar at 40°C, mass fraction of organics and water remained constant. At 50°C between 90 and 100 bar, phase behaviour changes as shown in the decreased slope for organics. But above 60°C, it seems that increasing pressure does not affect the mass fraction significantly. However, water enriched in the vapour phase showed that product quality decreases with increasing temperatures and pressures.

The total valuable aroma compounds i.e., hexanal and *trans*-2-hexenal presented similar trends to that obtained for the pure compounds. Therefore, improved enrichment of hexanal, *trans*-2-hexenal and hexanol in the vapour phase would be best achieved at lower conditions of 40°C and 70 bar as presented in Figure 4-40. However, operating at 70 bar would be below the critical pressure of CO_2. Thus, the data suggest that the separation would occur in the subcritical region of CO_2. But 70 bar is not significantly lower than the critical pressure of CO_2, therefore operation will be on the critical line or in the near-critical region.

It is evident from Figure 4-41 within single staged fractionation the hexanol and hexanal+*trans*-2-hexenal are inseparable. Hexanol content decreases in combination with hexanal+*trans*-2-hexenal content in the vapour phase with increasing temperatures. Therefore, a single-stage CC fractionation process can produce a product of higher quality but not able to separate undesirable (represented by hexanol) and valuable (represented by hexanal and *trans*-2-hexenal) fractions. Nevertheless, the product obtained is still an adequate product that would fetch a higher value on the market just based on the concentrations of organic compounds investigated. Therefore, the CC fractionation staged process clearly shows that separation is feasible as the water content is significantly reduced and ultimately increases product quality with a near perfect recovery for organics.

4.4.1.2. Process layout: Consideration 2

Three stages were selected because after the 3rd stage no traces of apple aroma compounds are present in the liquid phase based on previous layout. On the other hand, it comprised insignificant quantities in the liquid phase for fewer stages. Nonetheless, the extract was recycled to investigate further purification and the split fraction was investigated to establish the product quality, recovery and yield as presented in Table 4-12:

Table 4-12: Process layout consideration 2

Split Fraction	Vapour fraction			
	Water	**Hexanal**	***Trans*-2-hexenal**	**Hexanol**
0,1	0,734	7,822E-04	3,095E-03	0,262
0,2	0,734	7,822E-04	3,094E-03	0,262
0,3	0,734	7,822E-04	3,094E-03	0,262
0,4	0,734	7,822E-04	3,095E-03	0,262
0,5	0,734	7,822E-04	3,095E-03	0,262
0,6	0,734	7,822E-04	3,095E-03	0,262
0,7	0,734	7,822E-04	3,095E-03	0,262
0,8	0,734	7,822E-04	3,095E-03	0,262
0,9	0,734	7,822E-04	3,095E-03	0,262

Enriched liquid and vapour fractions for each compound remained constant. This was expected since separation occurs as a single stage. Therefore, adding a recycle will not make any difference.

4.5. Chapter outcomes

This chapter presented results to fulfil the requirements of the objectives set in Chapter 1. Steady-state operation established during pilot plant experiments enabled an equilibrium process model to be validated with experimental mass and energy balance data to fulfil the requirements of objective 1. A thermodynamic model regressed with literature VLE showed the model's accuracy. In addition, the validation with literature, experiments indicated the model's predictability is reasonable for S/F ratios above 5 and at higher feed concentrations. Correction factors obtained established degree of accuracy of the model estimated data. Results of multi-phase component behaviour attained objective 2 as it suggested that the S/F ratio had no impact on separability. Additionally, low temperatures and pressures favour the separation. Product quality and organics recovery from process layout scenarios indicated that separation occurs as a single-stage. Therefore, fulfilling part of the requirements for objective 3.

CHAPTER FIVE

Discussion of Results

5. DISCUSSION OF RESULTS

This section presents the discussion of the results presented in Chapter 4 and established whether the overall aim of the study was fulfilled. This included answering key research questions and comparison to literature findings. The economic evaluation based on the pilot plant and suggested retrofit presented fulfilled requirements of objective 3. In addition, a conclusion of the overall findings is presented.

5.1. Experimental product yield and quality

The data discussed in this section was based on data presented in 4.2.1, 4.2.2, and 4.2.3

The product yield between experiments 1 and 2 varied by 1%. In contrast, extract analysis showed that organics enriched in the vapour phase varied significantly between the two conditions. The extract obtained from experiment 1, comprised almost no water. Extract from experiment 2 comprised 94% water. Nearly the initial concentration of organics in feed. Thus, indicating that no separation occurred. There is a significant shift in the multicomponent phase behaviour of the process between the two conditions. The extract comprised a total sample from time 60 minutes. From steady state measurements, it was obvious that the system did not achieve a steady chemical composition. Therefore, the shift in the phase behaviour could be due to unsteady measurements. As a result, the water fraction would not be able to establish a constant composition. The raffinate obtained from the second experiment was not evaluated for a steady composition. Therefore, a validation of one of the experiments is required to account for the phase behaviour accurately. In addition, raffinate data in Table 4-5 shows that experiment 2 achieved a higher recovery of organics. However, as previously described, raffinate comprised of a combined average sample. Thus, the fraction for the organics does not represent the final concentration. But concentration data from 4.2.1, shows no *trans*-2-hexenal present. Therefore, organics final concentrations might differ. However, the fact that raffinate does not contain *trans*-2-hexenal indicates that *trans*-2-hexenal and other compounds are separable.

The CO_2 pump, P200, clearly posed a threat to the stability of the process. Throughout the experiments the pump fluctuated mainly between 4 to 6 kg/hr, obtaining an average of 5 kg/hr. This maintained the required set point flow rate for both experiments. In addition, during sampling from the column (the raffinate), the pressure would drop unavoidably and changed the steady pressure operation. However, a limitation on the sampling time of 30 seconds prevented significant decreases in pressure. Consequently, the CO_2 pump would increase the feed supply to compensate for the pressure lost in the column. Thus, the sudden increase and decrease the CO_2 flow rate shown in Figure 4-4. In addition, the automated valve, ARV400, closes to allow pressure to build to the required set point and then opens. This restricted extract

flow to the separators. Furthermore, pump operations posed a threat to the steady state operation of the process. The pump behaviour changed during experiment 2 as noted by the additional increase and decrease in flow rate presented in Figure 4-4. Diagnostics of the pump revealed a problem on one the valves located in the pump. Nonetheless, the range of the flow rate during operation remained stable.

The introduction of the disturbances clearly affected the steady state of the process. Therefore, the process established a new steady state operation through compensation of these disturbances. Considering the unavoidable disturbances, such as during sampling, the process maintained steady state well. The low standard deviations in Table 4-1 and Table 4-2, show that the disturbance did not have such a significant influence on the mechanical and thermal operations. Nonetheless, the changes that occurred during the introduction of the disturbance could have influenced the overall phase behaviour of the process. On the other hand, due to the low concentrations of organics present in the feed, slight changes could influence the enrichment of those organics into liquid and vapour phases. Therefore, the product quality obtained might not represent the actual phase behaviour of the but provides a reasonable estimation for the product quality that could be obtained.

The increased yield in experiment 2 was obtained at a lower product quality. This was because of the increased water fraction. Between experiments 1 and 2, product yield changes by 8%. Nonetheless, at a product yield of 25% for experiment 1, product quality was nearly at 100%. Based on the raffinate analysis at time 60, the extract comprised a mass fraction for hexanal at 2.64×10^{-4}, *trans*-2-hexenal at 6.50×10^{-3}, and hexanol 0.17. Note that this included the aromas lost to the solvent cycle because it relies on the mass balance in Table 4-3 and Table 4-4. Nonetheless, the conditions in experiment 1 favoured the fractionation of apple aroma constituents. In addition, the absence of *trans*-2-hexenal in the raffinate showed that process achieves a 100% recovery of characteristic apple aroma constituents. Furthermore, in the extract hexanol achieved a fold of 26, hexanal 32 and *trans*-2-hexenal 25. This indicated that process achieved an increased product quality but not as large as the 94% in Table 4-5. Which means that data in does not represent the actual concentrations recorded. Consequently, this would mean that the product quality for experiment 2 might not represent the final product quality at these conditions. However, based on the points mentioned, the product quality decreased from 40°C and 70 bar to 50°C and 100 bar at a low S/F ratio.

From experiment 1 to experiment 2, the CO_2 density changed from 198 kg/m^3 to 384 kg/m^3. Based on the data presented in Table 4-5, optimum fractionation of the model solution favours lower densities i.e., low temperature and pressure. In contrast, in the work of Bejarano & del Valle (2017), a density of 192 kg/m^{3,} recovered fewer organics in comparison to a density of 358 kg/m^3. These experiments were performed at 60°C, 80 bar and S/F ratio of 10 and 60°C,

110 bar and S/F ratio of 5. Which is in a much higher temperature range than the pilot plant experiments performed and a higher S/F ratio was investigated. On the other hand, the S/F ratio increases between these conditions. Therefore, when comparing the product quality at the same S/F ratio between 219 kg/m^3 and 684 kg/m^3, it decreased. At a density of 672 kg/m^3 the total organics enriched in the extract slightly increased but does not compare to the optimum recovery obtained at the density of 219 kg/m^3. However, reducing density further through increasing pressure at a high temperature resulted in decreasing the product quality. Temperature remained constant at 50^{o}C and pressure increased from 80 to 140 bar. In addition, these two conditions achieved the highest fraction of organics enriched in the vapour phase. Nonetheless, the overall phase behaviour suggested that increasing CO_2 flow rate resulted in decreased product quality. Therefore, indicating a consistency with the phase behaviour described in this work.

In addition, the feed in literature comprised of a lower concentration of hexanol. For the feed used in pilot plant experiments, hexanol comprised nearly 98% in the organic phase. Therefore, the feed investigated in this work was governed mainly by the phase behaviour of hexanol. For the work of Bejarano & del Valle (2017), hexanol comprised 57%. This could explain the deviations in the effect of the CO_2 density. In, Schultz (1969) obtained a 150 fold in Red Delicious apple essence at 63 bar and 25^{o}C. This indicated that CO_2 in its liquid phase could extract the apple aroma compounds present in the feed. The first experiment in this work occurred within the subcritical region of CO_2. Nonetheless, the concentration of organics improved from 5% to nearly 100% total organics. In comparison to the work of Schultz (1969), the most noticeable difference is the change in temperature. The pressure changed by 7 bar. The concentration of hexanol is significantly affected by temperature in comparison to pressure. At higher temperatures, the fraction hexanol enriched in the vapour phase increases (Elizalde-Solis *et al*., 2003; Secuianu *et al*., 2010). However, if that is the case, then it would be expected that the product yield would increase from experiment 1 to 2. Hexanal presented lower concentrations in the raffinate based on Figure 4-7. Therefore, achieving a greater fold in the extract. On the other hand, hexanol comprised <2% in the raffinate based on data presented in Figure 4-7. It presented significantly lower concentrations in the combined sample. It is thus obvious that the final fraction of hexanol did not establish a steady concentration. Most of the valuable fraction was recovered before the completion of the experiment. So, the process will not be capable of recovering all organics compounds in the vapour phase. But it is possible to recover most of the valuable apple aroma compounds. This does not mean that the separation of valuable fraction and undesired fractions were achieved.

For the separation of essential oil (that comprises volatile compounds) and seed oil in citrus SFF achieved the highest recovery of D-limonene at 60^{o}C. Yasumoto *et al.* (2015) indicated that the optimum recovery of the extract occurred at 30^{o}C. In addition, the solubility of D-

limonene significantly increased at 30°C and 80 bar. Thus, albeit the longer carbon chain in D-limonene, the process achieved greater results in the subcritical region of CO_2. In addition, the current work demonstrated that C6 volatiles can be fractionated in the subcritical region of CO_2. One would expect that the longer carbon chain would require a higher density of CO_2 to extract these compounds. However, within the subcritical region of CO_2, the solubility of volatiles increased.

For the fractionation of isopropanol alcohol (IPA) from aqueous mixtures, low temperatures and pressures favoured the recovery of IPA (Lalam *et al*., 2015). In this work, increasing pressure barely affected the fraction of organics enriched in the vapour phase as indicated by binary phase behaviour for organics/CO_2 (Elizalde-Solis *et al*., 2003; Secuianu *et al*., 2010; López-Porfiri *et al*., 2017; Villablanca-Ahues *et al.*, 2021). However, the hexanal and *trans*-2-hexenal vapour fraction increases with increasing pressure at a constant temperature. On the other hand, binary phase behaviour for hexanol/CO_2 shows that the vapour fraction decreases with increasing temperatures. Above 100 bar, especially in the higher-pressure regions, the phase behaviour changes and the hexanol vapour fraction increases (Secuianu *et al*., 2010; López-Porfiri *et al*., 2017). However, the experiments performed in this investigation was not performed in those higher-pressure region. Therefore, the increased recovery for *trans*-2-hexenal and hexanal was a result of increased solubility in CO_2. The low temperature and pressure that favoured the fractionation of C6 volatiles corresponded with the data obtained from Lalam *et al*. (2015). Similarly, the work presented by Señoŕns *et al.* (2001). shown that a temperature 40°C and low S/F ratios favoured the separation of valuable brandy aroma from alcoholic beverages.

In addition, generally, hydrocarbons present immiscibility in water due to the polar nature of water. Like usually dissolves like, thus hydrocarbons are likely more soluble in the nonpolar CO_2. Hence, the raffinate for chemical measurements in Figure 4-7 presented no traces of *trans*-2-hexenal. On the other hand, alcohols such as hexanol present miscibility in water to a certain extent (Claussen & Polglase, 1952; Hertel *et al*., 2007). Thus, explaining the high concentration comprised in the raffinate.

On the contrary, the valuable fraction (represented by hexanal+*trans*-2-hexenal) and the undesired fraction (represented by hexanol) will coexist in the vapour (extract) phase. This means that a product free from the undesired fraction of organics will not be obtained. This compares to data obtained from Bejarano & Del Valle (2017) and binary phase behaviour. However, a higher fold is achieved for the valuable fraction and not all undesirable hexanol will be recovered. Therefore, there is an increased value in the product obtained.

Nevertheless, the decreased organics fraction, indicated a higher product quality is achieved at low product yields. However, the product quality increased to 17% organics based on the raffinate analysis. Further lowering the product quality to increase yield, results in product fetching a lower value on the market. Thus, the increased organic fraction means that the product would fetch a higher value on the market. In addition, the increased organics enriched in the vapour phase means that higher purity water in raffinate was obtained. The water obtained in the raffinate could find various uses in the process for example cleaning, and ultimately reducing the production costs.

5.2. Process model development

The data discussed in this section is based on the results obtained in section 4.3.

5.2.1. Correlation data

Data shown in Figure 4-11 and Figure 4-12 indicated that the selected SRKKD thermodynamic model could estimate the binary phase behaviour for hexanal and *trans*-2-hexenal when compared to experimental data points. On the other hand, for Figure 4-13, it's obvious that the accuracy of the thermodynamic is decreased with increasing temperatures. Above 60^{o}C and 150 bar, the thermodynamic model's predictions deviated significantly with experimental data. The model presented the most deviations in the critical region of CO_2. In addition, the Aspen Plus® process simulator indicated that the regression cases for hexanal and hexanol were not tightly satisfied. Therefore, inaccurate prediction could be a result of incomplete regression. Contrastingly, the hexanal regression presented very low deviations from experimental measured VLE at between -3 to 2% deviations.

In general, the PR EoS is better at predicting the phase the density of many components in the liquid phase, especially those that are nonpolar in the high pressure range for supercritical CO_2 processes (Bejarano *et al*., 2011; Yazdizadeh *et al*., 2011; Effendi *et al.*, 2013; López-Porfiri *et al*., 2017; Lee *et al*., 2018; Villablanca-Ahues *et al*., 2021;). Differences of <8% in the liquid phase and <2% in the vapour phase was obtained using the PR EoS by Bejarano *et al*., (2011) for correlation of alkanols and CO_2. With the SRK thermodynamic model differences <6% was obtained, however, some data points were well underestimated (-10%), which can simply be adjusted with a correction factor. The PR EoS well underestimated liquid fractions in the lower temperature region. In contrast, the SRKKD model presented quite good correlation results in the lower temperature region for hexanol varying from -11 to 6%. A much larger range than PR EoS, however, most estimated values fell within a lower range of difference with experimental values. In the work by Villablanca-Ahues *et al*., (2021) the PR EoS model well underestimated liquid fractions and more so the vapour fractions for the *trans*-2-hexenal/CO_2 system. But in the case of the SRKKD model, most estimated values obtained

almost matched to experimental values. It is in the higher temperature and pressure region that the model overestimates the vapour and liquid fractions. Proving that the model was quite well in its phase behaviour correlations.

Considering that water is a polar molecule, the PR EoS might pose difficulty in its phase behaviour prediction. Binary interaction parameters obtained from the regressions are only determined based on the interaction of each compound with CO_2 (Peng & Robinson, 1976) however each compound is soluble to a certain extent in water as well and the Kabadi-Danner term for water accounts for this phase behaviour. Therefore, by including this term, the solubility of the hydrocarbons in water was also taken into consideration. This improved the thermodynamic model's predictability when compared to the PR EOS, which does not include a term for interactions with water. In addition, the feed mainly comprised of water and a very low concentration of aromatics, therefore it is crucial to include this parameter when working with a system of such. In addition, the model accounts for interactions with the water-rich liquid phase even if hydrocarbon presents immiscibility (Kabadi & Danner, 1985).

It is also obvious that the thermodynamic does not provide phase behaviour data in the critical region for hexanal and *trans*-2-hexenal, as there is no overlap between liquid and vapour phases predicted as shown in Figure 4-11 and Figure 4-12. The Aspen Plus® simulator uses an algorithm that presents difficulty in phase behaviour predictions in the critical region. Depending on the rigorousness of the calculations, errors in calculations might be obtained due to liquid and vapour like properties of supercritical fluids (AspenTech, 2011). However, the process simulator has been successful in modelling processes in the high pressure region for previous authors (Ajchariyapagorn *et al*., 2006; Lim *et al*., 2003; Manan *et a*l., 2009; Zamudio *et al.*, 2013; Rodrigues *et al*., 2019). Thus, indicating that the process simulator is more than capable of performing rigorous equations required to perform the regression.

By making the binary interaction parameters temperature-dependent results in increased accuracy in the prediction of the selected thermodynamic model. In general, thermodynamic models have difficulty in computing phase behaviour under these critical conditions due to CO_2's high compressibility in this region. For this reason, numerous experimental phase behaviour data regressed at various temperatures and pressures improved the accuracy of the regression. However limited experimental phase behaviour data available for the hexanal/CO_2 and *trans*-2-hexenal/CO_2 mixtures limited the conditions investigated. Nonetheless, the process simulator presented warnings for the hexanal/CO_2 and hexanol/CO_2 regression. For both cases, the regression converged within 5 iterations in comparison to *trans*-2-hexenal that converged within 11. Thus, indicating that the cases were not tightly satisfied and could explain the deviation in estimated and experimental measured data.

Even though vapour pressure data was not available for *trans*-2-hexenal, the model seems to be capable of predicting the experimental phase behaviour. The unsymmetric mixing term presented by Kabadi-Danner measures molecule-molecule interactions between hydrocarbons and water and the structural effect of the hydrocarbon and water in the water-rich phase. The model proved to overpredict alkanes and naphthenes and underpredict alkenes, dialkenes, cycloalkanes, acetylenes and aromatics (Kabadi & Danner, 1985). The mixing term includes the sum of the group contributions of all groups that comprise the hydrocarbon. All compounds have the same amount of carbons (6) contributing and one oxygen atom, however, the number of hydrogens differs. *Trans*-2-hexenal has the lowest number of hydrogen atoms at 10, hexanal 12 and hexanol 14. Therefore, the hydrogen interactions for the thermodynamic model had a significant impact on the outcomes of the regression.

As *trans*-2-hexenal had the lowest number of hydrogens, the regression case was tightly satisfied, thus presenting the low standard deviation obtained in Table 4-6. On the other hand, hexanal regression presented the least amount of differences in experimental and predicted data. However, the data was not as precise as for *trans*-2-hexenal. In addition, pure component data for hexanal and hexanol readily available in comparison to *trans*-2-hexenal meant that the process simulator relied on the estimated parameters for phase behaviour predictions. Therefore, parameters estimated by the model could have improved the overall accuracy in the data obtained for *trans*-2-hexenal.

The temperature range for the VLE collected for hexanol, was well above the required operating temperatures for the extraction of organic compounds from apple aroma concentrate, but well below the critical temperature of the water. As temperature increases the KD mixing term, a''_{wi}, decreased. This means that including the VLE obtained at 124.63°C, might have affected the results predicted by the thermodynamic model as an average absolute deviation was obtained for the binary interaction parameters regression as presented in equation (9).

On the other hand, the regression case for hexanal presented a negative binary interaction parameter when compared to *trans*-2-hexenal and hexanol. Hexanal is a nonpolar molecule, like *trans*-2-hexenal and hexanol, which means it is easily dissolved in CO_2, as it is a nonpolar molecule as well. However, hexanal is soluble in water but only at limited concentrations. With increasing temperature, hexanal's solubility in CO_2 and water increases (López-Porfiri *et al.*, 2017; Hertel *et al*., 2007). Therefore, there is a cross interaction between the CO_2-rich liquid phase and water-rich liquid phase for hexanal. There is also an interaction of hexanal and organics that occur. The low concentration of hexanal means that fewer molecules are available which means that the binary interaction is governed by hexanal and solvent interactions, as other interactions between organics are considered insignificant. However, the

solubility of hexanal in water does impact the interactions of the solute with the solvent. The addition of the water interaction term should account for this. However, binary interaction parameters for hydrocarbon systems fitted for the model are not available for aldehydes and alcohol homologous series. Therefore, the model assumes the values. Thus affecting the attractive energy contribution of the model, as the SRK EoS assumes a one fluid mixing rule (Soave, 1972). Contrastingly, not a significant impact as regression results shows very low to no deviations from experimental data.

Overall, the SRKKD thermodynamic seemed to be capable of predicting experimental VLE data for hexanal, *trans*-2-hexenal and hexanol using the binary interaction parameters presented in Table 4-6.

5.2.2. Multicomponent phase behaviour

The model developed in 4.3.2 was used to investigate the phase behaviour for the multicomponent mixture. The phase behaviour was predicted using the Gibbs flash algorithm and SRKKD thermodynamic model. Data discussed in this section was based on the results presented in 4.3.2.

5.2.2.1. Validation of model phase behaviour and correction factor

The model developed in 4.3.2 was used to investigate the conditions by Bejarano & del Valle, (2017) and pilot plant experiments. The results obtained from the process simulator are presented in combination with experimental data points. This established the error margin for the accuracy of the model. A correction factor was obtained to validate model data with experimental data presented in 4.3.2.1. The correction factors were then applied to the multicomponent phase behaviour such as to accurately describe the phase behaviour for the multicomponent mixture.

Validation with Bejarano and del Valle's (2017) findings

Data described in this section are based on Figure 4-15, Figure 4-16, Figure 4-17, Figure 4-18, Figure 4-19, Figure 4-20, and Table 4-9. As presented in the figures mentioned above, the model's accuracy increases with increasing feed concentration. Specifically for S/F ratios ≥10. Organics comprised a 0.175% feed concentration (within the 0.175% organics fraction comprised 0.57 hexanol, 0.29 *trans*-2-hexenal, and 0.14 hexanal) and this region of fractions are generally considered insignificant. However, the model predicted vapour and liquid phases for the conditions investigated with insignificant traces enriched in the liquid phase. Indicating that model over-estimated the mass fractions enriched in the vapour phase.

The model used to investigate the phase behaviour of the process was a two-outlet flash unit based on an equilibrium model. In the work of Bejarano & del Valle (2017), the product (extract) comprised distinct liquid and organic phases. Thus, indicating that a three-phase separation occurs i.e., vapour-liquid-liquid. Therefore, a three-outlet flash unit would be suitable to perform rigorous calculations required for the three-phase separation. However, the liquid-liquid phase is combined in the vapour-liquid phase calculation. Therefore, an additional liquid outlet could possibly not have a significant impact on the overall separability predicted by the model. In addition, the product consists of both phases.

The accuracy in the model's predictions relied on the regressed thermodynamic model and the flash model. Simply using a flash model already accounts for the discrepancy in the data. Vapour and liquid phase predictions are performed at equilibrium and generally, a system in industrial applications does not quite remain in equilibrium as presented in 4.2.1. Therefore, the overall inaccuracy in the data was expected. However, the model was more than capable of predicting the general phase behaviour regardless of the specific mass fractions. The FLASH2 model does not include the mass transfer of the process, which plays a crucial role in the SFE process. On the other hand, adjusted EoS that include the mass transfer of the process such as the Linear Combination of Vidal and Michelsen (LCVM) model presented by Boukouvalas *et al*., (1994) are developed. However, these models are not available on the Aspen Plus® database.

For hexanol and *trans*-2-hexenal most data points were within 50% difference overestimation region. Most data for hexanal were overestimated by 30% with some underestimated. There were much lower differences in the data predicted by hexanal. Water was completely underestimated. In the correlation data, hexanal presented the least amount of deviations with experimental data. Therefore, although the regression case for hexanal presented warnings the model still presented a higher accuracy when compared to other organics. In addition, the low deviations in estimated values obtained from the correlation show that the SRKKD model does indeed seem to predict the phase behaviour of hexanal within a low range of discrepancies.

Data in Figure 5-1 and Figure 5-2 presented the results obtained after applying the said correction factors for the 17.5% organics feed concentration from Table 4-9.

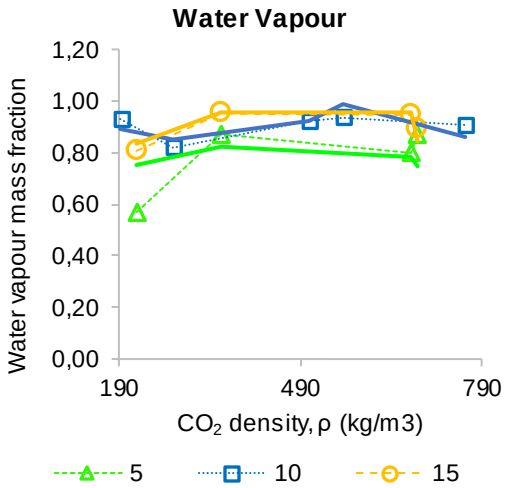

Figure 5-1: Variation of enriched vapour **water content** (mass fraction) **with CF** for 1**7.5% organics** with CO_2 density and S/F ratio. *The dotted symbols (–△–, ··□··, --○--) represent experimentally measured data and straight lines (——, ——, ——) model estimated data at S/F ratios 5, 10 and 15*

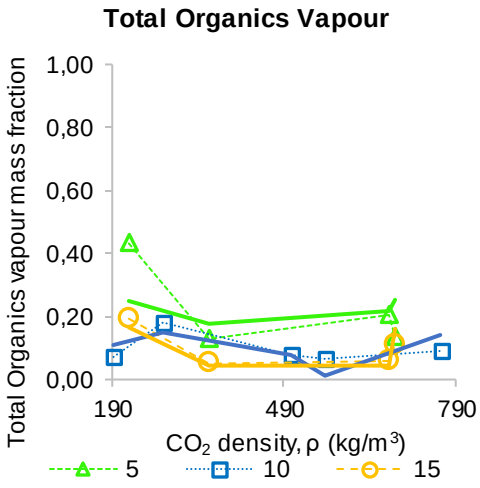

Figure 5-2: Variation of enriched vapour **water content** (mass fraction) **with CF** for 1**7.5% organics** with CO_2 density and S/F ratio. *The dotted symbols (–△–, ··□··, --○--) represent experimentally measured data and straight lines (——, ——, ——) model estimated data at S/F ratios 5, 10 and 15*

It was clear that the S/F ratio of 15 presented the best correlation with experimental data. The S/F ratio of 10 showed deviations with experimentally measured data, however, it presented an overall good fit with experimental data points. Based on Figure 5-1 and Figure 5-2 the model can overall predict phase behaviour trends but not mass fractions accurately.

The velocity at which the supercritical fluid passes through the liquid mixture plays a crucial role in the extraction rate as shown through the mass transfer. The velocity changes with mass flow rate. This is shown with the effect the S/F ratio has on the accuracy of the model as presented in Figure 5-1 and Figure 5-2. The CO_2 flow rate change with the S/F ratio, therefore changing the velocity. Since an equilibrium flash model was used in this case, the mass transfer of the process is thus not included. With that said, the model does not consider the superficial velocity. Therefore, discrepancies in model estimated data and experimental data should be expected.

In addition, regression had an impact on the model predicted data. As regression cases were not tightly satisfied, the multicomponent mixture's phase behaviour presented errors in accuracy. The SRKKD EoS might not be accurate in predicted mass fractions but presented the same phase behaviour trends as experimental data.

Overall, the model could predict the phase behaviour for experimental data for S/F ratios of ≥10.

Validation with pilot plant experiments

For the first experiment, the model presented the highest accuracy in the estimated phase behaviour for hexanol with a -7% deviation. As organics fraction mainly comprised hexanol, it was expected that water concentration would be overestimated. Pilot plant experiments clearly showed that a higher fraction for *trans*-2-hexanal was obtained in the extract and lower for hexanal. For the *trans*-2-hexenal model data deviated significantly from pilot plant experiments. The regression for *trans*-2-hexenal presented no warnings. But it had the least pure component data available in literature. Therefore, it was selected that the process simulator estimated all other properties. In addition, the experimental feed comprised 4.5% organics based on analysis. Whereas the process model was investigated with a 5% feed concentration. As a result, discrepancies in model estimated and experimentally measured data occurred.

On the other hand, the model completely overestimated the organic vapour fractions for the second experiment. In this case, hexanol enriched in the vapour phase presented the highest deviation. Experiment 2 occurred in a higher CO_2 density region, which means it is in a higher critical region. Therefore, this could possibly be from errors in predictability in the critical region. The phase behaviour of the model solution changes significantly between experiments 1 and 2. In addition, the CO_2 density increases from 198 to 384 kg/m^3. Therefore, the solubility of the total organics was significantly affected by the CO_2 density and previously described phase behaviour.

The model is therefore capable of predicting experimental phase behaviour in the low CO_2 density region. It should be noted that at higher densities, the model fails to correctly account for the phase behaviour of the system. Contrastingly, the CO_2 density had no impact on the estimated literature data presented in 4.3.2.1. But the S/F ratio impacted the phase behaviour predictions. Thus, indicating a likelihood of inaccurate measurements of concentrations during experiments. In addition, it could be that feed was not homogenously mixed, thus feed comprised inconsistent concentrations. Therefore, resulting in an unsteady process. Which means inconsistent vapour and liquid concentrations. However, chemical measurements in 4.2.1 indicated otherwise. Even so, the small deviation from set points has a significant impact on the mass transfer of the process. But overall, the system maintained steady-state quite well. In addition, the column packing (pall rings) is random which affected the liquid-to-solvent contact time and liquid distribution in the column which affects the liquid-fluid exchange area. The model used does not include the packing, thus explaining the deviation in simulation data and experimental data.

On the other hand, this could also indicate that during experiments liquid-to-solvent exchange area was affected by the column packing. That could explain the low yield obtained in experiment 2 which was caused by the poor mass transfer efficiency. In addition, a validation experiment will confirm the concentration data obtained, which was also noted in the product quality discussed in 5.1. But the process model can predict phase behaviour in the low CO_2 density region. Therefore, the process model is still suitable for evaluating the system energy requirements and optimising the process for optimum extraction to obtain the objective.

5.2.2.2. Multicomponent phase behaviour and separability

The regressed thermodynamic model previously discussed was used to develop a process model to simulate the CC fractionation of apple aroma concentrate. The phase behaviour of the multicomponent mixture of the process model was investigated using the Gibbs flash algorithm simulated as a two outlet flash drum.

Based on the data presented in Figure 4-21, Figure 4-22 and Figure 4-23, the optimum separability for total organics and water was obtained at 40°C. From Figure 4-24, Figure 4-25, and Figure 4-26 it is obvious that the S/F ratio had no impact on the separability of the multicomponent mixture. Validation with literature data presented in 4.3.2.1, the model can predict the phase behaviour for the multicomponent mixture. However, organic phases are overestimated by the model and the water phase was underestimated but model still predicted overall trends,

At 40°C and 100 bar, the total organics/water reached maximum separation. With increasing CO_2 densities, the separability decreases. In contrast, 60°C favours hexanal+*trans*-2-hexenal/hexanol separation and presented a significant impact on the hexanal+*trans*-2-hexenal/water separation above 100 bar. However, the separation is still favoured at low temperatures and pressures. In addition, literature indicates that hexanal+*trans*-2-hexenal and hexanol phases are not separable as they coexist in their concentration presented (Bejarano & Del Valle, 2017). Therefore, although hexanal+*trans*-2-hexenal and hexanol phases present separability this is based on model predictions. It is thus obvious that investigating the separation would not be feasible as shown through the low separation factors obtained. Moreover, the low separation factors indicate difficulty in separation. In combination with the polarity in water, the separation might not be achieved.

Hexanal enriched in vapour phase favours high temperatures based on the binary phase behaviour of hexanal/CO_2. For *trans*-2-hexenal low temperatures favours the separation. And hexanol presents a higher recovery in the vapour at higher temperatures; (Elizalde-Solis *et al*., 2003; Secuianu *et al*., 2010; López-Porfiri *et al.,* 2017; Villablanca-Ahues *et al.*, 2021). On the other hand, the multicomponent mixture indicated that the separation favoured low temperatures and pressures. This corresponded with the binary phase behaviour of *trans*-2-

hexenal. Hexanal comprised the lowest concentration (ppb) in the feed, thus explaining the deviation of model predicted phase behaviour. In addition, as previously indicated, regression cases for hexanal and hexanol were not tightly satisfied. However, the optimum low operating conditions (i.e., low CO_2 density) compared to product quality obtained from pilot plant experiments. Therefore, the model predicted the multicomponent mixtures phase behaviour at low conditions.

The absurd separation factors obtained for organics/water and hexanal+*trans*-2-hexenal/water indicate that separation is well over-achieved. This also means that the separation occurs as a single stage. Bejarano & del Valle, (2017) confirm this for the fractionation of apple aroma compounds. This was also validated with the process layout scenarios investigated. Therefore, modifications to a single-stage would not affect the process outcomes by much because separation is easily achieved.

The total organics/water separation is favoured by decreasing temperature and pressure as presented in Figure 4-21, thus at lower CO_2 densities. However, at 100 bar the density of CO_2 significantly increases, thus resulting in increased solubility in the vapour phases. Optimum aromas (hexanal+*trans*-2-hexenal) yield was obtained at 50°C and 110 bar based on literature for the extraction of apple aroma compounds. Best extraction yields are obtained between CO_2 densities 300 and 500 kg/m^3 (Bejarano & Del Valle, 2017). At 50°C model data follows a similar trend as the 40°C, however, the model presents the best separability at 40°C at much higher solvent densities. In addition, experimental data indicate that the S/F ratio had a significant impact on the extraction yield of aromas. High S/F ratios seemed to favour aromas yield. Thus, indicating that increasing the S/F ratio would increase the rate at which hexenal and *trans*-2-hexenal are enriched in the vapour phase.

However, deviations in model data and experimental data could be a result of the different feed concentrations investigated. The model solution obtained from literature comprised 14% hexanal, 29% *trans*-2-hexenal and 57% hexanol in the organic phase. Whereas the model investigated in the current investigation comprised 0.29% hexanal, 1.16% *trans*-2-hexenal and 98.54% hexanol. Therefore, the phase behaviour of the organics was mainly governed by the concentration of hexanol in this case. For the literature model, hexanal and *trans*-2-hexenal presented much higher concentrations, therefore fractionation occurs. However, due to the low concentration of the organics mentioned, most of the compounds are enriched in the vapour phases with insignificant traces present in the liquid phases. Thus, explaining the differences in conditions obtained.

Based on the multicomponent phase behaviour, it is obvious that low operating conditions favour the separation of total organics and water. 40°C was thus selected as the optimum temperature for extraction of apple aroma compounds, albeit 60°C presenting rapidly

increased separability. The same separability is achieved at a lower pressure, therefore, to reduce the energy requirements of the process 40°C was selected. Water and organic phases are easily separable as shown in the high separation factors obtained, thus presenting great technical feasibility in separation.

5.3. Retrofitting of a CC scCO2 fractionation column to the current process layout

The process model for the suggested process was developed using the Aspen Plus® process simulator regressed with experimental vapour-liquid phase equilibrium, mass, and energy data. Vapour-liquid phase equilibrium and other thermodynamic properties data were regressed using the Property Method option, which is discussed in Chapter 3. Based on the model developed in 4.3.2, a best-suited process layout scenario retrofitted to the current conventional industrial process based on process layout scenarios. Further, the suggested process layout was optimised.

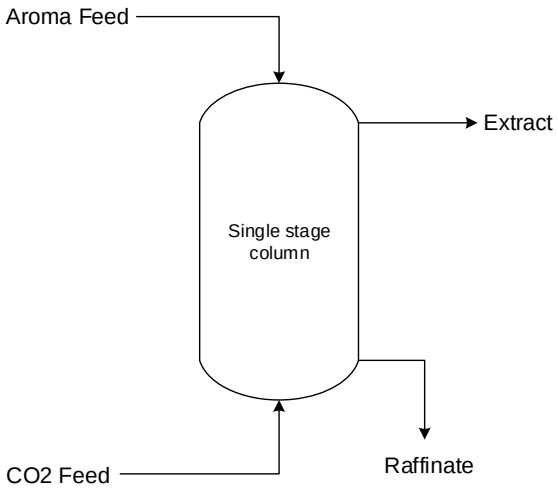

Figure 5-3: PFD for base/control case

The process model developed in 5.2.2.2 was selected as the base case for the development of the process layout scenarios investigated to enable the comparison of the product quality, product recovery, yield, and energy consumed. For the base case, the feed and desired product specifications were considered. The base case comprised of a single-stage fractionation column (separation vessel) as presented in Figure 5-3.

As the water concentration is minimised in the vapour phase, the concentration of volatile compounds enriched in the vapour phase increases, resulting in a product of higher purity, ultimately increasing the product quality. However, as previously discussed; it cannot be disregarded that this is at risk of lower product yields. On the other hand, a product of higher purity will fetch a higher value on the market. Optimising the water enriched in the liquid phase

will reduce the amount of water enriched in the vapour phase, therefore the optimum operating conditions were set at a point at which the water enriched in the vapour is at its minimum but accounting for the near-critical conditions of CO_2.

Results presented in 4.4.1.1 shows that a single-stage process at equilibrium will be able to concentrate/fold the given feed by enriching most of the water into the liquid phase, however not all key aroma compounds present in the aroma concentrate feed were recovered. Figure 4-28, Figure 4-29, Figure 4-30 indicated that the number of stages will have no significant effect on the water enriched in the vapour phase (ultimately product quality) for a feed concentration ≤50%. It is only for a feed concentration of 90% that the water mass fraction increases with an increasing number of stages. Consequently, lowering the product quality of the feed. Similarly, the product yield is not affected by the addition of the number of stages. The effect of the number of stages is influenced by the increasing S/F ratio for the 90% concentration feed. However, for this case, the product stream changes from vapour to liquid. Thus, the top notes of volatiles are lost in the process. Therefore, reintroducing a 90% feed would not be feasible as a higher concentration of organics are already sufficient for uses as is.

The fraction of water enriched in the vapour phase increases with both increasing temperatures and pressures in Figure 4-36. It is at 90 bar where a change in the slope is observed for both 40°C and 60°C, with a steadily increasing slope for 50°C. The results presented indicate that the process achieves optimum fractionation at low operating conditions i.e., temperature, pressure, and solvent-to-feed ratio.

This corresponds to the low temperatures required for the extraction of volatiles from literature (Reverchon, 1997; Laitinen, 1999; Señoŕns *et al.*, 2001; Yousefi *et al.*, 2019;). The fact that the separation occurs as a single-stage shows that fractionation can be easily achieved. Especially for the total organics and water separation. Similar phase behaviour is followed with the adjusted correction factors however, the simulation cannot predict the mass fractions accurately. This was previously indicated with the multicomponent phase behaviour.

With that said, intermolecular interactions between organics in the water-rich and CO_2-rich phase cannot be disregarded as it plays a crucial role. In addition, previously described polarity differences between organics and water had a significant impact on the solubility in CO_2. Consequently, this means increased separability

As a result of deviation of model estimated and experimental data, a FLASH3 unit was investigated. The fact that water and liquid phases were separated, it was expected that the model would produce more accuracy in phase behaviour predictions. Seeing that separation has already proven to be single staged, a single staged FLASH3 unit was selected. Data

obtained for the vapour phase are presented in Figure 5-4 and Figure 5-5. The FLASH3 unit has the vapour (V), liquid (L) and liquid/water (L) phase outlet streams. Water stream were calculated separately from other compounds.

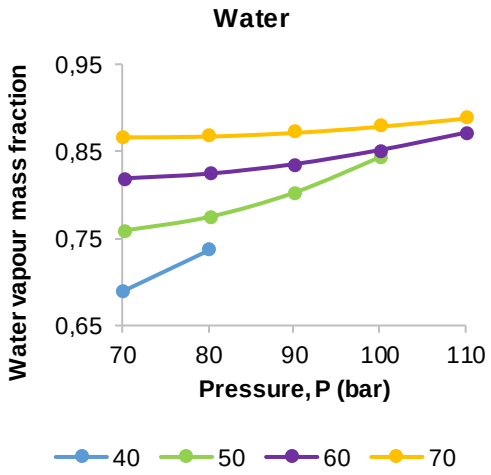

Figure 5-4: FLASH3 variation of enriched **vapour mass fraction** for **water** with T and P

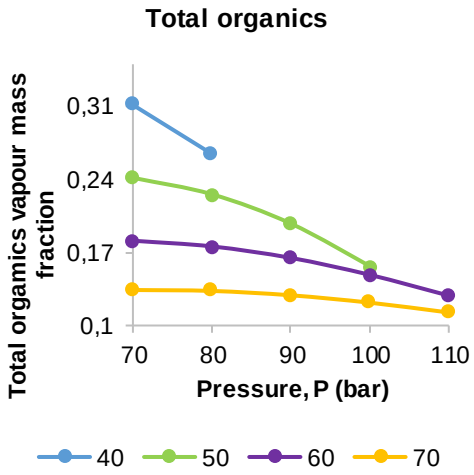

Figure 5-5: FLASH3 variation of enriched **vapour mass fraction** for **total organics** with T and P

Results showed similar phase behaviour as in the FLASH2 unit above 50°C. At 40°C all compounds were enriched in the liquid phase above 80 bar. Thus, no separation occurred. Similarly, conditions at 50°C and pressures above 100 bar showed no presence of compounds in the vapour. However, based on pilot plant experiments, there is separation in those phases. Therefore, model does not accurately predict the phase vapour and liquid fractions of the multicomponent mixture. In addition, the Liquid and Water phases both comprised water. Thus, indicating that model did not separate water. Which could be due to the thermodynamic model selected Additionally, the FLASH3 model predicts the same phase behaviour as the FLASH2 model. Thus, the FLASH2 model results were deemed more accurate than the FLASH3.

In summary, the process does not require further optimisation to improve product quality. Separation clearly occurs as a single stage therefore separation is easily achieved. Based on the data presented the optimum product quality and recovery would be obtained at 40°C, 70 bar and a S/F ratio of 5.

5.4. Economic evaluation based on Pilot Plant data and suggested retrofit

This section is based on the energy requirements of the process for the total product quality obtained. Energy requirements were obtained from the process model. The simulated pilot plant using the Aspen Plus® simulator is presented in Figure 5-6. The process model represented the total recycling process of CO_2.

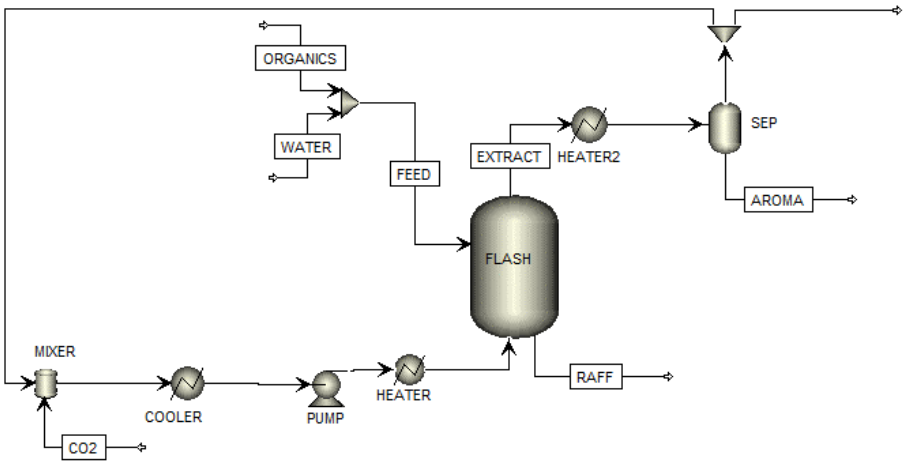

Figure 5-6: CO_2 recycle process for energy evaluation

The CO_2 flowrate and recycling equated to the required S/F ratio in the output stream from the mixer unit. The sequence of units represented the pilot plant used in experimental work. A cooler represented the energy to liquefy CO_2 for pumping from the mixer. The pump evaluated the power required to maintain system pressure. A heater selected evaluated the energy required for heating CO_2 to above critical temperature. Followed by a FLASH2 unit to represent the energy to fractionate feed with the best process layout scenario previously selected. HEATER2 evaluated the energy required to prevent Joule Thompson expansion. SEP represented separation energy for CO_2 and EXTRACT. The split unit accounted for CO_2 losses in the recycle.The conditions for each unit shown in Table 5-1 represented previously indicated optimum conditions. Temperature for the cooler (before the CO_2 feed pump) was selected to maintain CO_2 in the liquid phase. Separator pressure operated at 50 bar and 60°C to preserve thermal labile compounds. Heaters were selected to obtain energy requirements for heat exchangers of the process. A recycle of 80% CO_2 was selected. Allen & Muse (2017) showed that higher recycling ratios reduce energy requirements.

Table 5-1: Conditions for units set using the Aspen Plus® simulator

Unit	Conditions
Cooler (heater)	To = 14.27° P = 50 bar
Pump	Discharge P = 70 bar
Heater (heater)	To = 40°C P = 70 bar
Column (FLASH2)	T = 40°C P = 70 bar
Heater after column (heater)	To = 50°C P = 70 bar
Separator (FLASH2)	T = 40°C P =50 bar

The mass fractions of organics obtained in extract established the cost of the product. A basis of 50 kg/hr feed was assumed which equated to a production output of 100 tonnes per year.

This yields a product value of 99% organics. CO_2, in Figure 5-6, was set a flowrate of 50 kg/hr. The required 250 kg/hr (for the S/F ratio) was maintained with CO_2 in the recycle. The heat duty and power required from simulation established the energy requirements of the process.

The process simulator estimated a total energy requirement of 348 MJ/kg product. This value was significantly greater than the expected low energy requirements for similar SFE processes. However, this value represents an upscale production rate. Further evaluation revealed that the cooler, heater and separator contributed to the significantly high energy requirement (at $\times 10^4$ GJ/hr) obtained. Thus, the pump and column (represented by FLASH) energy requirements were insignificant. In addition, the temperature selected in the condenser does not liquefy CO_2 completely. But cool it to the dew point temperature of CO_2. This resulted in vapour flow in the pump as indicated by the process simulator. Vapour in the pump causes cavitation and inconsistent pump behaviour (Sinnott, 2005). Thus, the cooler should operate at a temperature below the dew point of CO_2.

Phase change occurs in the heater and cooler. The estimated duty accounted for the phase change. The significantly high values obtained indicates that phase change should occur over two heat exchangers. As a result, the addition of a condenser after the cooler was investigated. The cooler was set at 15^{o}C and the condenser at 9^{o}C. The low condenser temperature prevented that phase change occurred in the pump The estimated heat duty increased over the two heat exchangers by 4.90×10^3 GJ/hr. This was expected as the condenser was set at a lower temperature. By considering the temperature difference, the energy consumption reduced but not significantly. In addition, this resulted in an increased energy requirement for the CO_2 heater. However, this indicated that energy for one heat exchanger equates to dividing energy over two heat exchangers. Ultimately, the energy requirement for liquefying CO_2 remained the same.

On the other hand, the cooler required 2.18×10^4 less energy than the condenser. Therefore, the large energy requirement resulted due to the phase change between 15^{o}C and 9^{o}C. From saturated vapour to saturated liquid. Thus the energy requirements equate to the latent heat of CO_2 (Smith *et al*., 1999). Precooling recycling could reduce the energy requirements of the cooler because CO_2 leaves the mixer at 45^{o}C. Thus, reducing the energy required for the cooler. However, this would not reduce the energy requirements of the condenser. This indicated that a subcooler was required after the condenser to reduce the temperature difference. However, as previously indicated the model would just split the energy requirements over the two units. But it does show a reduction. Therefore, the addition of more heat exchangers would reduce energy requirements but not significantly. Furthermore, an additional heat exchanger increases utility costs.

Replacing the pump with a compressor means that condensation of CO_2 is not necessary. Most industrial-scale SFE processes include compressors. However, compressors tend to be more expensive pumps. In addition, it requires more power and interstage cooling (i.e., a heat exchanger) to account for Joule Thompson expansion. Plus, it might require a storage vessel to draw CO_2 gas from (Sinnott, 2005). However, this requires validation. Additionally, pump cycles present lower exergy losses than compressor cycles. Especially in the saturation region (Smith *et al.*, 1999).

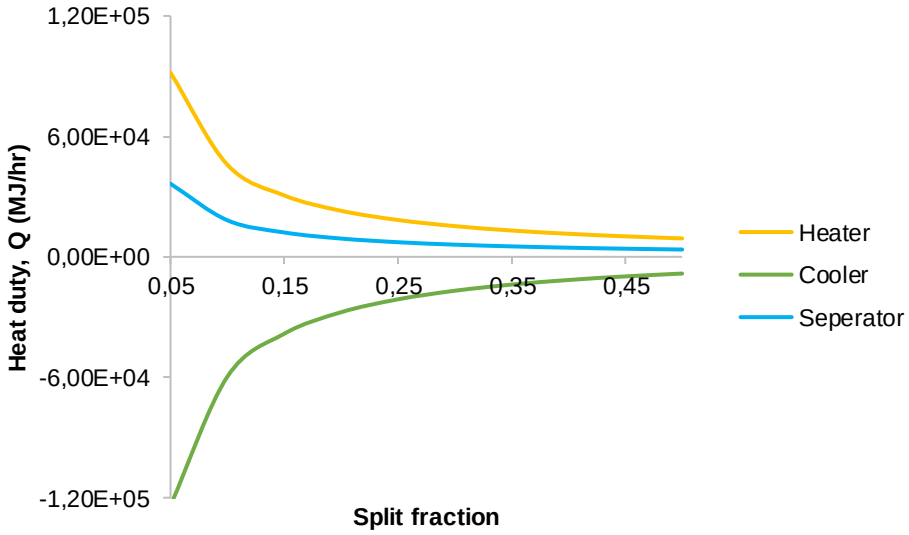

Figure 5-7: Energy requirements for the heater, cooler and separator with **variation in CO_2 recycling**

The effect of the CO_2 recycling on the energy requirements for the heater, cooler and separator are shown in Figure 5-7. Energy requirements reduces with increasing fraction of CO_2 leaving the process. A decreased fraction of CO_2 in the recycle means that the CO_2 in the system is reduced. Therefore, the amount of CO_2 processed was less. Thus, explaining the reduced energy requirements. As a result, the CO_2 added to the process must be increased. This means that the processing capacity for the units would remain the same. Therefore, the energy requirements would remain unchanged. So, changing the split fraction does not affect the energy requirements but the CO_2 added to the process. Ultimately, the cost of CO_2. Thus, higher CO_2 recycling is beneficial for the process i.e., a lower split fraction.

The extraction of butanol and hexanol from an aqueous solution required 4 and 2.4 MJ/kg products (Tompsett *et al.*, 2018). Alcohols separation from water requires more energy. On the other hand, the process presented required much more energy. However, it was less than the extraction of *Eucalyptus globulus* bark. A processing output of 311 to 362 ton product per year required 1.46 to 2.10 GJ/kg product (Rodrigues *et al.*, 2019). This process included ethanol as a modifier and a 0 to 5 wt% ethanol in the feed. Lower concentrations of ethanol required less

energy. The feed in this work comprised of 0.3% organics. The product obtained comprised 99% organics at a yield of 25%. So, the process produces a low product yield due to the low initial organics concentration. Therefore, the amount of feed processed is significantly greater. In addition, the CO_2 flow rate increased. As a result, units required a higher processing capacity. Consequently, increased energy requirement. This indicated that process energy requirements compare to solid extractions of higher carbon groups. However, high energy requirements resulted from high processing capacity at low product output. But the product comprised 99% organics.

A 200 kg/hr feed oregano required 281 MJ/tonne feed and 265 MJ/tonne feed for rosemary (Moncada *et al*., 2016). This included heating and cooling. After heat integration, the energy requirements were reduced by more than half. Therefore, heat integration could be applied to reduce the overall energy requirement. For the separation unit, energy requirements included pressurisation energy. Thus, the inclusion of a pressure-reducing unit will reduce the overall energy requirement. Also, an additional separator could reduce energy requirements for the separator. Which indicates that energy requirements can be reduced. However, this requires validation.

In summary, the process presents similar energy requirements as presented by solid extractions. However, heat integration could reduce the overall energy required. The process recovers nearly all organics present in the feed. The product comprised 99% organics. This was obtained at lower yields (25%). Therefore, processing capacity for product output is quite high. However, the energy requirements could be reduced. Still, this means that the product will have to fetch a high value on the market to account for processing costs.

5.5. Outcomes for investigation

This investigation was aimed at establishing the economic viability of retrofitting an apple aroma production facility. SFF achieves a high recovery of apple aroma constituents based on literature. South African produced apple aroma was modelled in a FLASH2 unit using the Aspen Plus process simulator. The SRKKD EoS selected predicted experimental literature phase behaviour data above S/F ratio of 10 and 10^2 times initial concentration. For validation pilot plant experiments, model estimation favoured low operating conditions. The process route layout scenarios considered proved that a single-stage flash achieved a near 100% recovery of organics. The CO_2 recycling process developed indicated significantly high energy requirements for the process, which attained the aim of the study.

6. CONCLUSION AND RECOMMENDATIONS

In this work, the application of retrofitting a sub-concentration process to an apple production facility was presented. SFF pilot and literature experiments indicated technical viability in the recovery of valuable apple aroma compounds. Literature obtained binary phase behaviour was correlated with the SRKKD EoS in the Aspen Plus® process simulator to model the multicomponent mixture. The process model was further developed into process layout scenarios such as to attain the best layout for the economic evaluation of the process.

The model could estimate literature measured concentration above S/F ratios of 5 at 10^2 times the initial feed concentration. The model presented accuracy in estimated pilot plant concentration. However, higher CO_2 densities affect the phase behaviour of organics significantly. Thus, the model was not capable of predicting the phase behaviour in that region. In addition, interactions of organics with water also affected the mass transfer of the process. On the other hand, data obtained from the second experiment could be inaccurate because of unsteady measurements. Therefore, this requires validation.

Experimental data showed that low operating conditions favour the fractionation of organics. This was confirmed with model data for organics/water separation. In addition, multicomponent phase behaviour shows that separation was easily achieved. As a result, process layout scenarios presented a single staged flash unit as the best-suited layout. Process optimum conditions were obtained at 40^{o}C, 70 bar and S/F ratio of 5. Which is in the lower CO_2 density range and operating at 70 bar is just below the critical pressure of CO_2. Therefore, the process operates best at the critical operating line or near saturation.

The complete CO_2 recycling process revealed that the process had a significant energy requirement per product output. Significantly greater than similar processes and like solid extractions. At optimum conditions energy requirement of 348 GJ/kg product was obtained. This was obtained at a product purity of 99%. However, the application of heat integration could reduce overall energy requirements for heating and cooling of CO_2. In addition, including a pressure reducing unit before the separator and an additional separator unit could reduce the energy requirements of the separator.

The high product purity and recovery of organics indicates that the product could fetch a higher value on the market, thus indicating feasibility.

7. REFERENCES

Ajchariyapagorn, A., Douglas, S., Douglas, P.L. & Pongamphai, S. 2006. Simulation of Safe Processes Using Aspen Plus : an Economic Evaluation. *Proceedings of the 1st International Conference on Natural Resources Engineering & Technology 2006*, (July): 479–483. http://eprints.utm.my/id/eprint/248/1/ArayaAjchariyapagorn2006_Simulationofsafeprocesesusing.pdf.

Allen, A.J. & Muse, S.K. 2017. *Energy Analysis of Butanol Extraction Using Supercritical Carbon Dioxide*. Worcester Polytechnic Institute. https://digitalcommons.wpi.edu/mqp-all/3282.

Anthony, M. 2007. Ingredients and Formulation: The Importance of Aroma.[Online] *Food Processing*. Available at: https://www.foodprocessing.com/articles/2007/291/ [Accessed 11 March 2019].

Arthey, D. & Ashurst, P.R. 1996. *Fruit processing*. First. UK: Springer Science+Business Media Dordrecht.

AspenTech. 2011. Introduction to Aspen Plus. *Teach Yourself the Basics of Aspen Plus™*.

Associated Fruit Processors. Apple Aroma Product Specification. https://www.afp.co.za/our-products/aroma/ 13 August 2019.

Attokaran, M. 2011. Solvent Extraction. In *Natural Food Flavors and Colorants*. John Wiley & Sons: 29–34.

BCCPublishing, 2014. *Flavours and fragrances markets report* [Online] Available at: https://www.bccresearch.com/market-research/chemicals/flavors-and-fragrances-markets-report. [Accessed 28 October 2020].

Bejarano, A., Gutiérrez, J.E., Araus, K.A. & De La Fuente, J.C. 2011. Measurement and modeling of high-pressure (vapor+liquid) equilibria of (CO_2+alkanol) binary systems. *Journal of Chemical Thermodynamics*, 43(5): 759–763. https://doi.org/10.1016/j.jct.2010.12.018.

Bejarano, A., López, P.I., Del Valle, J.M. & De La Fuente, J.C. 2015. High-pressure (vapour + liquid) equilibria for ternary systems composed by {(E)-2-hexenal or hexanal + carbon dioxide + water}: Partition coefficient measurement. *Journal of Chemical Thermodynamics*, 89: 79–88. https://doi.org/10.1016/j.jct.2015.05.003.

Bejarano, A., Simões, P.C. & Del Valle, J.M. 2016. Fractionation technologies for liquid mixtures using dense carbon dioxide. *Journal of Supercritical Fluids*, 107: 321–348. https://doi.org/10.1016/j.supflu.2015.09.021.

Bejarano, A. & Del Valle, J.M. 2017. Countercurrent fractionation of aqueous apple aroma constituents using supercritical carbon dioxide. *Journal of Supercritical Fluids*, 120: 266–274. https://doi.org/10.1016/j.supflu.2016.08.001.

Börjesson, J., Karlsson, H.O.E. & Trägårdh, G. 1996. Pervaporation of a model apple juice aroma solution: Comparison of membrane performance. *Journal of Membrane Science*, 119(2): 229–239. https://doi.org/10.1016/0376-7388(96)00123-8.

Boukouvalas, C., Splitios, N., Coutsikos, P., Tzouvaras, N. & Tassios, D. 1994. Prediction of vapor-liquid equilibrium with the LCVM model : a linear combination of the Vidal and Michelsen mixing rules coupled with the original UNIFAC and the t-mPR equation of state. *Fluid Phase Equilibria*, 92: 75–106. https://doi.org/10.1016/0378-3812(94)80043-X.

Brunner, G. 2010. Applications of Supercritical Fluids. *Annual Review of Chemical and Biomolecular Engineering*, 1(1): 321–342. https://doi.org/10.1146/annurev-chembioeng-073009-101311.

Brunner, G. 2009. Counter-current separations. *Journal of Supercritical Fluids*, 47(3): 574–582. https://doi.org/10.1016/j.supflu.2008.09.022.

Catharino, R.R., Leal, P.F., Meireles, M.A.A., Carmello, Q.A.C., Maia, N.B. & Eberlin, M.N. 2007. Sweet Basil (Ocimum basilicum) Extracts Obtained by Supercritical Fluid Extraction (SFE): Global Yields, Chemical Composition, Antioxidant Activity, and Estimation of the Cost of Manufacturing. *Food and Bioprocess Technology*, 1(4): 326–338. https://doi.org/10.1007/s11947-007-0030-1.

Classen, C., Howes, D. & Synnott, A. 1994. *Aroma: The Cultural History of Smell*. 1st ed. London: Routledge. https://books.google.co.za/books?id=ywGIAgAAQBAJ&printsec=frontcover#v=onepage&q&f=false.

Claussen, W.F. & Polglase, M.F. 1952. Solubilities and Structures in Aqueous Aliphatic Hydrocarbon Solutions. *Journal of the American Chemical Society*, 74(19): 4817–4819. https://doi.org/10.1021/ja01139a026.

Coelho, J.A.P., Filipe, R.M., Palavra, A.F., Naydenova, G.P., Yankov, D.S. & Stateva, R.P. 2016. Semi-Empirical Models and Cubic Equations of State for Correlation of Solids

Solubility in $scCO_2$: From Simple to Complex Substances. *The Open Chemical Engineering Journal*, 10(Suppl-1, M5): 29–40. https://doi.org/ http://dx.doi.org/10.2174/1874123101610010029.

Corbo, M.R., Lanciotti, R., Gardini, F., Sinigaglia, M. 2002, & Guerzoni, M.E. Effects of Hexanal, trans -2-Hexenal, and Storage Temperature on Shelf Life of Fresh Sliced Apples. *Journal of Agricultural and Food Chemistry*, 48(6): 2401–2408. https://doi.org/10.1021/jf991223f.

Crocker, E.C. 2009. The chemistry of flavor. *Journal of Chemical Education*, 22(11): 567. https://doi.org/10.1021/ed022p567.

Dahl, S., Fredenslund, A. & Rasmussen, P. 1991. The MHV2 Model : A UNIFAC-Based Equation of State Model for Prediction of Gas Solubility and Vapor-Liquid Equilibria at Low and High Pressures. *Industrial and Engineering Chemistry Research*, 30(8): 1936–1945. https://doi.org/10.1021/ie00056a041.

Dahl, S. & Michelsen, M.L. 1990. High-Pressure Vapor-Liquid Equilibrium with a UNIFAC-Based Equation of State. *AIChE Journal*, 36(12): 1829–1836. https://doi.org/10.1002/aic.690361207.

Dimick, P.S. & Hoskin, J.C. 1983. Review of apple flavor — state of the art. *C R C Critical Reviews in Food Science and Nutrition*, 18(4): 387–409. https://doi.org/10.1080/10408398309527367.

Dixon, J. & Hewett, E.W. 2000. Factors affecting apple aroma / flavour volatile concentration : A Review. *New Zealand Journal of Crop and Horticultural Science*, 28(3): 155–173. https://doi.org/10.1080/01140671.2000.9514136.

Effendi, C., Shanty, M., Ju, Y.H., Kurniawan, A., Wang, M.J., Indraswati, N. & Ismadji, S. 2013. Measurement and mathematical modeling of solubility of buttery-odor substance (acetoin) in supercritical CO_2 at several pressures and temperatures. *Fluid Phase Equilibria*, 356: 102–108. https://doi.org/10.1016/j.fluid.2013.07.035.

Elhadi M. Yahia. 1994. Apple Flavor.pdf. *Horticulture Reviews*. John Wiley & Sons Inc. 16: 197–233. https://books.google.co.za/books?hl=en&lr=&id=fFj92fyIIhkC&oi=fnd&pg=PA197&dq=Elhadi+M.+Yahia.+1994.+Apple+Flavor.&ots=dvS2FXq5qC&sig=3IaqczyUly7OIrO_kvBeNdfhmH4#v=onepage&q&f=false.

Elizalde-Solis, O., Galicia-Luna, L.A., Sandler, S.I. & Sampayo-Hernández, J.G. 2003. Vapor-

liquid equilibria and critical points of the CO_2 + 1-hexanol and CO_2 + 1-heptanol systems. *Fluid Phase Equilibria*, 210(2): 215–227. https://doi.org/10.1016/S0378-3812(03)00170-5.

Espino-Díaz, M., Sepúlveda, D.R., González-Aguilar, G. & Olivas, G.I. 2016. Biochemistry of apple aroma: A review. *Food Technology and Biotechnology*, 54(4): 375–394. https://doi.org/10.17113/ftb.54.04.16.4248.

Espinosa, S., Diaz, S. & Brignole, E.A. 2002. Thermodynamic modeling and process optimization of supercritical fluid fractionation of fish oil fatty acid ethyl esters. *Industrial and Engineering Chemistry Research*, 41(6): 1516–1527. https://doi.org/10.1021/ie010470h.

Fernandes, J., Ruivo, R. & Simões, P.C. 2007. Dynamic Model of a Supercritical Fluid Extraction Plant. *AICHE Journal*, 53(4): 825–837. https://doi.org/10.1002/aic.11123.

Fiori, L., Manfrini, M. & Castello, D. 2014. Supercritical CO_2 fractionation of omega-3 lipids from fish by-products: Plant and process design, modeling, economic feasibility. *Food and Bioproducts Processing*, 92(2): 120–132. https://doi.org/10.1016/j.fbp.2014.01.001.

Flath, R.A., Black, D.R., Guadagni, D.G., Mcfadden, W.H. & Schultz, T.H. 1967. Identification and Organoleptic Evaluation of Compounds in Delicious Apple Essence. *Journal of Agricultural and Food Chemistry*, 15(1): 29–35. https://doi.org/10.1021/jf60149a032.

Fornari, T., Vicente, G., Vázquez, E., García-Risco, M.R. & Reglero, G. 2012. Isolation of essential oil from different plants and herbs by supercritical fluid extraction. *Journal of Chromatography A*, 1250: 34–48. https://doi.org/10.1016/j.chroma.2012.04.051.

Fourie, F.C. van N., Schwarz, C.E. & Knoetze, J.H. 2019. CO_2 + n-dodecane + 1-decanol: High pressure experimental phase equilibria data and thermodynamic modelling. *Journal of Supercritical Fluids*, 151: 49–62. https://doi.org/10.1016/j.supflu.2019.04.019.

Frey, C. 2009. Natural Flavors and Fragrances: Chemistry, Analysis, and Production. *ACS Symposium Series,* 908: 3–19. 10.1021/bk-2005-0908.ch001.

Gañán, N. & Brignole, E.A. 2011. Fractionation of essential oils with biocidal activity using supercritical CO2- Experiments and modeling. *Journal of Supercritical Fluids*, 58(1): 58–67. https://doi.org/10.1016/j.supflu.2011.04.010.

Garcez, J.J., Barros, F., Lucas, A.M., Xavier, V.B., Fianco, A.L., Cassel, E. & Vargas, R.M.F. 2017. Evaluation and mathematical modeling of processing variables for a supercritical fluid extraction of aromatic compounds from Anethum graveolens. *Industrial Crops and*

Products, 95: 733–741. https://doi.org/10.1016/j.indcrop.2016.11.042.

Geankoplis, C. 2003. *Transport Processes And Unit Operation*. 3rd ed. Upper Saddle River: Prentice-Hall.

Gonçalves, B., Oliveira, I., Bacelar, E., Morais, M.C., Aires, A., Cosme, F., Ventura-Cardoso, J., Anjos, R. & Pinto, T. 2018. Aromas and Flavours of Fruits. *Generation of Aromas and Flavours*. London: IntechOpen: 10-20 http://dx.doi.org/10.5772/intechopen.76231.

Gracia, I., Rodríguez, J.F., García, M.T., Alvarez, A. & García, A. 2007. Isolation of aroma compounds from sugar cane spirits by supercritical CO_2. *Journal of Supercritical Fluids*, 43: 37–42. https://doi.org/10.1016/j.supflu.2007.04.010.

Guo, J., Yue, T., Yuan, Y., Sun, N. & Liu, P. 2020. Characterization of volatile and sensory profiles of apple juices to trace fruit origins and investigation of the relationship between the aroma properties and volatile constituents. *LWT - Food Science and Technology*, 124 (February): 109203. https://doi.org/10.1016/j.lwt.2020.109203.

El Hadi, M.A.M., Zhang, F.J., Wu, F.F., Zhou, C.H. & Tao, J. 2013. Advances in fruit aroma volatile research. Molecules, 18(7): 8200–8229. https://doi.org/10.3390/molecules18078200.

Hannay, J.B. & Hogarth, J. 1879. On the Solubility of Solids in Gases. *Proceedings of the Royal Society of London*, 29(196–199): 324–326. https://doi.org/10.1098/rspl.1879.0104.

Hertel, M.O., Scheuren, H. & Sommer, K. 2007. Solubilities of hexanal, benzaldehyde, 2-furfural, 2-phenylethanol, Phenylethanal, and γ-nonalactone in water at temperatures between (50 and 100)°C. *Journal of Chemical and Engineering Data*, 52(6): 2143–2145. https://doi.org/10.1021/je700122y.

HortGro. 2017. *KEY DECIDUOUS FRUIT STATISTICS 2017*. [Online] Available at: www.hortgro.co.za [Accessed 12 March 2019.]

Jafarian Asl, P. & Niazmand, R. 2020. Modelling and simulation of supercritical CO_2 extraction of bioactive compounds from vegetable oil waste. *Food and Bioproducts Processing*, 122: 311–321. https://doi.org/10.1016/j.fbp.2020.05.005.

Jiang, Y., Song, J., Osorio, S., Muñoz, C., Valpuesta, V., Bayarri, S., Costell, E., Macedo, G.A., Macedo, J.A., Fleuri, L.F. & Pelayo-Zaldívar, C. 2010. Fruit Flavors: Biology, Chemistry and Physiochemistry. In Y. H. Hui, ed. *Handbook of Fruit and Vegetable Flavours*. New Jersey: John Wiley & Sons Inc: 1–73. http://priede.bf.lu.lv/grozs/AuguFiziologijas/Augu_resursu_biologija/gramatas/Handbook

of Fruit and Vegetable Flavors.pdf.

Kabadi, V.N. & Danner, R.P. 1985. A Modified Soave-Redlich-Kwong Equation of State for Water-Hydrocarbon Phase Equilibria. *Industrial and Engineering Chemistry Process Design and Development*, 24(3): 537–541. https://doi.org/10.1021/i200030a004.

Kimbaris, A.C., Siatis, N.G., Daferera, D.J., Tarantilis, P.A., Pappas, C.S. & Polissiou, M.G. 2006. Comparison of distillation and ultrasound-assisted extraction methods for the isolation of sensitive aroma compounds from garlic (Allium sativum). *Ultrasonics Sonochemistry*, 13(1): 54–60. https://doi.org/10.1016/j.ultsonch.2004.12.003.

Knez, Markočič, E., Leitgeb, M., Primožič, M., Knez Hrnčič, M. & Škerget, M. 2014. Industrial applications of supercritical fluids: A review. *Energy*, 77: 235–243. https://doi.org/10.1016/j.energy.2014.07.044

Koch, J., 1976. Zur beurteilung von natuerlichem fruchtsaftaroma. Meran, Kongress-Bericht XIV Int. Fruchtsaft-Kongress.

Koshima, C.C., Nakamoto, K.T., Aracava, K.K., Oliveira, A.L. & Rodrigues, C.E.C. 2015. Fractionation of bergamot and lavandin crude essential oils by solvent extraction: Phase equilibrium at 298.2 K. *Journal of Chemical and Engineering Data*, 60(1): 37–46. https://doi.org/10.1021/je500581h.

Lalam, R., Chamali, S., Camy, S., Rouzineau, D., Kessas, R. & Condoret, J.S. 2015. Fractionation of aqueous isopropanol mixtures in a countercurrent packed column using supercritical CO2. Journal of Supercritical Fluids, 101: 24–35. http://dx.doi.org/10.1016/j.supflu.2015.02.032

Laitinen, A. 1999. *Supercritical fluid extraction of organic compounds from solids and aqueous solutions*. Helsinki University of Technology Dissertation. http://www.inf.vtt.fi/pdf/.

Laitinen, A. & Kaunisto, J. 1999. Supercritical fluid extraction of 1-butanol from aqueous solutions. *Journal of Supercritical Fluids*, 15(3): 245–252. https://doi.org/10.1016/S0896-8446(99)00011-X.

Lane, H.P., Fielder, S., Hunt, M.B., Rowan, D.D. & Allen, J.M. 2002. Biosynthesis of 2-Methylbutyl, 2-Methyl-2-butenyl, and 2-Methylbutanoate Esters in Red Delicious and Granny Smith Apples Using Deuterium-Labeled Substrates. *Journal of Agricultural and Food Chemistry*, 44(10): 3276–3285. https://doi.org/10.1021/jf9508209

Lee, W.J., Tan, C.P., Sulaiman, R. & Chong, G.H. 2018. Solubility of red palm oil in supercritical carbon dioxide: Measurement and modelling. *Chinese Journal of Chemical*

Engineering, 26(5): 964–969. https://doi.org/10.1016/j.cjche.2017.09.024.

Lim, C.S., Manan, Z.A. & Sarmidi, M.R. 2003. Simulation Modeling of the Phase Behavior of Palm Oil-Supercritical Carbon Dioxide. *JAOCS, Journal of the American Oil Chemists' Society*, 80(11): 1147–1156. https://doi.org/10.1007/s11746-003-0834-6

López-Porfiri, P., Villablanca-Ahues, R., Bejarano, A. & de la Fuente, J.C. 2017. High-pressure (vapor + liquid) equilibria for binary systems containing carbon dioxide and key apple odorants, hexanal and ethyl-2-methylbutyrate. *Journal of Chemical Thermodynamics*, 115: 269–275. https://doi.org/10.1016/j.jct.2017.08.008.

López, M.L. & Echeverría, G. 2010. Apple (Malus × domestica Borkh.). In Y. H. Hui, ed. *HANDBOOK OF FRUIT AND VEGETABLE FLAVORS*. Hoboken, NJ: John Wiley & Sons Inc: 247–264. http://priede.bf.lu.lv/grozs/AuguFiziologijas/Augu_resursu_biologija/gramatas/Handbook of Fruit and Vegetable Flavors.pdf.

Lucintel, 2020. Flavour and fragrances market [Online] Available at: https://www.lucintel.com/flavor-and-fragrances-market.aspx [Accessed 22 October 2020].

Madzimbamuto, T.F.N., Schwarz, C.E. & Knoetze, J.H. 2016. Supercritical fractionation of Agathosma (buchu) essential oil. Part I: Measurement of binary phase equilibria. *Journal of Supercritical Fluids*, 107: 612–623. http://dx.doi.org/10.1016/j.supflu.2015.07.023.

Manan, Z.A., Siang, L.C. & Mustapa, A.N. 2009. Development of a new process for palm oil refining based on supercritical fluid extraction technology. *Industrial and Engineering Chemistry Research*, 48(11): 5420–5426. https://doi.org/10.1021/ie801735y.

Manjare, S.D. & Dhingra, K. 2019. Supercritical fluids in separation and purification: A review. *Materials Science for Energy Technologies*, 2(3): 463–484. https://doi.org/10.1016/j.mset.2019.04.005.

Mattheis, J.P., Fellman, J.K., Chen, P.M. & Patterson, M.E. 1991. Changes in Headspace Volatiles during Physiological Development of Bisbee Delicious Apple Fruit. *Journal of Agricultural and Food Chemistry*, 39(11): 1902–1906. https://doi.org/10.1021/jf00011a002

McCabe, W., Smith, J. & Harriot, P. 1993. *Unit Operations Of Chemical Engineering*. 5th ed. J. J. Carberry, J. R. Fair, W. P. Schowalter, M. Tirrell, & J. Wei, eds. New York: McGraw Hill.

Mckenzie, D.-L. 1988. *Physical and Chemical Properties of Apple Juice and Apple Juice Particulate*. The University of British Columbia. http://dx.plos.org/10.1371/journal.ppat.1005459%5Cnhttp://doi.wiley.com/10.1002/9780470015902.a0022859.

Mehinagic, E., Prost, C. & Demaimay, M. 2004. Optimization of extraction of apple aroma by dynamic headspace and influence of saliva on extraction of volatiles. *Journal of Agricultural and Food Chemistry*, 52(16): 5175–5182. https://doi.org/10.1021/jf049577g.

Mezzomo, N., Martínez, J. & Ferreira, S.R.S. 2011. Economical viability of SFE from peach almond, spearmint and marigold. *Journal of Food Engineering*, 103(4): 473–479. https://doi.org/10.1016/j.jfoodeng.2010.10.032.

Michelsen, M.L. 1990. A method for incorporating excess gibbs energy models in equations of state. *Fluid Phase Equilibria*, 60: 47–58. https://doi.org/10.1016/0378-3812(90)85042-9.

Moncada, J., Tamayo, J.A. & Cardona, C.A. 2016. Techno-economic and environmental assessment of essential oil extraction from Oregano (Origanum vulgare) and Rosemary (Rosmarinus officinalis) in Colombia. *Journal of Cleaner Production*, 112: 172–181. http://dx.doi.org/10.1016/j.jclepro.2015.09.067.

MordorIntelligence, 2019. South Afican food flavour and enhancer market industry. [Online] Available at: https://www.mordorintelligence.com/industry-reports/south-africa-food-flavor-and-enhancer-market-industry [Accessed 25 October 2020].

Mouahid, A., Dufour, C. & Badens, E. 2017. Supercritical CO_2 extraction from endemic Corsican plants; Comparison of oil composition and extraction yield with hydrodistillation method. *Journal of CO2 Utilization*, 20(June): 263–273. http://dx.doi.org/10.1016/j.jcou.2017.06.003.

Mukhopadhyay, M. 2000. *Natural Extracts using Supercritical Carbon Dioxide*. Boca Raton: CRC Press LLC.

Nikfardjam, M.P. & Maier, D. 2011. Development of a headspace trap HRGC/MS method for the assessment of the relevance of certain aroma compounds on the sensorial characteristics of commercial apple juice. *Food Chemistry*, 126(4): 1926–1933. http://dx.doi.org/10.1016/j.foodchem.2010.12.021.

Niu, Y., Wang, R., Xiao, Z., Zhu, J., Sun, X. & Wang, P. 2019. Characterization of ester odorants of apple juice by gas chromatography-olfactometry, quantitative measurements, odour threshold, aroma intensity and electronic nose. *Food Research International*,

120(January): 92–101. https://doi.org/10.1016/j.foodres.2019.01.064.

Novella, A., Camy, S. & Condoret, J. 2020. Fractionation of a dilute acetic acid aqueous mixture in a continuous countercurrent packed column using supercritical CO_2: Experiments and simulation of external extract reflux. *The Journal of Supercritical Fluids*, 157: 104680. https://doi.org/10.1016/j.supflu.2019.104680.

Núñez, G.A., Gelmi, C.A. & del Valle, J.M. 2011. Simulation of a supercritical carbon dioxide extraction plant with three extraction vessels. *Computers and Chemical Engineering*, 35(12): 2687–2695. https://doi.org/10.1016/j.compchemeng.2011.04.002

Parhi, R. & Suresh, P. 2013. Supercritical Fluid Technology: a Review. *Journal of Advanced Pharmaceutical Science And Technology*, 1(1): 13–36. https://doi.org/10.14302/issn.2328-0182.japst-12-145

Peach, J. & Eastoe, J. 2014. Supercritical carbon dioxide: A solvent like no other. *Beilstein Journal of Organic Chemistry*, 10: 1878–1895. https://doi.org/10.3762/bjoc.10.196

Peng, D.Y. & Robinson, D.B. 1976. A New Two-Constant Equation of State. *Industrial and Engineering Chemistry Fundamentals*, 15(1): 59–64. https://doi.org/10.1021/i160057a011.

Plaza, F. 2019. OVERVIEW GLOBAL APPLE MARKET- January 2019. *FarmingPortal.co.za*. [Online] Available at: http://www.farmingportal.co.za/index.php/agri-index/68-crops/1403-overview-global-apple-market-january-2019 [Accessed 12 March 2019].

Pourmortazavi, S.M. & Hajimirsadeghi, S.S. 2007. Supercritical fluid extraction in plant essential and volatile oil analysis. *Journal of Chromatography A*, 1163(1–2): 2–24. https://doi.org/10.1016/j.chroma.2007.06.021

Rao, M. 1989. *Processed Apple Products*. D. Downing, ed. New York: Springer.

Reverchon, E. 1997. Supercritical fluid extraction and fractionation of essential oils and related products. *Journal of Supercritical Fluids*, 10(1): 1–37. https://doi.org/10.1016/S0896-8446(97)00014-4

Reverchon, E. & De Marco, I. 2006. Supercritical fluid extraction and fractionation of natural matter. *Journal of Supercritical Fluids*, 38(2): 146–166. https://doi.org/10.1016/j.supflu.2006.03.020

Reverchon, E., Porta, G. Della & Senatore, F. 1995. Supercritical CO_2 Extraction and Fractionation of Lavender Essential Oil and Waxes. *Journal of Agricultural and Food*

Chemistry, 43(6): 1654–1658. https://doi.org/10.1021/jf00054a045

Rocha-Uribe, J.A., Novelo-Pérez, J.I. & Araceli Ruiz-Mercado, C. 2014. Cost estimation for CO2 supercritical extraction systems and manufacturing cost for habanero chili. *Journal of Supercritical Fluids*, 93: 38–41. http://dx.doi.org/10.1016/j.supflu.2014.03.014.

Rodrigues, V.H., de Melo, M.M.R., Portugal, I. & Silva, C.M. 2019. Simulation and techno-economic optimization of the supercritical CO_2 extraction of Eucalyptus globulus bark at industrial scale. *Journal of Supercritical Fluids*, 145(December 2018): 169–180. https://doi.org/10.1016/j.supflu.2018.11.025.

Rodrigues, V.M., Rosa, P.T.V., Marques, M.O.M., Petenate, A.J. & Meireles, M.A.A. 2003. Supercritical extraction of essential oil from aniseed (Pimpinella anisum L) using CO_2: Solubility, kinetics, and composition data. *Journal of Agricultural and Food Chemistry*, 51(6): 1518–1523. https://doi.org/10.1021/jf0257493

Root, W.H. 1996. Apples and Apple Processing. In Y. H. Somogyi, L., Barrett D.M. and Hui, ed. *Processing Fruits Science and Technology - Volume 2: Major Processed Products*. Boca Raton: CRC Press: 1–33. www.crcpress.com.

Root, W.H. & Barrett, D.M. 2004. Apples and Apple Processing. In *Processing Fruits: Science and Technology*. Boca Raton: CRC Press: 455–480.

Rosa, P.T.V. & Meireles, M.A.A. 2005. Rapid estimation of the manufacturing cost of extracts obtained by supercritical fluid extraction. *Journal of Food Engineering*, 67(1–2): 235–240. https://doi.org/10.1016/j.jfoodeng.2004.05.064

Rowe, D.J. 2005. *Chemistry and Technology of Flavours and Fragrances*. CRC Press LLC.

Sabanoglu, T., 2020. Value global flavor and frangrance market. [Online] Available at: https://www.statista.com/statistics/475081/value-global-flavor-and-fragrance-market/ [Accessed 19 January 2021].

Saffarionpour, S. & Ottens, M. 2018. Recent Advances in Techniques for Flavor Recovery in Liquid Food Processing. *Food Engineering Reviews*, 10(2): 81–94. https://doi.org/10.1007/s12393-017-9172-8.

Saravacos, G.D., Moyer, J.C. & Wooster, G.D. 1970. Concentration of liquid foods in a pilot-scale falling film evaporator. *New York State Agricultural Experiment Station Food and Life Sciences Bulletin*, (4). https://hdl.handle.net/1813/4031.

Schneider, G.M., Kautz, C.B. & Tuma, D. 2000. Physico-chemical principles of supercritical

fluid science. In E. Kiran, P. G. Debenedetti, & C. J. Peters, eds. *Supercritical Fluid - Fundamentals and Applications*. Kemer: Springer Science+Business Media: 31–68.

Schultz, W.G. 1969. Process for extraction of flavors. *United States Patent Office Number 3477856*.

Seader, J.D., Henley, E.J. & Roper, D.K. 2011. *Separation Process Principles: Chemical and Biochemical Operations*. Third. J. Welter & D. Matteson, eds. United States of America: John Wiley & Sons, Inc.

Secuianu, C., Feroiu, V. & Geană, D. 2010. High-pressure phase equilibria in the (carbon dioxide + 1-hexanol) system. *Journal of Chemical Thermodynamics*, 42(10): 1286–1291. https://doi.org/10.1016/j.jct.2010.05.006.

Señoráns, F.J., Ruiz-Rodríguez, A., Ibañez, E., Tabera, J. & Reglero, G. 2001. Optimization of countercurrent supercritical fluid extraction conditions for spirits fractionation. *Journal of Supercritical Fluids*, 21(1): 41–49. https://doi.org/10.1016/S0896-8446(01)00086-9.

Señoŕans, F.J., Ruiz-Rodríguez, A., Ibañez, E., Tabera, J. & Reglero, G. 2001. Countercurrent supercritical fluid extraction and fractionation of alcoholic beverages. *Journal of Agricultural and Food Chemistry*, 49(4): 1895–1899. https://doi.org/10.1016/S0896-8446(02)00154-7.

Shen, Z., Palmer, M. V., Ting, S.S.T. & Fairclough, R.J. 1996. Pilot Scale Extraction of Rice Bran Oil with Dense Carbon Dioxide. *Journal of Agricultural and Food Chemistry*, 44(10): 3033–3039. https://doi.org/10.1021/jf950761z.

Sheth, K. 2018. Top Apple Producing Countries In The World. [Online] *WorldAtlas*. Available at: https://www.worldatlas.com/articles/top-apple-producing-countries-in-the-world.html [Accessed: 11 March 2019].

Simándi, B., Deák, A., Rónyai, E., Yanxiang, G., Veress, T., Lemberkovics, É., Then, M., Sass-Kiss, Á. & Vámos-Falusi, Z. 1999. Supercritical carbon dioxide extraction and fractionation of fennel oil. *Journal of Agricultural and Food Chemistry*, 47(4): 1635–1640. https://doi.org/10.1021/jf9809535

Sinnott, R.K. 2005. Coulson & Richardson's Chemical Engineering Series: Chemical Engineering Design. *ELSEVIER - Coulson & Richardson's Chemical Engineering series*, 6(4).

Smith, R.L., Inomata, H., Kanno, M. & Arai, K. 1999. Energy analysis of supercritical carbon dioxide extraction processes. *Journal of Supercritical Fluids*, 15(2): 145–156.

https://doi.org/10.1016/S0896-8446(98)00134-X

Soave, G. 1972. Equilibrium constants from a modified Redlich-Kwong equation of state. *Chemical Engineering Science*, 27(6): 1197–1203. https://doi.org/10.1016/0009-2509(72)80096-4

Spaho, N. 2017. Distillation Techniques in the Fruit Spirits Production,. In M. Mendes, ed. *Distillation–Innovative Applications and Modeling. InTech*. BoD-Books on Demand: 129–152. https://www.intechopen.com/books/distillation-innovative-applications-and-modeling/distillation-techniques-in-the-fruit-spirits-production.

Spiliotis, N., Magoulas, K. & Tassios, D. 1994. Prediction of the solubility of aromatic hydrocarbons in supercritical CO_2 with EOS/GE models. *Fluid Phase Equilibria*, 102: 121–141. https://doi.org/10.1016/0378-3812(94)87072-1

Symoneaux, R., Mehinagic, E., Royer, G., Prost, C. & Jourjon, F. 2006. Characterization of Odor-Active Volatiles in Apples: Influence of Cultivars and Maturity Stage. *Journal of Agricultural and Food Chemistry*, 54(7): 2678–2687. https://doi.org/10.1021/jf052288n.

TheInsightPartners, 2021. *Aroma chemical market 2021 report opportunities, growth factors, key players and regional forecast 2027*. [Online] Available at: https://ksusentinel.com/2021/01/12/aroma-chemicals-market-2021-report-oppurtunities-growth-factors-key-players-and-regional-forcast-2027/ [Accessed 18 January 2021].

Tompsett, G.A., Boock, J.T., DiSpirito, C., Stolz, E., Knutson, D.R., Rivard, A.G., Overdevest, M.R., Conlon, C.N., Prather, K.L.J., Thompson, J.R. & Timko, M.T. 2018. Extraction Rate and Energy Efficiency of Supercritical Carbon Dioxide Recovery of Higher Alcohols from Dilute Aqueous Solution. *Energy Technology*, 6(4): 683–693. https://doi.org/10.1002/ente.201700626

Turton, R., Bailie, R.C., Whiting, W.B. & Shaelwitz, J.A. 1998. *Analysis, Synthesis and Design of Chemical Processes*. Third edit. Upper Saddle River: CRC Press.

Vallat, A., Gu, H. & Dorn, S. 2005. How rainfall, relative humidity, and temperature influence volatile emissions from apple trees in situ. *Phytochemistry*, 66(13): 1540–1550. https://doi.org/10.1016/j.phytochem.2005.04.038.

Del Valle, J.M. 2015. Extraction of natural compounds using supercritical CO_2: Going from the laboratory to the industrial application. *Journal of Supercritical Fluids*, 96: 180–199. http://dx.doi.org/10.1016/j.supflu.2014.10.001.

Del Valle, J.M., Núñez, G.A. & Aravena, R.I. 2014. Supercritical CO_2 oilseed extraction in multi-

vessel plants. 1. Minimization of operational cost. *Journal of Supercritical Fluids*, 92: 197–207. https://doi.org/10.1016/j.supflu.2014.05.018

Varasteh, A. 2012. Modeling of Vapour Liquid Equilibrium Data for Thyme Essential Oil Based on UNIQUAC Thermodynamic Model. *Journal of Chemical Engineering & Process Technology*, 04(01): 1–5. https://www.omicsonline.org/modeling-of-vapour-liquid-equilibrium-data-for-thyme-essential-oil-based-on-uniquac-thermodynamic-model-2157-7048.1000145.php?aid=11088.

Veggi, P.C., Cavalcanti, R.N. & Meireles, M.A.A. 2014. Production of phenolic-rich extracts from Brazilian plants using supercritical and subcritical fluid extraction: Experimental data and economic evaluation. *Journal of Food Engineering*, 131: 96–109. https://doi.org/10.1016/j.jfoodeng.2014.01.027.

Viganó, J., Machado, A.P.D.F. & Martínez, J. 2015. Sub- and supercritical fluid technology applied to food waste processing. *Journal of Supercritical Fluids*, 96: 272–286. https://doi.org/10.1016/j.supflu.2014.09.026

Villablanca-Ahues, R., López-Porfiri, P., Canales, R.I. & de la Fuente, J.C. 2021. High-pressure vapor + liquid equilibria for the binary system CO2 + (E)-2-hexenal. *Journal of Supercritical Fluids*, 168. https://doi.org/10.1016/j.supflu.2020.105027

Wong, V., Wyllie, S.G., Cornwell, C.P. & Tronson, D. 2001. Supercritical fluid extraction (SFE) of monoterpenes from the leaves of Melaleuca alternifolia (Tea Tree). *Molecules*, 6(2): 92–103. https://doi.org/10.3390/60100092

Xu, Y., Fan, W. & Qian, M.C. 2007. Characterization of Aroma Compounds in Apple Cider Using Solvent-Assisted Flavor Evaporation and Headspace Solid-Phase Microextraction. *Journal of Agricultural and Food Chemistry*, 55(8): 3051–3057. https://doi.org/10.1021/jf0631732

Yasumoto, S., Quitain, A.T., Sasaki, M., Iwai, H., Tanaka, M. & Hoshino, M. 2015. Supercritical CO_2-mediated countercurrent separation of essential oil and seed oil. *Journal of Supercritical Fluids*, 104: 104–111. https://doi.org/10.1016/j.supflu.2015.05.008.

Yazdizadeh, M., Eslamimanesh, A. & Esmaeilzadeh, F. 2011. Thermodynamic modeling of solubilities of various solid compounds in supercritical carbon dioxide: Effects of equations of state and mixing rules. *Journal of Supercritical Fluids*, 55(3): 861–875. https://doi.org/10.1016/j.supflu.2010.10.019.

Yousefi, M., Rahimi-Nasrabadi, M., Pourmortazavi, S.M., Wysokowski, M., Jesionowski, T.,

Ehrlich, H. & Mirsadeghi, S. 2019. Supercritical fluid extraction of essential oils. *TrAC - Trends in Analytical Chemistry*, 118: 182–193. https://doi.org/10.1016/j.trac.2019.05.038

Zamudio, M., Schwarz, C.E. & Knoetze, J.H. 2013. Experimental measurement and modelling with Aspen Plus® of the phase behaviour of supercritical CO_2 + (n-dodecane + 1-decanol + 3,7-dimethyl-1-octanol). *Journal of Supercritical Fluids*, 84: 132–145. https://doi.org/10.1016/j.supflu.2013.09.015

Zamudio, M., Schwarz, C.E. & Knoetze, J.H. 2011. Phase equilibria of branched isomers of C_{10}-alcohols and C_{10}-alkanes in supercritical carbon dioxide. *Journal of Supercritical Fluids*, 59(3): 14–26. https://doi.org/10.1016/j.supflu.2011.07.004